CANCER IMMUNOTHERAPY TARGETING T CELL COSTIMULATORY MOLECULES

by

Angela D. Pardee

B.A., Boston University, 2005

Submitted to the Graduate Faculty of

the School of Medicine in partial fulfillment

of the requirements for the degree of

Doctor of Philosophy

University of Pittsburgh

2010

UNIVERSITY OF PITTSBURGH

SCHOOL OF MEDICINE

This dissertation was presented

by

Angela D. Pardee

It was defended on

September 24, 2010

and approved by

Lisa H. Butterfield, Ph.D., Associate Professor, Department of Medicine

Nick Giannoukakis, Ph.D., Associate Professor, Department of Pathology

Michael Shurin, M.D., Ph.D., Associate Professor, Department of Pathology

Angus Thomson, Ph.D., D.Sc., Professor, Department of Surgery

Simon Watkins, Ph.D., Professor, Department of Cell Biology and Physiology

Dissertation Advisor: Walter J. Storkus, Ph.D., Professor, Department of Dermatology

CANCER IMMUNOTHERAPY TARGETING T CELL COSTIMULATORY MOLECULES

Angela D. Pardee, Ph.D.

University of Pittsburgh, 2010

According to the American Cancer Society, over 1.5 million new cancer cases will be diagnosed this year, a figure that is expected to rise with the aging population. Chemotherapy and radiation are the current "gold standards" for cancer treatment, but these therapies are marginally effective, toxic, and serve to diminish the quality of life for cancer patients. Immunotherapy represents an attractive alternative to these traditional treatment regimens. Despite overwhelming evidence that the immune system is capable of recognizing and eliminating tumors, both spontaneously and in response to immune-based therapy, such protection is abrogated in the face of compensatory immunosuppressive events characteristic of progressive disease. Thus, a major goal of novel immune-based therapies is the coordinate silencing of regulatory circuits and amplification of protective T cell function.

While immune modulating reagents that trigger the T cell costimulatory molecules OX40 and GITR are currently being evaluated in early-phase clinical trials, little pre-clinical information is available regarding the efficacy and mechanism(s) of action for these agents in the setting of advanced, well-established disease. To further characterize the molecular, cellular, and treatment-associated consequences of OX40 and GITR engagement, novel agonistic reagents directed against murine OX40 and GITR (ligand-Fc fusion proteins) were recently constructed and characterized *in vitro*. We now show that the growth of well-established, day 17 sarcomas is significantly inhibited or ablated by a short course of either treatment, with OX40L-Fc

demonstrating superior anti-tumor efficacy over GITRL-Fc at comparable dosing. Both treatments were capable of eliminating regulatory T cells within tumors, inducing profound proliferation of T effector cells in the tumor-draining lymph node, and promoting the recruitment of these expanded effector cells to the tumor microenvironment. However, OX40L-Fc therapy mediated additional, T cell-independent effects, including the activation of tumor-localized dendritic and endothelial cell subsets. These changes rendered the tumor microenvironment more immunogenic and permissive to the infiltration of treatment-induced, protective immune cells. The pleiotropic anti-tumor effects demonstrated in this model by OX40L-Fc, and to a lesser extent GITRL-Fc, strongly supports the further translation of such modalities into human clinical trials, either as single agents or in the context of combinational immunotherapy.

TABLE OF CONTENTS

LIST OF FIGURES

PREFACE

I need to first and foremost acknowledge my mentor, Walt, for sharing his considerable scientific knowledge, for his critical reading and comprehensive (i.e. at times slightly verbose) editing of my abstracts and manuscripts, for encouraging me to pursue supplemental training in clinical and translational research over the course of my dissertation studies, for his unwavering patience and guidance, and for having confidence in me when I didn't. I was lucky to have been able to work alongside Drs. Amy Wesa and Jennifer Taylor, who served as additional, unofficial mentors throughout my graduate studies, and I am very grateful for their beneficial discussion and advice regarding career and life aspirations. I additionally need to thank past and current lab members for providing technical support, scientific discussion, optimism, laughter and friendship.

To my late uncle Gary, whose battle with cancer opened my eyes to the injustice of this disease, to my mother and father, who never let me believe that anything was out of my reach and who gave me the opportunity to leave a small town and make something out of myself, to my brother and sister, who inspire me daily, and to Willis, for sharing my highs and lows and letting me share yours, I dedicate this dissertation.

1.0   INTRODUCTION

Developing tumors are typically recognized and eliminated by a protective mechanism of immunosurveillance, failure of which results in the prevalence of tumor tolerance over immunity (1, 2). The goal of tumor immunotherapy is to break such tolerance and initiate a robust, prolonged tumor-specific immune response without the harsh toxicities that traditional cancer therapies impart. High-profile accomplishments in the field have recently been made, including FDA-approval of the first cellular vaccine for cancer (3), and demonstration that a small minority of patients with metastatic melanoma can be, for all intents and purposes, cured upon antibody-mediated blockade of the T cell inhibitory molecule CTLA-4 (4). Median overall survival in both trials, however, was only increased by 4 months. While these milestones should be celebrated as proof-of-concept that T cell-based immunotherapy of cancer is feasible and relatively effective (compared to standard of care treatment), there is clearly room for improvement.

Costimulatory members of the tumor necrosis factor (TNF) receptor family, including OX40 and GITR, are essential components of functional immunity, regulating T cell survival and activation at naïve, effector, and memory stages of the adaptive immune response (5). Accumulating pre-clinical data suggests that engagement of costimulatory members of the TNF receptor (TNFR) family may counteract tumor-mediated immunosuppression by directly reactivating tumor-specific T cells and/or inhibiting dominant suppressive mechanisms that prevent T cell effector function(s) *in vivo* (6). Based on this duality of immunostimulatory

function, TNFR-based agonistic modalities, administered alone or in combination with other immunotherapies, possess high potential for use in treating cancer, a notion that was recently supported by the prioritization of such agents for clinical translation by the National Cancer Institute (7).

1.1 IMMUNOSURVEILLANCE OF CANCER

1.1.1 Immunosurveillance: a primer

The theory that pre-neoplastic lesions can be recognized and eliminated by the immune system was first proposed by Ehrlich in 1909, and the term immunosurveillance was later coined by Burnet and Thomas (1, 8). This theory could not be tested experimentally, however, until our understanding of immunobiology had matured and immunodeficient mouse models became available. Although early experiments indicated that carcinogen-induced tumors grew equivalently in immunocompetent and immunodeficient mice, refuting the cancer immunosurveillance hypothesis, it was later determined that these "immunodeficient mice" in fact contained natural killer (NK) cells and low frequencies of T cells (9). Years later, immunosurveillance became a hot topic again when IFN-γ neutralizing antibodies were found to accelerate tumor growth (10), consistent with later observations made in IFN-$\gamma^{-/-}$ mice (11). Perforin, as well as NK and NKT cells, were identified as additional factors integral to protective anti-cancer immunity, as perforin- or NK1.1-deficient mice, respectively, developed tumors at higher rates than their wild-type counterparts (11, 12). Finally, the most compelling data in support of the cancer immunosurveillance hypothesis came when carcinogen-induced tumor

incidence was found to be enhanced in Rag-2$^{-/-}$ mice that lack T, B, and NKT cells (13). Observational data from humans further supports the existence of a cancer immunosurveillance process. Immunosuppressed transplant recipients, for example, exhibit higher incidences of cancers of non-viral origin than the general population (14), while the density of tumor-infiltrating lymphocytes (TIL) is associated with favorable clinical outcome in cancers of various histological origins (15-17). In summary, the plethora of experimental data from mice and correlative clinical data validate the concept that the immune system can protect against tumor growth and progression.

1.1.2 Elimination

A series of sequential cellular and molecular events are though to be necessary for the recognition and immune-mediated elimination of developing tumors (1, 18). First, the normal tissue surrounding cancer cells is disrupted as a consequence of tumor expansion, resulting in the subsequent release of "danger" signals (19), which serve as agonists for pattern-recognition receptors expressed by cells of the innate immune system (20). A positive feedback system between tumor-infiltrating macrophages, dendritic cells (DC) and NK cells then amplifies the production of pro-inflammatory cytokines (i.e. type I and II interferons, IL-12) and induce a state of acute inflammation (21-23). Next, tumor-infiltrating DC, which are considered professional antigen-presenting cells (APC), acquire antigens released by dying tumor cells (24), mature, and migrate to the tumor-draining lymph node (TDLN) (25, 26). These mature DC process and present tumor antigen in the context of MHC class I molecules via the cross-presentation pathway to activate CD8$^+$ cytotoxic T lymphocytes (CTL) (27). Priming of MHC class II-restricted CD4$^+$ T cells by DC also occurs in the TDLN (28). These activated Th1 CD4$^+$ T cells

further amplify the adaptive immune response by "licensing" DC-mediated priming of CD8$^+$ T effector cells via CD40/CD40L interactions and the secretion of IFN-γ (29, 30). Efficient T cell priming by DC involves two signals: i.) interactions between the T cell receptor (TCR) on T cells and MHC-peptide complexes on DC, and ii.) engagement of the costimulatory receptor CD28 on T cells with CD80 and CD86 on DC. Additionally, T cell differentiation towards Th1 (pro-inflammatory) or Th2 (anti-inflammatory) can also be facilitated through provision of a polarization signal, or "signal 3" (31). The concept of T cell plasticity has become exceedingly complex in recent years, with 7 unique subsets of CD4$^+$ T cells currently defined (32). Finally, activated tumor-primed CD4$^+$ and CD8$^+$ T effector cells home to the tumor microenvironment (TME) in response to CXCR3 chemokine ligands (CXCL-9, -10 and -11) and carry out their tumoricidal activity (33, 34).

During the effector phase of an anti-tumor immune response, the functions of IFN-γ are multi-fold. Produced primarily by CD4$^+$ Th1 cells and NK cells in the TME, IFN-γ exhibits potent anti-proliferative (35) and angiostatic (36, 37) effects on tumor cells and surrounding structural cells, respectively. Additionally, stimulation of innate immune cells and structural cells in the TME by IFN-γ induces the production of CXCR3 ligands (1). CXCL9 and CXCL10 not only serve as chemoattractants for T effector cell and NK cell recruitment into tumor lesions, but they are also powerful inhibitors of angiogenesis (38). Moreover, IFN-γ enhances the immunogenicity of tumor cells by inducing MHC up-regulation and antigen presentation to CTL (39). Finally, NK cell and CD4$^+$ T cell "help" appears to potentiate the effector function of CTL through their direct production of IFN-γ in tumor lesions (40).

Cells with cytolytic capability (i.e. NK cells and CTLs) are essential players in the anti-tumor effector phase (41). Tumor cells commonly down-regulate MHC class I to avoid a CTL

attack (42). Ironically, these cells simultaneously up-regulate MHC class I chain-related proteins A and B (MICA/B) (43), rendering them susceptible to attack by NK cells, which express the MICA/B receptor NKG2D (44). NK cells carry out their cytotoxic effector activity primarily through the perforin/granzyme granule exocytosis pathway. In brief, lytic granules containing perforin and granzymes are secreted by NK cells upon contact with the target cell. Perforin, a membrane-disruption protein, forms pores on the target cell's plasma membrane, which allows the entry of serine proteases known as granzymes. These molecules then initiate a proteolytic caspase cascade that results in DNA fragmentation and target cell apoptosis (45). NK cells can also induce target cell apoptosis by signaling through TRAIL, an apoptosis-inducing member of the TNF superfamily (44).

The cumulative data from experimental murine tumor models (46-48) and immuno-monitoring of human cancer patients (16, 49) strongly suggests that CD8$^+$ T cells are integral to immune-mediated tumor elimination, perhaps more than any other immune cell subset. In contrast to NK cells, CD8$^+$ CTL exert their tumoricidal activity in an MHC class I-restricted tumor-specific manner, although their effector functions are similar. CTLs also mediate target cell apoptosis through secretion of lytic granules and signaling through an apoptosis-inducing member of the TNF superfamily, in this case FasL (45). An additional and significant function of CD8$^+$ T cells is the production of IFN-γ, the numerous anti-tumor activities of which are described above.

1.1.3   Tumor antigens

A requirement for tumor elimination mediated by the adaptive immune system is the existence of immunogenic tumor antigens presented in the context of MHC class I molecules. Viral antigens,

5

expressed by virally-induced cancers such as cervical cancer and Burkitt's lymphoma (50), are considered tumor-specific antigens (TSA) because their expression is restricted to cancer cells. However, because most human cancers are non-viral in etiology and therefore recognized by the immune system as "self," the ability of humans to mount tumor-specific immune responses against such cancers was doubted (51). Following the landmark observation that tumor-specific T cell-mediated immunity can spontaneously arise in a small subset of patents (52), the first non-viral tumor antigen, MAGE-1, was identified by Boon and colleagues (53). Importantly, this HLA-A1-restricted antigen was expressed by primary melanoma cells and melanoma cell lines, but not normal tissues.

The evolution of sequencing technologies and cell propagation techniques has allowed the characterization of over 1000 human tumor antigens (1). Tumor antigens fall into two broad categories: i.) tumor-specific antigens (TSA), which include viral antigens as well as antigens that arise as a result of somatic mutations in the cancer cell (i.e. p53 mutations), and ii.) tumor-associated antigens (TAA), which represent the majority of human tumor antigens. TAAs are non-mutated self molecules that are preferentially expressed by cancer cells, but can be expressed by normal cells as well (54). Because of the less restricted expression profile of these antigens, compared to TSAs, T cell-targeting of TAAs carries a higher risk of correlative autoimmunity. TAAs can be further divided into three sub-categories (1): i.) *differentiation antigens*, which are expressed by cancer cells and normal cells of the same origin (i.e. MART-1, tyrosinase, gp100), ii.) *overexpressed antigens*, which are amplified in cancer cells and expressed in normal tissues at low levels (i.e. HER-2/neu), and iii.) *cancer-testis antigens*, which are normally expressed only by germ cells in the testis, but are aberrantly expressed by cancer cells as a result of genetic instability (i.e. MAGE, NY-ESO-1) (55).

Additionally, recent advances by our group and others have indicated that antigens expressed by the tumor stroma can serve as valuable targets of anti-tumor T cells. Solid tumors (i.e. carcinomas and sarcomas) are comprised of cancer cells and additional non-transformed cells of that make up the tumor stroma. Stromal cell subsets include bone-marrow-derived cells (i.e. monocytes, granulocytes, lymphocytes), endothelial cells, supporting vascular cells (i.e. pericytes), and tissue-associated fibroblasts (56). These stromal cells support tumor cell fitness by providing nutrients (i.e. oxygen), growth factors, and cytokines (55). Together, cancer cells and the surrounding stroma make up what is known as the tumor microenvironment, or TME (57). We have recently demonstrated that prophylactic vaccination against hemoglobin-β, which is aberrantly expressed by tumor-associated pericytes, protects mice against subsequent tumor challenge (58). Additional "stroma-associated antigens" that have exhibited immunogenicity in murine tumors models include fibroblast activation protein (FAP) and vascular-endothelial growth factor receptor 2 (FLK-1) (59, 60). Of particular therapeutic significance, it has been reported that TAAs can be acquired and cross-presented by the tumor stroma, followed by CTL-mediated elimination of these TAA-expressing stromal cells (56, 61). Furthermore, cancer cells that lost TAA expression (antigen loss variants) were simultaneously eliminated via an unknown mechanism when CTL killing of TAA-expressing stromal cells occurred. Given that tumor cells commonly lose MHC class I expression (42), while stromal cells do not, targeting of stroma-associated antigens or TAA cross-presented by stromal cells represents an attractive immunotherapeutic approach.

1.2   MECHANISMS OF IMMUNE ESCAPE

Needless to say, the cancer immunosurveillance process is not always effective, and clinically-apparent disease can develop. Although immune evasion was not designated by Hanahan and Weinberg (55) ten years ago as a "hallmark of cancer," likely because the cancer immunosurveillance theory remained controversial at the time, the ability of tumors to evade an immune response is now recognized as an essential characteristic of malignant disease. Tumors employ a variety of mechanisms to evade the immune response, both locally in the tumor microenvironment (effector phase tolerance) and distally in the TDLN (suboptimal T cell priming) (2, 62). The concepts of inadequate tumor cell recognition (immunologic ignorance), intrinsic T cell dysfunction, and extrinsic suppression of T cells by immunoregulatory molecules and cells will now be discussed.

1.2.1   Immunologic ignorance

Human tumors that are not eliminated in the process of immunosurveillance or as a result of therapy can remain in a state of dormancy that can last decades (63). Indeed, cancer recurrence following long periods of remission is commonly observed (64, 65). Moreover, cancers have been inadvertently transferred from donor to recipient upon organ transplantation, even when the donors had been diagnosed as cancer-free for many years prior to transplantation (66). Tumor dormancy can also be experimentally induced in mice, and it has been demonstrated that sculpting of the tumor cell repertoire by the immune system occurs during this "equilibrium phase" (63, 67). In one study, tumors were grown in either immunocompetent (wild-type) or immunodeficient (RAG-2$^{-/-}$) mice and then transplanted into wild-type mice. Tumors isolated

8

from wild-type mice grew progressively in the recipients, while tumors that were grown in immunodeficient more were rejected, suggesting that these tumors are more immunogenic than those isolated from wild-type controls (13). The concept that the immune system eliminates highly-immunogenic tumor cells and spares those of low immunogenicity has been termed "immunoediting" (1). The end product of this process, however, is the outgrowth of poorly-immunogenic tumor cell variants that can escape immune recognition.

Additional mechanisms inhibit the ability of the immune system to recognize tumor cells. As noted above, tumor cells commonly down-regulate MHC class I (42), but components of the antigen processing and presentation machinery (i.e. β2-microglobulin and TAP1) in these cells can also be dysregulated (68). Insensitivity of tumor cells to the many effects of IFN-γ signaling can also develop during the course of disease progression (69). Finally, tumor cells can "hide" from an NK cell attack via shedding of MICA/B, molecules that serve as ligands for the activating NK cell receptor NKG2D, thereby preventing MICA/B-NKG2D interactions and protecting against NK cell-mediated tumor lysis (70).

1.2.2   T effector cell anergy/dysfunction

T effector cell hyporesponsiveness, another major barrier to effective anti-tumor immunity, occurs through: i.) the induction of systemic TAA-specific T cell anergy, and ii.) T effector cell dysfunction upon infiltration of tumor lesions. T cell anergy, a consequence of inefficient priming, is characterized by an inability to respond to TCR stimulation, resulting in impaired T cell proliferation and/or effector function upon MHC-peptide engagement (71). It has been proposed that T cell anergy represents a significant barrier to spontaneous and therapeutic anti-tumor immunity (72). The activation of tumor-specific T cells is dependent on cross-presentation

of tumor antigen by APC in the TDLN, rather than through direct presentation by tumor cells themselves (73), indicating that dysfunctional APCs are responsible for the generation of systemic TAA-specific anergy (74). Indeed, poorly-immunogenic, or "tolerogenic," DC have recently been characterized and determined to play an important role in this process (75, 76). These DC exhibit an immature phenotype (i.e. low surface expression of CD40 and CD86) and produce minimal amounts of IL-12 (77, 78). Additionally, secretion of the enzyme indoleamine 2,3-dioxygenase (IDO) by DC at the time of T cell priming results in durable antigen-specific anergy (79).

Moreover, T effector cells that are sufficiently-activated in the TDLN can lose functionality upon infiltration of tumor lesions. T cell-intrinsic dysfunction, characterized by suboptimal granule exocytosis, cell cycle arrest, and defective cytokine secretion, has been attributed to tumor-induced inhibition of proximal TCR signaling (80-82). TIL hypo-responsiveness may also be a consequence of prolonged antigen signaling within the tumor mass and subsequent T cell "exhaustion" (83). Indeed, TIL that were isolated and expanded *ex vivo* displayed optimal anti-tumor activity when the time in culture (i.e. rounds of *in vitro* stimulation) was minimized (84).

1.2.3   Active suppression of T effector cells

Tumor cells themselves employ an expansive arsenal of weapons to evade an immune attack, including surface expression of inhibitory molecules and secretion of immunosuppressive cytokines (2). Although structurally related to the costimulatory receptor ligands CD80/B7.1 and CD86/B7.2, PD-L1/B7-H1 and B7-H4 send inhibitory signals upon T cell engagement and are therefore referred to as co-inhibitory molecules (85, 86). Elevated expression of both PD-L1 and

B7-H4 on tumor cells has been reported and is associated with poor clinical prognosis (87, 88). Tumor cells are also known to produce high levels of the pleiotropic immunosuppressive cytokines IL-10 (89) and TGF-β (90, 91).

Contrary to the anti-tumor properties of lymphoid and myeloid immune cells discussed above, immune-suppressive subsets of these cells that exert pro-tumorigenic activity have also been identified. At this point, CD4$^+$ regulatory T cells (Treg) and myeloid-derived suppressor cells (MDSC) are the best characterized of these suppressor cells. Naturally-occurring CD4$^+$CD25$^+$ Tregs, which develop in the thymus with specificity to self antigen, are identified by constitutive expression of the transactivator protein Foxp3 and represent 5-10% of peripheral CD4$^+$ T cells (92, 93). Once activated by TCR engagement, natural CD4$^+$CD25$^+$ Tregs suppress non-specifically and through direct cell-to-cell contact that may involve surface-bound TGF-β (94, 95). Regulatory T cells can also develop in the periphery from naïve CD4$^+$ T cells after chronic stimulation by immature DC or in the presence of IL-10 or TGF-β (96, 97). These peripherally-induced Tregs appear to function via IL-10 secretion (98). In tumor-bearing hosts, Tregs exert their immunosuppressive activity in both the TDLN and TME. In murine models, TDLN Tregs inhibit anti-tumor T effector cell priming (99), and have been found to increase in frequency and suppressor activity over the course of disease progression (100). In the TME, Treg induction, expansion, and/or recruitment all contribute to the abrogation of anti-tumor immunity. For example, increased proportions of TGF-β and IL-10-secreting Tregs capable of suppressing CTL proliferation were observed in late-stage cancer patients (101), while Curiel and colleagues reported preferential migration of Foxp3$^+$ Tregs into ovarian tumors and ascites, which correlates with poor prognosis (102). In addition to TGF-β and IL-10 secretion, proposed suppressive

11

mechanisms of these intratumoral Tregs include competitive consumption of IL-2, perforin- or granzyme-dependent killing of T effector cells, and induction of tolerogenic DC (103).

Additional inhibitory-type cells that accumulate dramatically in tumors include myeloid-derived suppressor cells (MDSC), a heterogeneous population that is identified by CD11b$^+$Gr-1$^+$ co-expression and exhibit properties of both macrophages and granulocytes (104). Since these cells phenotypically and functionally resemble alternatively activated, or M2, macrophages, it is currently unknown whether MDSC and M2 macrophages represent distinct cellular subsets or are a result of myeloid cell plasticity (105). Regardless, CD11b$^+$Gr-1$^+$ cells isolated from tumor-bearing mice potently inhibit anti-tumor T effector cell immunity (106), primarily through the production of enzymes (i.e. arginase-1) that interfere with T cell amino acid metabolism (107). Correlative clinical data also implicates a key role for these cells in tumor immune evasion (108).

1.2.4 Impaired tumor homing

In addition to the ability of tumor microenvironmental factors to disable anti-tumor T cell activity, the TME can physically impede the migration and infiltration of effector cells. A clear correlation between T cell infiltration of tumors and overall survival has been routinely observed (17, 109). Circulating T cells extravasate into peripheral tissues through recognition of adhesion molecules, including ICAM and VCAM, which are up-regulated by vascular endothelial cells (VEC) in response to inflammatory conditions, followed by chemokine-mediated migration to the target site (110). This process is complicated in the cancer setting, however, due to tumor-induced vascular alterations and limited chemokine and adhesion molecule expression. The vasculature of solid tumors is characterized by disorganized, tortuous vessels that restrict the infiltration of nutrients, oxygen, therapeutic drugs, and tumor-primed T cells (111). The

importance of IFN-γ-inducible chemokine (i.e. CXCL9/Mig and CXCL10/IP-10) production in the TME has also been demonstrated, as high IP-10 levels correlated with favorable prognosis of patients with uterine/cervical cancers (112). Strategies to "normalize" the tumor vasculature and induce chemokine and adhesion molecule up-regulation have shown efficacy in pre-clinical models (113-115).

1.3   CANCER IMMUNOTHERAPY

Recent conceptual advancements have improved our understanding of tumor biology and the paradoxical effects of the immune system in the setting of cancer. These advancements have also facilitated the evidence-based design of a plethora of novel immunotherapeutic strategies, the goals of which are to: i.) enhance suboptimal host immunity through administration of activation stimuli or preformed tumor-specific antibodies or T cells (i.e. passive immunotherapy), ii.) generate *de novo* tumor-specific T cell immunity through active immunization, and/or iii.) counteract the immunosuppressive mechanisms discussed above. Ultimately, it is expected that optimal therapeutic benefit will require treatment regimens that engage multiple immune effector mechanisms. Immunotherapeutic modalities that have been FDA-approved or are in late-phase clinical development will now be addressed.

1.3.1   Passive Immunotherapy

Passive immunotherapy is an umbrella term for a variety of treatment modalities, including tumor-targeting mAbs, immune adjuvants, cytokine therapy, immune-modulating mAbs, and

adoptive T cell therapy (116). Monoclonal antibody (mAb) therapy is the most widely used form of passive cancer immunotherapy. These mAbs target molecules preferentially expressed on the surface of tumor cells in an MHC-unrestricted manner. Several FDA-approved mAbs target proteins that are expressed by hematologic malignancies (i.e. leukemias and lymphomas), including CD52, CD33, and CD20. Solid tumors can also be treated by mAb therapy. FDA-approved mAbs against EGFR and HER2/*neu* expressed by tumors of epithelial origin are indicated for use in breast and colorectal cancers. Moreover, the vasculature of solid tumors can be targeted by anti-VEGF mAbs. Tumor-targeting mAbs can exert their effector function through several mechanisms, including signaling blockade, complement activation, and antibody-dependent cellular cytotoxicity, although the activity of each reagent is dependent on the Fc region of the antibody (116).

Systemic treatment with cytokines, including IL-2 and IFN-α, has been approved for clinical use. Although the exact anti-tumor function of these cytokines *in vivo* is unclear, severe adverse events are common and often dose limiting (116). Novel approaches to cytokine-based therapy include conditional cytokine expression by gene-engineered dendritic cells (117).

The primary goal of next-generation passive immunotherapies is to abrogate tumor-induced immunosuppression. As described above, blockade of the T cell inhibitory molecule CTLA-4 in a Phase III clinical trial improved overall survival of patients with metastatic melanoma (4). FDA approval of this reagent is expected within a year. Antibody-mediated blockade of PD-1, an additional T cell inhibitory molecule, has also demonstrated therapeutic benefit in early-phase clinical trials, but unlike anti-CTLA-4, only minor adverse events were reported upon PD-1 blockade (118). Moreover, Treg-depleting reagents, such as denileukin diftitox (Ontak), that target the constitutively-expressed molecule CD25, have been shown to

effectively eliminate circulating Tregs without coordinate depletion of activated, CD25-expressing T effector cells (119).

1.3.2   Active Immunotherapy

Active immunotherapy is defined as the *de novo* generation of tumor-specific immunity, mediated primarily through vaccination. Two prophylactic vaccines against virally-induced cancers have been approved by the FDA: i.) the HBV vaccine to prevent the development of hepatocellular carcinoma, and ii.) the HPV vaccine against cervical cancer, but also additional forms of genital epithelial tumors and some forms of head and neck cancer (116). However, most human cancers are non-viral in etiology and express patient-specific antigens. Prophylactic vaccination against these spontaneously-occurring cancers is therefore unrealistic. Instead, several therapeutic vaccination strategies have been developed, including purified peptide or protein vaccines, tumor cell vaccines, and DC vaccines (120).

As mentioned previously, the first cellular vaccine for cancer, sipuleucel-T (Provenge), was approved earlier this year and is indicated for castration-resistant prostate cancer. This product has been marketed as a DC vaccine, although it is actually a mixture of autologous lymphocytes and myeloid cells that are loaded *ex vivo* with a prostate-associated antigen and then re-infused into patients (3).

Whole tumor cell vaccines have the advantage of providing multiple tumor antigens Several types of these vaccines are currently in late-phase clinical development, including GVAX, which is comprised of cultured tumor cell lines (allogeneic), irradiated and engineered to secrete the DC growth-promoting cytokine GM-CSF (121). Finally, peptide-based vaccines, targeting TAAs such as MAGE-A3 and NY-ESO-1, may be the most cost-effective and least

labor-intensive of these vaccination strategies, but clinical benefit has been limited (116). Next-generation approaches may involve co-administration of adjuvants, including CpG oligodeoxynucleotides (TLR9 agonists), which are expected to enhance the immunogenicity of peptide vaccines (122).

1.4   COSTIMULATORY TNFR FAMILY

Costimulation is classically defined as the engagement of receptors secondary to T cell receptor (TCR) signaling that functions to lower the activation threshold of naïve T cells (123, 124). The primary costimulatory receptor on T cells is CD28, which upon binding of its ligands B7.1/CD80 or B7.2/CD86 initiates high-level IL-2 production and clonal T cell expansion. Additional costimulatory molecules, including members of the TNF receptor family, function subsequent to CD28 engagement to enhance the activation, survival, and differentiation of T effector and memory cells (5). Unlike CD28, which is constitutively expressed by T cells, TNFR costimulatory molecules, including 4-1BB/CD137, OX40/CD134, GITR, and CD30, are up-regulated shortly after activation and down-regulated soon thereafter. TNFR ligands are biologically active as trimers, which induce corresponding trimerization of their receptors upon binding. This has been observed for OX40 and GITR ligation in both mouse and human cells (5). Recently it was reported that murine GITR ligand (GITRL) may exert stronger activity when in a dimer conformation (125), while human GITRL can exist and signal effectively in multiple states of oligomerization (126), suggesting that structural diversity can exist among TNFR ligands. Upon ligand engagement, multiple TNF receptor-associated factor (TRAF) molecules are recruited to the intracellular domain of costimulatory TNF receptors and initiate JNK, p38, and

NF-κB signaling pathways (5). Alterations in signaling cascades elicited by various TNFR family members may be attributed to divergent affinities for TRAF proteins and the existence of at least six unique TRAF isoforms.

1.4.1   OX40

OX40 is restricted to naturally-occurring Treg and activated T effector cells (preferentially CD4$^+$), with expression typically peaking 48-72 hours after TCR engagement (5, 127, 128). Administration of agonist OX40 mAb enhances the primary clonal expansion of both CD4$^+$ and CD8$^+$ TCR transgenic T cells *in vivo* (129-131), perhaps due to the OX40-dependent down-regulation of the inhibitory costimulatory receptor CTLA-4 (132). While early studies suggested that OX40 ligation preferentially yielded Type-2 effector cytokine production by CD4$^+$ T cells, accumulating evidence now indicates that OX40/OX40L interactions enhance ongoing Type-1 or Type-2 responses and do not bias the functional polarity of CD4$^+$ T effector cells (5). Experimentally-induced CD4$^+$ T cell anergy can also be abrogated by OX40 engagement (133), and it has recently been reported that genetic mutations leading to OX40 over-expression predispose individuals to systemic lupus erythematosus (134), suggesting that OX40 ligation can potently reverse established T cell tolerance.

Costimulatory TNFR signaling is also thought to play a dominant role in T cell survival and the generation of memory following initial clonal expansion; this topic has been comprehensively discussed in recent reviews (5, 135). Consistent with this notion, the primary role of OX40 signaling appears to involve the extension of T cell survival following initial clonal expansion and differentiation into T cell memory. OX40-deficient CD4$^+$ and CD8$^+$ T cells undergo premature apoptosis *in vivo* (131, 136), while agonist mAb-mediated OX40

17

costimulation prolongs CD8$^+$ T cell survival that can be further augmented by co-treatments incorporating 4-1BB agonist mAb (137, 138). Furthermore, the lack of OX40 signaling impairs the maintenance of CD8$^+$ memory and CD4$^+$ T effector but not central memory T cells (139, 140). OX40/OX40L interactions may help to establish a "CD4 memory niche" involving the IL-7-dependent up-regulation of OX40 expression on CD4$^+$ T cells (135). Finally, the role of OX40 in both natural and inducible regulatory T cells (nTreg and iTreg, respectively) has recently received significant attention (141). OX40 signaling does not appear to play a significant role in the peripheral maintenance of nTreg, as similar numbers of these cells are observed in the peripheral tissues of OX40$^{-/-}$ and wild-type mice (142). OX40 ligation on nTreg can induce their proliferation, but it has not been conclusively demonstrated that these expanded nTreg retain their suppressor function. It does appear, however, that OX40 engagement may antagonize nTreg function in the absence of cell proliferation (142, 143). Naïve CD4$^+$CD25$^-$ T cells can also acquire regulatory activity upon culture with low dose antigen and TGF-β, for example (144). Recent reports suggest, however, that the induction of Foxp3 gene expression can be inhibited through OX40/OX40L interactions that may involve the manipulation of TGF-β signaling pathways (142, 144, 145). Alternatively, OX40 signaling may indirectly subvert Treg function by rendering T effector cells refractory to the action of Treg (143). Hence, OX40 appears to interface a number of divergent mechanisms that limit Treg-mediated immune suppression, including the prevention of iTreg generation, direct inhibition of nTreg function, and by conferring resistance of effector cells to Treg-dependent inhibition.

18

1.4.2 GITR

GITR and its human ortholog AITR are expressed on nTreg and activated B cells, macrophages, DC, NK cells, and effector T cells (5, 127, 146). On T effector cells, GITR is up-regulated earlier than OX40, peaking approximately 24 hours after T cell activation. Interestingly, it was recently shown that GITR expression is induced in Treg by a complex between Foxp3 and the transcription factor NFAT (147), whereas in activated T effector cells NFAT inhibits while NFκB induces GITR up-regulation (148), suggesting that distinct regulatory mechanisms control GITR expression in different cell subsets. Similar to OX40, GITR ligation enhances primary T cell expansion and effector cytokine secretion in the presence of low-dose antigen (149, 150). Likewise, GITR/GITRL interactions can reverse T cell tolerance via a Treg-independent mechanism, as depletion of CD25^{hi} Treg does not yield a similar phenotype (151). GITR engagement has also been reported to sustain the survival of activated T cells and to prevent activation-induced cell death (AICD) in wild-type versus GITR$^{-/-}$ T cells (152, 153). Moreover, IL-15 appears to be important for GITR-based maintenance of the CD8 memory pool in particular, as this cytokine induces GITR up-regulation and may contribute to a unique "CD8 memory niche" (135).

Despite accumulating evidence that GITR signaling directly augments the immune function of T effector cells, considerably more attention has been paid to investigating the impact of GITR on regulatory T cell activity. In this regard, only a limited role for GITR in the development, maintenance, and function of nTreg has been shown in GITR$^{-/-}$ mice (154). As with OX40, GITR ligation can induce the proliferation of both murine and human nTreg, but conflicting reports exist regarding the function of these expanded Treg (155-157). A recent study

by Wang and colleagues suggest that GITR engagement can prevent the conversion of naïve $CD4^+$ T cells into $Foxp3^+$ iTreg in the presence of TGF-β (158). Although GITR/GITRL interactions may contribute directly to the regulation of Treg subsets, elegant experiments from the Shevach group using combinations of wild-type or $GITR^{-/-}$ effector cell/Treg co-cultures indicate that effector T cells are the primary target of GITR costimulation (154, 159). While $GITR^{-/-}$ $CD4^+CD25^+$ Treg exhibit similar suppressive capacity as wild-type Treg, the proliferation of $GITR^{-/-}$ but not wild-type $CD4^+CD25^-$ effector T cells is inhibited upon stimulation with GITR agonist mAb, suggesting that GITR ligation renders effector T cells resistant to Treg-mediated suppression. Finally, although GITR is expressed by activated human NK cells, it is unclear whether GITR signaling mediates activating or inhibitory signals in these cells (160, 161), despite clear evidence that GITR stimulation enhances the proliferation and effector cytokine production of murine NKT cells *in vitro* and *in vivo* (162).

1.5   THERAPEUTIC COSTIMULATORY TNFR AGONISTS

The National Cancer Institute recently published a priority list of immunotherapy agents with anticipated anti-tumor potential, placing an emphasis on agents that are not commercially available or fully-developed for testing in humans at this time (7). Agonist antibodies targeting OX40 and GITR, a type of passive immunotherapy, were among the 20 agents emphasized from a list of over 100 novel modalities. Based on the aggregate conclusions from a large volume of murine tumor studies, described below, it is clear that TNFR-targeting therapeutics have tremendous potential to augment anti-tumor immunity and ultimately, the survival of cancer patients. Contrary to the severe adverse events reported from clinical trials of CD28 agonistic

and CTLA-4 blocking mAbs (163, 164), the efficacy of TNFR-based therapy has been consistently demonstrated in pre-clinical tumor models in the absence of pathologic inflammatory responses, likely attributable to the action of inducible rather than constitutively expressed TNF receptors on T cells (165).

1.5.1 OX40

Most mechanistic studies in murine tumor models have utilized depleting antibodies specific for various immune cell subsets and immunodeficient mice to define requisite cell types linked to drug impact. For example, a number of groups have reported that the therapeutic efficacy of OX40 agonists appears to rely heavily on $CD8^+$ T cells, as tumors rapidly progress upon depletion of this immune cell subset (166-172). $CD4^+$ T cells appear to play an even greater role in treatment outcomes associated with OX40-based therapy (166-170). Pan and colleagues reported that co-administration of agonist OX40 significantly enhances the tumor infiltration and *ex vivo* tumoricidal activity of $CD8^+$ T cells isolated from mice treated with anti-4-1BB and IL-12 gene therapy, while $CD4^+$ T cell depletion abrogates this effect (173). Moreover, a recent study using OVA-transduced tumors and adoptive transfer of OX40-stimulated OT1 (anti-OVA $CD8^+$) T cells suggests that the accumulation of Type-1, tumor-specific $CD8^+$ T cells in the tumor microenvironment is dependent on endogenous $CD4^+$ T cells, as $CD8^+$ TIL are absent in homologous models established in MHC Class II-deficient ($CD4^+$ T cell-deficient) mice (174). OX40-mediated signals thus appear to augment the helper function of $CD4^+$ T cells, thereby indirectly promoting the optimal effector function of anti-tumor $CD8^+$ T cells. However, this notion has not been universally observed in experimental models, since OX40-dependent, $CD8^+$ T cell-mediated therapeutic efficacy is preserved in $CD4^+$ T cell-deficient mice (131, 175). This

suggests that OX40-associated signals may directly result in the stimulation of CD8$^+$ T cells under such conditions, or that an alternative cell type may provide OX40-dependent "help" to developing CD8$^+$ T cells in the CD4-deficient host. Support for the latter was recently provided by Zaini and colleagues, who found that OX40-mediated therapy of B16 melanoma is abrogated in NKT cell-deficient mice (170). In this regard, it is important to note that although OX40 expression is thought to be restricted to T cells, 20% of OX40$^+$ TIL in this model exhibit an NKT cell phenotype. The authors propose that OX40L-transduced DC activate tumor-localized NKT cells to secrete IFN-γ, which acts to facilitate the priming of Type-1 T cells via DC maturation and functional "licensing" (176) or the direct differentiation of CD8$^+$ T effector cells (40, 177). Two additional recent studies suggest that OX40 agonists may abrogate tumor-induced immunosuppression by either preventing the conversion of naïve CD4$^+$ T cells into Foxp3$^+$ Treg (172), or by limiting the frequency and function of MDSC (178).

A variety of OX40-targeted modalities exist as potential therapeutic agents, including agonist antibodies, ligand-Fc fusion proteins (179), ligand-expressing viral vectors, and ligand-transduced DC or tumor cell vaccines (6). Weinberg and colleagues initially assessed the therapeutic efficacy of agonist OX40 mAb and recombinant OX40L-Fc fusion protein, concluding that when administered early after tumor inoculation (i.e. by day 3), overall tumor-free survival was significantly enhanced in model systems employing a range of tumor cell lines exhibiting variable inherent immunogenicities (180). Using a clinically-relevant model of tumor antigen tolerance, transgenic *neu*-N mice bearing established *neu*-expressing tumors were immunized with GM-CSF-transduced versions of the same tumor as a vaccine (175). Notably, enhanced survival of these mice could only be achieved when OX40 mAb was co-administered along with the vaccine.

A substantial literature exists regarding the expression of OX40 in cancer patients (180-182). For example, OX40 was found to be expressed by approximately 30% of TIL and draining lymph node cells in patients with head and neck squamous cell carcinoma (HNSCC) or melanoma (183). Furthermore, high levels of OX40 expression in the TIL of colorectal cancer or melanoma patients have been positively-correlated with prolonged patient survival (184, 185). Initial screening of an agonist OX40 mAb of murine origin in nonhuman primates revealed no overt toxicities despite its potent immunostimulatory properties, i.e. the induction of long-lived anti-SIV humoral and T cell responses (186). In addition, a recombinant human OX40L-Fc fusion protein has recently been developed that appears capable of stimulating peripheral blood T cells in a manner comparable to that noted for agonist mAb (187). A phase I dose escalation trial was recently conducted with the murine antibody administered within a five day window (188). An extended treatment period was unfeasible due to the generation of human anti-murine immunity (i.e. HAMA responses). Although none of the treated patients exhibited tumor regression that met the criteria for partial response, 2- to 4-fold increases in $CD4^+Foxp3^-$ and $CD8^+$ T cells, as well as NK cells, were observed in the peripheral blood of these patients, demonstrating for the first time that OX40-based therapy can augment the adaptive immune response in humans.

1.5.2   GITR

Because GITR was characterized more recently than OX40, it is not surprising that substantially less data exists regarding the functional mechanisms and therapeutic efficacy of GITR agonists in pre-clinical tumor models (159). Ramirez-Montagut *et al.* showed that GITR-mediated tumor rejection is abrogated upon depletion of $CD4^+$, $CD8^+$, and $NK1.1^+$ cell subsets and in mice

23

deficient in expression of IFN-γ and FasL (189), consistent with results reported by other groups using different tumor models (190-192). Treatment of progressing CT26 colon carcinomas with agonist GITR mAb led to increased numbers of activated CD4$^+$ T cells, CD8$^+$ T cells, and NK cells in the tumor-draining lymph nodes (191). However, this effect was abrogated when CD4$^+$ T cells were depleted prior to treatment, indicating that CD4$^+$ T cells play an indispensable role in the GITR-dependent priming of therapeutic anti-tumor CD8$^+$ T cells and NK cells. Not unexpectedly, increased numbers of Foxp3$^+$ Treg are observed in the spleen and tumor-draining lymph nodes of GITR-treated mice (189, 191), yet despite the ability of these Treg to secrete IL-10, responder anti-tumor CD4$^+$CD25$^-$ T cells in these animals appear refractory to Treg-mediated suppression (191). This observation is likely due to the direct costimulatory effect of GITR ligation on CD4$^+$ T effector cells, rather than via the abrogation of Treg function (154). Further support for this conclusion is provided by studies performed by Ramirez-Montagut and colleagues, who reported that GITR-mediated tumor rejection is enhanced by CD25 depletion, indicating that the abrogation of Treg function is not the primary mechanism of GITR-based therapy (189). Thus, despite the availability of only a limited data set, GITR agonists appear to foster anti-tumor immunity *in vivo* by primarily targeting fully-differentiated CD8$^+$ T cells and by augmenting the ability of CD4$^+$ T helper cells to activate secondary waves of tumoricidal T cells.

The agonist GITR mAb, clone DTA-1, has been the most common GITR-stimulating reagent utilized in murine tumor models to date (6). BALB/c mice treated with DTA-1 within 8 days of syngeneic MethA fibrosarcoma inoculation rapidly reject their tumors and exhibit specific resistance to tumor re-challenge (190). GITRL-Fc fusion proteins have also demonstrated potent agonist activity in Colon 26 (colorectal carcinoma) and RENCA (renal

carcinoma) models (192). Similarly, intratumoral injection of recombinant adenovirus encoding GITRL leads to significant inhibition of poorly-immunogenic B16 melanoma growth in C57BL/6 mice (193).

Recent reports suggest that human tumors are enriched in CD4^{+} TIL expressing a CD25^{hi}Foxp3^{+} phenotype, consistent with Treg cells (194). Such Treg also express GITR and exhibit strong suppressor function *ex vivo*, mediated primarily through IL-10 and TGF-β, while Treg in the peripheral blood of patients do not express GITR and exhibit minimal suppressor activity (194). Tumor-localized GITR[+] Treg may thus be more sensitive to GITR ligation than circulating Treg. One mechanism that tumor cells employ to evade immune-mediated destruction is the down-regulation or "shedding" of costimulatory receptors and the subsequent induction of tumor-specific T cell anergy (195, 196). In fact, soluble tumor-shed GITRL has been reported in the sera of patients with various malignancies but not healthy controls (197, 198), where it is has been shown to blunt the function of NK cells (198, 199). However, GITR engagement activates human T lymphocytes *in vitro* (126), suggesting that GITRL signals may only be inhibitory to NK cell-mediated, rather than T cell-mediated anti-tumor immunity. While clinical-grade GITR agonists are in their early stages of development, a fully humanized agonist GITR mAb, TRX518, has recently been developed by Tolerx Inc. (Cambridge, MA, USA). Initial characterization studies indicate that TRX518 is agonistic for human PBMC *in vitro* and that it fails to bind Fc receptors, thus limiting the theoretical likelihood of antibody- or complement-mediated deletion of GITR^{+} cells *in vivo* (200).

1.6   STATEMENT OF THE PROBLEM

Despite the induction of potent anti-tumor immunity by certain immunotherapy regimens in murine tumor models, the results of large, randomized trials of these therapies have generally been disappointing (i.e. low objective clinical response rates) (201). One key factor involved in these high clinical attrition rates is the use of poorly predictive animal models. Although transplantable murine tumors are widely used for experimental immunotherapy studies, most treatments are initiated within the first week following tumor inoculation and appear to induce immune-based tumor rejection (202). However, when these same therapies were administered to mice bearing established tumors (i.e. day 10 post-tumor inoculation), therapeutic benefit was completely abolished (202). In order to maximize the likelihood that our results would have some predictive value for efficacy in patients, a primary objective of our study was to test the efficacy of our costimulatory therapies in the setting of well-established tumors.

The anti-tumor efficacy of agonistic mAbs towards OX40 and GITR has already been widely explored in numerous murine tumor models (6). However, recombinant TNFR ligand-Fc fusion proteins serve as an attractive alternative to agonist antibodies, given the comparable or in some cases enhanced degree of efficacy observed for ligand-Fc reagents and agonist antibodies in mouse models (171, 192). Due to their lower avidity and bioavailability, ligand-Fc fusion proteins may also represent a safer alternative to costimulatory agonist antibodies, which can elicit significant collateral toxicity (203). Our initial aim, therefore, was to assess the relative therapeutic efficacy of OX40L-Fc and GITRL-Fc reagents in the well-established disease setting.

Although T cell costimulatory agonists targeting OX40 and GITR are currently being evaluated in early-phase clinical trials, the mechanism(s) through which such reagents function remain controversial, particularly for advanced-stage disease. This problem is considerable, as

the rational design of combinational therapies is unfeasible without knowledge of the mechanistic activity of these reagents. For example, combination of two therapies with overlapping mechanisms would result in a lack of synergistic benefit (in addition to the waste of resources and unnecessary burden to patients and clinical personnel). Through a longitudinal analysis of treatment-induced alterations in both the tumor-draining lymph node and the tumor microenvironment, we were able to identify the molecular and cellular alterations associated with the anti-tumor efficacy of therapies based on the use of OX40L-Fc and GITRL-Fc reagents.

2.0 A THERAPEUTIC OX40 AGONIST DYNAMICALLY ALTERS DENDRITIC, ENDOTHELIAL AND T CELL SUBSETS WITHIN THE ESTABLISHED TUMOR MICROENVIRONMENT

Angela D. Pardee[1], Dustin McCurry[1], Sean Alber[2], Peisheng Hu[3],

Alan L. Epstein[3] and Walter J. Storkus[1,4,5]

From the Departments of [1]Immunology, [2]Cell Biology and Physiology and [4]Dermatology, University of Pittsburgh School of Medicine, Pittsburgh, PA 15213, and the [3]Department of Pathology, Keck School of Medicine, University of Southern California, Los Angeles, CA 90033, and the [5]University of Pittsburgh Cancer Institute, Pittsburgh, PA 15213.

2.1   ABSTRACT

Little preclinical modeling currently exists to support the use of OX40 agonists as therapeutic agents in the setting of advanced cancers, as well as, the mechanisms through which therapeutic efficacy is achieved. We demonstrate that treatment of mice bearing well-established day 17 sarcomas with a novel OX40 ligand-Fc fusion protein (OX40L-Fc) resulted in tumor regression or dormancy in the majority of treated animals. Unexpectedly, dendritic cells (DC) in the progressive tumor microenvironment (TME) acquire OX40 expression and bind fluorescently-labeled OX40L-Fc. Furthermore, longitudinal analyses revealed that DC become enriched in the tumor-draining lymph node (TDLN) of both wild-type and Rag$^{-/-}$ mice within three days after OX40L-Fc treatment. By day 7 after treatment, a significant expansion of CXCR3^{+} T effector cells was noted in the TDLN, and by day 10 post-treatment, Type-1 polarized T cells exhibiting a re-activated memory phenotype had accumulated in the tumors. High levels of CXCL9 (a CXCR3 ligand) and enhanced expression of VCAM-1 by vascular endothelial cells (VEC) were observed in the TME early after treatment with OX40L-Fc. Notably, these vascular alterations were maintained in Rag$^{-/-}$ mice, indicating that the OX40L-Fc-mediated activation of both DC and VEC occur in a T cell-independent manner. Collectively, these findings support a paradigm in which the stimulation of DC, T cells and the tumor vasculature by an OX40 agonist dynamically orchestrates the activation, expansion and recruitment of therapeutic T cells into established tumors.

2.2 INTRODUCTION

As tumors develop and progress, a number of regulatory mechanisms are responsible for maintaining immune tolerance in the tumor microenvironment (TME). Poor tumor homing and penetration of T effector cells, a consequence of aberrant vasculature and limited chemokine and adhesion molecule expression in the TME (113, 204), is one major barrier to anti-tumor immunity (15). Furthermore, tumor-specific T cells that effectively infiltrate tumors may be rendered inactive by soluble factors and inhibitory signals associated with tumor cells and through the negative impact of both myeloid- and lymphoid-derived suppressor cells (2, 205). While systemic immunity may be affected to a variable degree, immune suppression is typically most profound within the TME, with tumor-infiltrating lymphocytes (TIL) exhibiting severe deficiencies in $CD8^+$ T cell-mediated cytotoxic function (206). In murine tumor models, TIL dysfunction becomes pronounced only at later stages of solid tumor growth, at which point a mature tumor stroma comprised of both bone marrow- and non-bone marrow-derived cells has been established (56, 207).

Given the perceived importance of T cell-mediated immunity underlying effective immunotherapy (41) and better clinical outcome (15), substantial emphasis has recently been placed on the development of treatment modalities that are capable of restoring T cell function and enhancing tumor penetration in the tumor-bearing host. In particular, immune-stimulating agents that target the costimulatory TNF receptor (TNFR) family member OX40, have demonstrated anti-tumor efficacy in pre-clinical models (165). Costimulatory members of the TNFR family are up-regulated shortly after TCR engagement on naïve and antigen-experienced cells, where they serve as key modulators of cell activation, survival, and differentiation (5, 135). OX40 is expressed by activated T effector cells and OX40-mediated signals provided during

priming regulate CD4$^+$ and CD8$^+$ T cell activation and clonal expansion *in vivo* (129, 131, 143).

Furthermore, anergic or hypo-responsive OX40$^+$ T cells may be re-activated by OX40 agonists

(133). OX40 is also constitutively expressed by CD4$^+$Foxp3$^+$ regulatory T cells (Treg) (127).

Indeed, recent studies have demonstrated that agonist signaling through OX40 inhibits the

suppressor function of natural Foxp3$^+$ Treg (208), prevents the induction of Treg from CD4$^+$ T

effector cells (144), and confers resistance to effector cells against Treg-mediated inhibition

(143).

To characterize the molecular, cellular, and treatment-associated consequences of OX40

engagement in the setting of well-established tumors, a novel agonistic reagent directed against

murine OX40 (OX40 ligand-Fc fusion protein; OX40L-Fc) was recently constructed and

characterized *in vitro* (171). We observed that the progressive growth of well-established day 17

sarcomas was inhibited by a short course of OX40L-Fc therapy, with complete tumor regression

or extended disease stabilization (i.e. tumor dormancy) observed in the majority of treated

animals. Comparable findings were obtained in both the MCA205 (H-2^b) and CMS4 (H-2^d)

sarcoma models. We noted that i.p. injection of OX40L-Fc induced significant expansion of T

effector cells in the TDLN, resulting in the accumulation of activated, Type-1 polarized T cells

in the TME within 10 days of initiating OX40L-Fc therapy. Moreover, our therapy appeared to

dynamically affect DC and vascular endothelial cells (VEC) in both wild-type and Rag$^{-/-}$ mice

bearing well-established tumors. The extensive molecular and cellular alterations observed in

this model strongly support the translation of OX40 agonists into human clinical trials, either as

single agents or in the context of combinational immunotherapy (6).

2.3   MATERIALS AND METHODS

Mice. Six to ten week old female C57BL/6 (H-2^b), B6.129S7-Rag1^{tm1Mom} (Rag$^{-/-}$; H-2^b) and BALB/cJ (H-2^d) mice were purchased from The Jackson Laboratory and maintained in the pathogen-free animal facility in the Biomedical Sciences Tower at the University of Pittsburgh. All animal work was done in accordance with a protocol approved by the Institutional Animal Care and Use Committee.

Tumor Establishment. The MCA205 (H-2^b) sarcoma cell line was purchased from the American Type Culture Collection (ATCC). The CMS4 (H-2^d) sarcoma has been described in detail previously (209). Cell lines were cultured in complete media (CM; RPMI-1640 supplemented with 100 U/ml penicillin, 100 μg/ml streptomycin, 10 mM L-glutamine and 10% heat-inactivated fetal bovine serum (all reagents from Life Technologies) in a humidified incubator at 37° C and 5% CO_2. All cell lines were negative for known mouse pathogens. Tumors were established by injection of 5 x 10^5 tumor cells s.c. into the right flanks of syngeneic mice, with tumor size assessed every 3 to 4 days and recorded in mm^2. Mice were sacrificed when tumors became ulcerated or reached a maximum size of 400 mm^2.

Costimulatory Therapy. Tumor-bearing mice were injected i.p. with 100 μg of OX40L-Fc or rat IgG isotype control antibody (Sigma-Aldrich) in a total volume of 100 μl PBS on days 17 and 20 post-tumor inoculation when tumors were approximately 30-50 mm^2 in size. The mOX40L-Fc fusion protein has been previously described (171).

Isolation of Tumor, LN and Spleen cells. Single cell suspensions were obtained from TDLN as previously described (209). For TIL, tumors were enzymatically digested with 0.1% w/v collagenase, 1% w/v hyaluronidase, and 0.1% w/v DNase (all from Sigma), with

lymphocytes isolated as buoyant cells after discontinuous density centrifugation as previously described (210).

   In Vitro Stimulation (IVS) of T cells. Bulk TIL (*n* = 1 per group) were restimulated *in vitro* with irradiated (100 Gy) MCA205 cells for 5 days at a T cell-to-tumor ratio of 10:1 in CM with 20 U/ml recombinant human IL-2. Recovered T cells were then cultured in media alone (to determine background cytokine levels) or with 5μg/ml anti-CD3 (BioLegend) for 72 hours. Cell-free supernatants were then harvested and assessed for levels of mIFN-γ using a specific OptEIA ELISA set (BD Biosciences) according to the manufacturer's instructions with a lower limit of detection of 32.5 pg/ml. Data are reported as the mean ± SD of duplicate determinations.

   RT-PCR. Total RNA was isolated from TIL on days 3, 7, and 10 after the initial treatment (day 17 post-tumor inoculation), as indicated, using RNeasy Micro kit (Qiagen), according to the manufacturer's instructions. For semi-quantitative RT-PCR, TIL were cultured with 5 μg/ml anti-CD3 (BioLegend) for 24 hours, followed by RNA isolation and cDNA preparation using random hexamer primers (Applied Biosciences). PCR was performed using the following primer pairs: β-actin (forward), 5'-GGCATCGTGATGGACTCCG-3'; β-actin (reverse), 5'-GCTGGAAGGTGGACAGCGA-3'; IFN-γ (forward), 5'-GAAAGCCTAGAAAGTCTGAATAAC-3'; IFN-γ (reverse), 5'-ATCAGCAGCGACTCCTTTTCCGCT-3'; IL-10 (forward), 5'-AGTGGAGCAGGTGAAGAGTGATT-3'; IL-10 (reverse), 5'-TCATGTATGCTTCTATGCAGTTGATG-3'; T-bet (forward), 5'-AACCAGCACCAGACAGAGATG-3'; T-bet (reverse), 5'-TAGAAGAGGTGAGAAGGGGTC-3'; Foxp3 (forward), 5'-GGCCCTTCTCCAGGACAGA-3'; Foxp3 (reverse), 5'-GCTGATCATGGCTGGGTTGT-3'. Cycling times and temperature

33

were as follows: initial denaturation at 94°C for 2 min (1 cycle), denaturation at 94°C for 30 s, annealing at 60-65°C for 30 s and elongation at 72°C for 1 min (35-40 cycles), final extension at 72°C for 5 min (1 cycle). Following gel electrophoresis, PCR products were imaged and band density quantified using LabWorks Software (PerkinElmer). For quantitative RT-PCR, reverse transcription and PCR amplification was performed by the University of Pittsburgh's Genomics and Proteomics Core Laboratories (a shared resource). For quantitative analysis of T-bet, IFN-γ, and control β-actin, previously published primer pairs were used (211), and cDNA was amplified using SYBR® Green PCR Master Mix (Applied Biosystems). For quantitative analysis of Foxp3, IL-10, and control β-actin, RT^2 qPCR Primer Assays (SABiosciences) were used and cDNA was amplified using RT^2 SYBR Green qPCR Master Mix (SABiosciences). For each sample, the cycle threshold (Ct) values for β-actin gene were determined for normalization purposes and the ΔCt between β-actin and T-bet, Foxp3, IFN-γ and IL-10 were calculated. ΔΔCt were calculated to isotype treatment samples. Relative RNA expression for each gene is depicted as $2^{ΔΔCt}$.

Confocal Immunofluorescence Staining and Imaging. Tumor tissue was processed and sectioned as previously reported (209), followed by immunofluorescence staining and confocal microscopy. The following primary antibodies were used for staining sections: rat anti-mouse CD31 (BD Biosciences), goat anti-mouse OX40 (Santa Cruz Biotechnology), rat anti-mouse OX40 (eBioscience), hamster anti-mouse CD11c (BD Biosciences), rat anti-mouse VCAM-1 (Santa Cruz Biotechnology), and goat anti-mouse CXCL9 (R&D Systems). The following secondary antibodies were used: donkey anti-rat Alexa Fluor 488 (Molecular Probes), donkey anti-goat Cy3 (Jackson ImmunoResearch), donkey anti-hamster Alexa Fluor 488 (Molecular Probes), donkey anti-rat Cy3 (Jackson ImmunoResearch), goat anti-rat Fab1 fragment Cy3

34

(Jackson ImmunoResearch), and goat anti-rat Alexa Fluor 488 (Molecular Probes). All sections were briefly incubated with DAPI (Sigma) and then mounted. Images were acquired using an Olympus Fluoview 1000 confocal microscope (Olympus). Isotype control and specific antibody images were taken using the same level of exposure on the channel settings.

Flow Cytometry. Before all stainings, cells were Fc-blocked with anti-CD16/CD32 (BD). Single-cell suspensions were stained using the following antibodies: PerCP- and PE-conjugated CD4 and CD8, PE-conjugated Gr-1, FITC-conjugated CD80 and CD25, and PerCP-Cy5.5-conjugated Ki67 (all BD), FITC-conjugated CD27, Class II and F4/80, PE-conjugated CCR7 and OX40, and APC-conjugated CD11c, CD44, CXCR3, and CD11b (all eBioscience) or appropriate-matched, fluorochrome-labeled isotype control mAb. For Foxp3 intracellular staining, $CD4^+$ T cells were surface stained as described above and then further processed using an APC anti-mouse/rat Foxp3 Staining kit (eBioscience) according to the manufacturer's instructions. FITC-conjugation of OX40L-Fc was performed using a FITC protein labeling kit (Molecular Probes). Cells were analyzed using an LSR II flow cytometer (Beckman Coulter), with corollary data assessed using FlowJo software (version 7.6.1; Tree Star, Inc.).

Statistical Analysis. All comparisons of inter-group means were performed using a two-tailed Student's *t* test, with *P* values < 0.05 considered significant.

2.4   RESULTS

2.4.1   OX40L-Fc treatment elicits potent anti-tumor activity against well-established tumors.

A novel OX40 agonist, consisting of mOX40L linked to the C-terminus of the Fc fragment of immunoglobulin, was recently constructed and shown to be curative in early day 5 (H-2^d) Colon 26 and RENCA tumor models (171). In contrast, an agonist anti-OX40 (OX86) mAb was only able to extend median survival by approximately 2 weeks in these models. To determine whether OX40L-Fc would be efficacious in a more established and potentially clinically-relevant disease model, we treated H-2^b mice bearing day 17 MCA205 sarcomas via i.p. injection of 100 μg of OX40L-Fc or control rat IgG. A second identical dose was provided three days later. Tumors in all control-treated mice grew progressively and exhibited a rapid expansion in size around day 30 post-inoculation, necessitating euthanasia by day 40 (Figure 1A). In contrast, OX40L-Fc-treated mice exhibited reduced, stabilized tumor size by day 27 that was durable through day 40. Although OX40L-Fc treatment resulted in the long-term survival of only 13% of treated animals (Figure 1B), 50% of this cohort exhibited small (~20-40 mm^2) lesions that remained "dormant" for more than 6 weeks, before eventually progressing. Growth of representative tumors exhibiting dormancy in OX40L-Fc-treated mice is shown in Figure 1C.
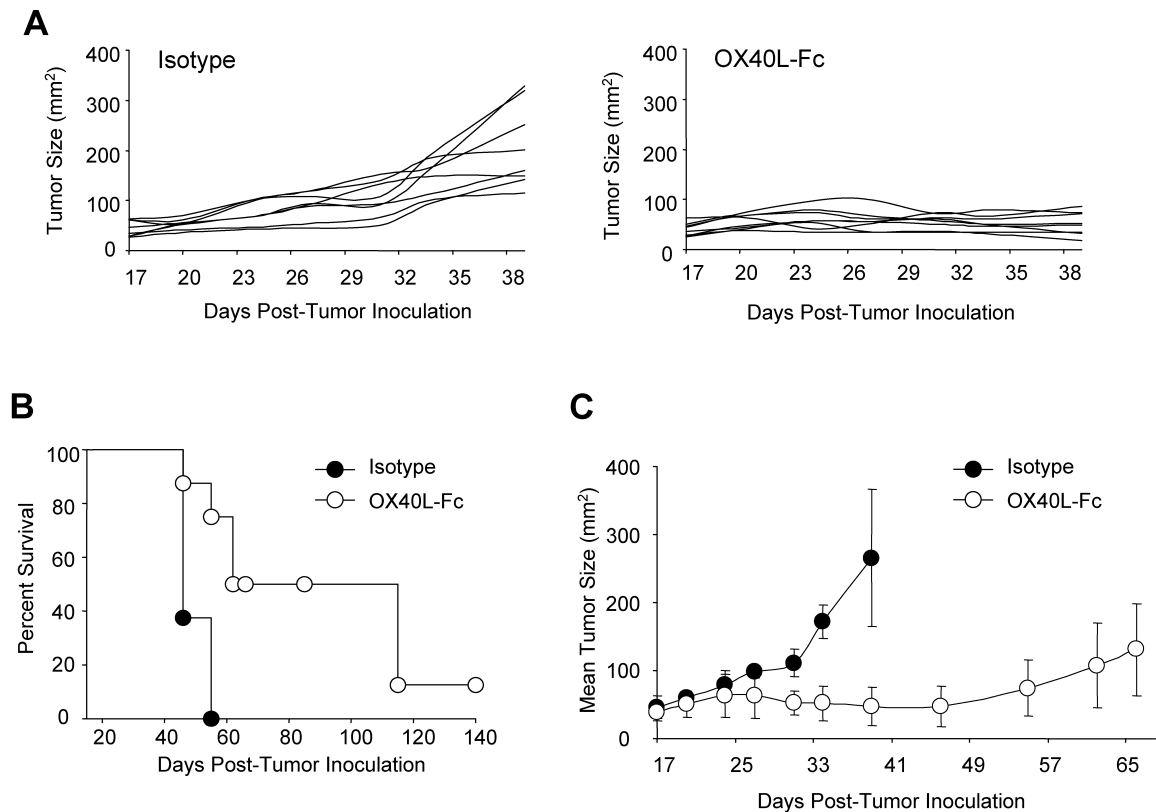
Figure 1. Systemic OX40L-Fc treatment is therapeutic against well-established tumors in wild-type mice.

(A) MCA205 sarcomas (*n* = 8 per group) were injected s.c. into the right flank of C57BL/6 wild-type mice. Mice bearing established day 17 tumors (~30 to 50 mm^2 in area) were treated i.p. with 100 μg of rat IgG isotype control mAb or OX40L-Fc, as indicated. Treatment was repeated on day 20 after tumor inoculation. Tumor areas (mm^2) were calculated every 3 days, with the data for individual animals reported. (B) Data from Figure 1A are presented in a Kaplan-Meier plot. (C) Mean tumor areas ± SD are shown for representative OX40L-Fc-treated mice exhibiting tumor dormancy (*n* = 3), with data obtained from isotype-treated control animals (*n* = 3) shown for comparison. Data are representative of two independent experiments performed.

Similar therapeutic benefits were observed in the CMS4 (H-2^d) sarcoma model, where over 80% of animals rejected their tumors after OX40L-Fc treatment on days 17 and 20 (Appendix Figure 1). Despite the superior efficacy observed for OX40L-Fc in the CMS4 model,

all remaining data were collected in the MCA205 tumor model due to the tendency of progressor CMS4 tumors to ulcerate, necessitating pre-mature euthanasia per IACUC regulations.

2.4.2   T cell and DC expression of OX40 is elevated in the progressor TME.

To identify the *in situ* cellular targets of OX40L-Fc-based therapy, we next assessed OX40 expression on T cell subsets within the TDLN and the TME of untreated MCA205 tumor-bearing mice between days 17 and 20 post-tumor inoculation. While OX40 was barely detectable on $CD4^+Foxp3^-$ and $CD8^+$ T cells in the TDLN, approximately 50% of $CD4^+Foxp3^+$ T cells expressed OX40 (Figure 2A), consistent with previous reports indicating that OX40 expression is restricted to the regulatory subset of resting T cells in peripheral tissues (143). Conversely, OX40 expression was up-regulated on all T cell subsets in the untreated TME, including a median of over 20% of $CD8^+$ T cells and over 60% of $CD4^+Foxp3^-$ T cells.

Because NK and NKT cells can express OX40 under certain conditions (170, 212), we hypothesized that non-T cell subsets may also represent targets for interaction with OX40L-Fc in the progressor TME. Indeed, OX40 expression was highly up-regulated on $CD11c^+CD11b^+ClassII^{hi}$ tumor-infiltrating DC (TIDC) when compared to TDLN-localized DC (median of 37.6% vs. 2.3% $OX40^+$, respectively; Figure 2B). OX40 was also detected on TIDC via confocal immunofluorescence microscopy (Figure 2C). Furthermore, FITC-labeled OX40L-Fc was found to bind to TIDC, but not to TDLN-localized DC (Figure 2D). These data suggest that although $CD4^+Foxp3^+$ T cells may represent the exclusive expressors of OX40 in the periphery, $CD4^+Foxp3^-$ and $CD8^+$ T effector cells, as well as DC, contain substantial $OX40^+$ populations in the TME, making each of these cell types plausible targets of OX40L-Fc-based therapy.
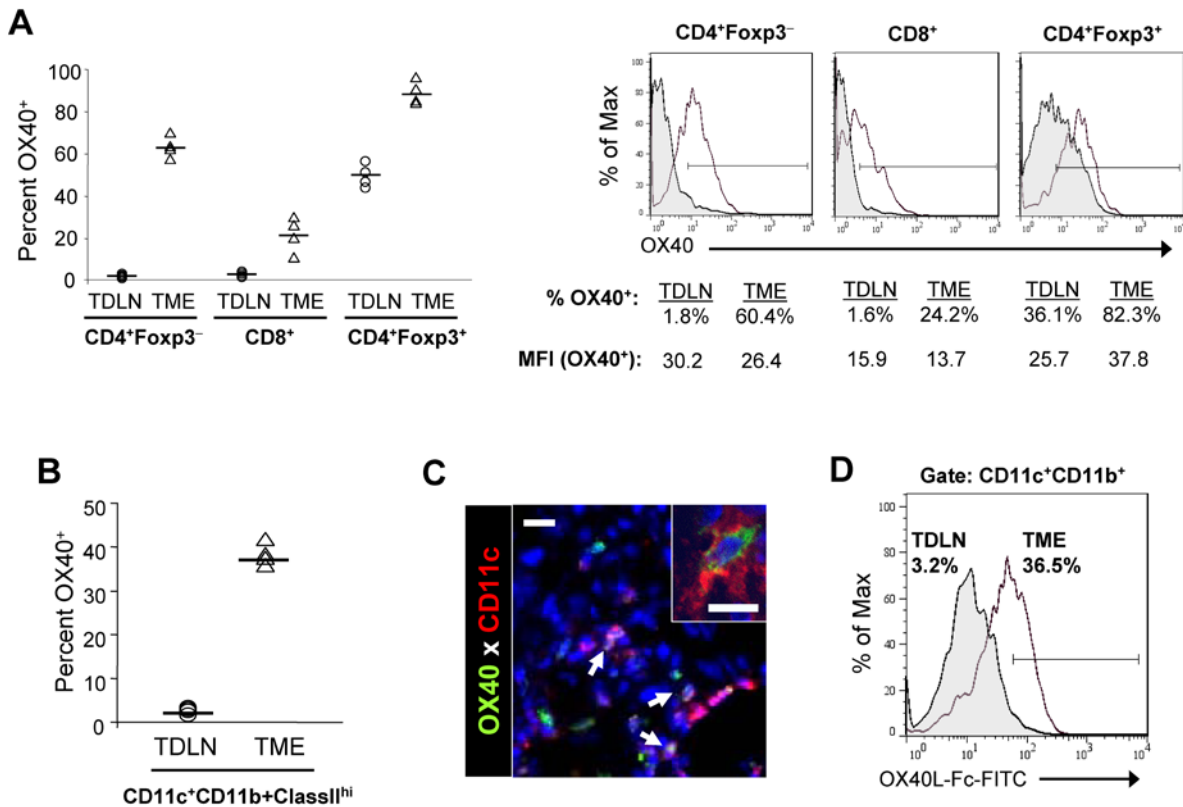
Figure 2. T cell and DC expression of OX40 is elevated in the progressive TME in wild-type mice.

(A and B) Single-cell suspensions ($n = 4$) were prepared from untreated MCA205 tumors (TME) and tumor-draining lymph nodes (TDLN) isolated between days 17 and 20 post-tumor inoculation. (A) Percentages of OX40$^+$ T cells among the indicated gated cell populations are shown (left panel). Each symbol corresponds to an individual tumor-bearing mouse (bar = median value). Representative histograms are depicted (right panel), with percentages of OX40$^+$ T cells and mean fluorescence intensity (MFI) of OX40$^+$ T cells indicated. Filled histograms represent cells isolated from the TDLN; open histograms represent cells isolated from the TME. (B) Percentages of DC (CD11c$^+$CD11b$^+$ClassII^{hi}) expressing OX40 in the TDLN and TME are reported (bar = median value). (C) Untreated MCA205 tumors were isolated between days 17 and 20 post-tumor inoculation, then sectioned, stained and analyzed by confocal fluorescence microscopy as described in Materials and Methods. Representative staining of DAPI (blue), OX40 (green) and CD11c (red) is shown, with arrows indicating CD11c$^+$OX40$^+$ cells. Inset reflects higher power (60x magnification) image. Bars, 10 μm. (D) Representative staining of gated CD11c$^+$CD11b$^+$ DC

with FITC-labeled OX40L-Fc. Filled histogram represents cells isolated from the TDLN; open histogram represents cells isolated from the TME. Experiments were repeated two times with similar results obtained in each instance.

2.4.3 T cell-independent enrichment of mature DC expressing the LN-homing receptor CCR7 in the TDLN shortly after treatment with OX40L-Fc.

Given the observed high levels of OX40 expressed by TIDC in untreated tumor-bearing mice, we next evaluated how DC populations were altered in response to OX40L-Fc treatment. By day 3 after the first OX40L-Fc treatment, TIDC expression of the costimulatory molecules CD80 and CD86 was augmented (data not shown), and a concordant increase in $CD11c^+CD11b^+$ DC within the TDLN was observed when compared to isotype mAb-treated control mice (Figure 3A). These TDLN DC populations expressed elevated levels of CD80 and the lymph node-homing chemokine receptor CCR7 when compared to TDLN isolated from isotype mAb-treated control animals (Appendix Figure 2). Moreover, enrichment of DC upon OX40L-Fc treatment was similarly observed in the TDLN of $Rag^{-/-}$ mice bearing established MCA205 tumors (Figure 3B). These data are consistent with the T cell-independent activation/maturation of $OX40^+$ TIDC to become competent for trafficking to the TDLN within the initial 3 days of OX40L-Fc-based therapy. Longitudinal analysis suggests that treatment-induced migration of TIDC to the TDLN persists through day 7 of the therapy period, with a return to control conditions by day 10 (data not shown). Such trafficking of activated DC would be anticipated to sponsor the cross-priming of anti-tumor T cell responses in the TDLN. We observed no substantial alterations, however, in DC frequency or phenotype in non-TDLN (data not shown).
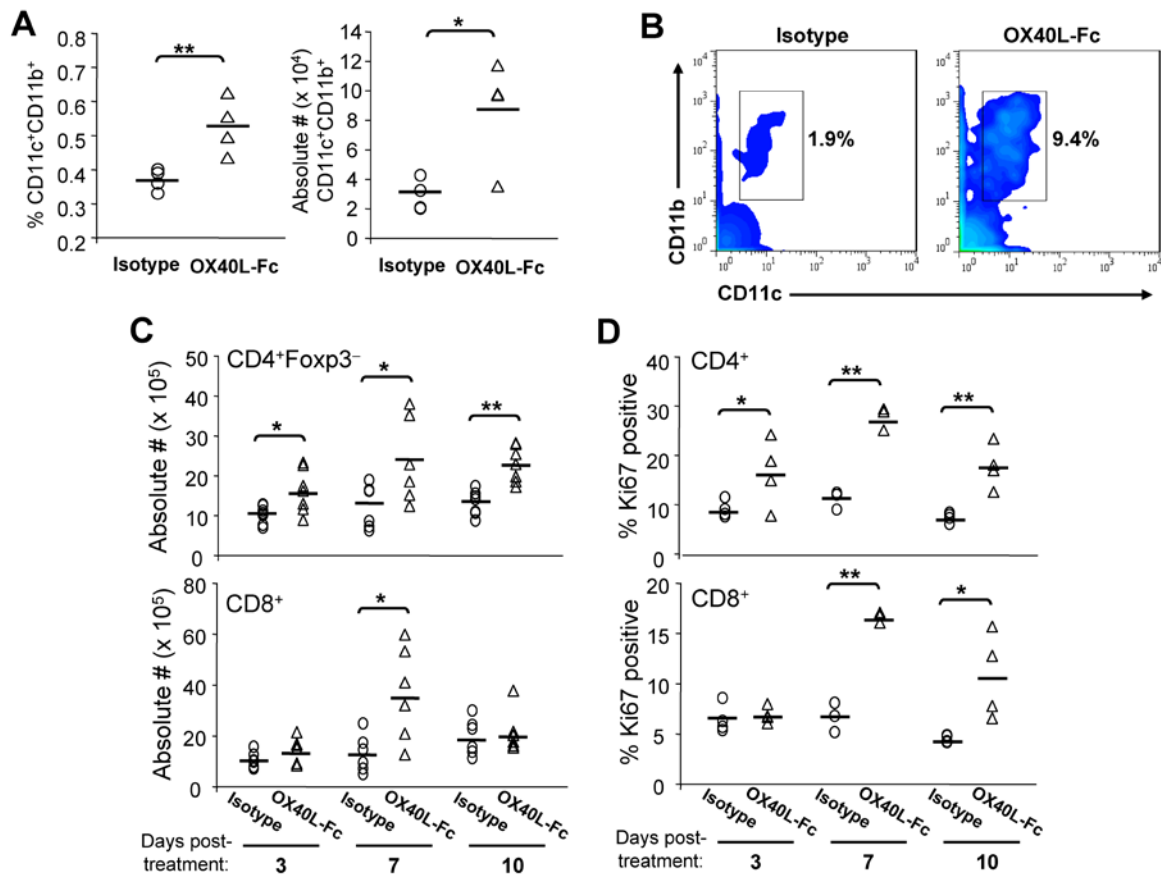
Figure 3. Longitudinal analysis of TDLN populations following OX40L-Fc treatment.

MCA205 tumor-bearing wild-type or Rag$^{-/-}$ mice were treated as in Figure 1 and TDLN cells were isolated on day 3 after treatment with isotype control antibody or OX40L-Fc ($n = 4$ per group). In A, the percentages and absolute numbers (x 10^4) of CD11c$^+$CD11b$^+$ DC among gated live cells are shown for wild-type mice. Each symbol corresponds to an individual animal. The solid line represents the median value. In B, a representative density plot is shown, with percentages indicated for CD11c$^+$CD11b$^+$ DC among total TDLN cells isolated from Rag$^{-/-}$ mice. For panels C and D, TDLN cells were isolated from wild-type mice on days 3, 7, and 10 after treatment. Graphs show absolute numbers (x 10^5) of CD4$^+$Foxp3$^-$ and CD8$^+$ T cells (C) and the percentages of Ki67$^+$ T cells (D). Data are representative of results obtained in 2 independent experiments in each case. *, $P < 0.05$; **, $P < 0.01$.

2.4.4 OX40L-Fc treatment promotes the expansion of TDLN T cells expressing the tissue-homing Type-1 chemokine receptor CXCR3.

To assess alterations in the TDLN T cell compartment following OX40L-Fc treatment and TIDC trafficking to the TDLN, we harvested TDLN from mice on days 3, 7, and 10 after initiating treatment and determined absolute numbers of $CD4^+Foxp3^-$ and $CD8^+$ T effector cells. Time-dependent increases in both T cell sub-populations were noted as a consequence of OX40L-Fc treatment, with numbers of TDLN T cells peaking at day 7 post-treatment (Figure 3C). Indeed, 7 days after initiating OX40L-Fc treatment, highly significant up-regulation in expression of the proliferation marker Ki67 was observed for both $CD4^+$ and $CD8^+$ T cell subsets within the TDLN ($P < 0.01$; Figure 3D). Although these T cells did not exhibit any alterations in activation marker expression (CD25 and CD69; data not shown), both $CD4^+$ and $CD8^+$ T cells expanded from OX40L-Fc-treated versus control mAb-treated mice were enriched in the $CD44^{hi}$ phenotype at day 7 post-treatment (Appendix Figure 3A), supporting the ability of OX40L-Fc therapy to preferentially stimulate memory T cells.

It has recently been demonstrated that Type-1 polarized $CD8^+$ T cells are effectively recruited to tumor sites via CXCR3-mediated chemotaxis in response to the CXCL9-11 chemokines produced within the TME (33). To determine whether TDLN T cells in OX40L-Fc-treated animals are differentially competent to migrate to the TME based on this index, we assessed $CD4^+$ and $CD8^+$ T cells for their expression of CXCR3 7 days after the initiation of therapy. As shown in Appendix Figure 3B, we found that the $CXCR3^+$ sub-population of $CD4^+$ and $CD8^+$ T cells was increased after OX40L-Fc versus control mAb treatment. These data suggest that OX40 agonist therapy not only stimulates expansion of TDLN T cells, but also

licenses these cells for trafficking to peripheral tissue sites in which CXCR3 ligands are expressed, such as the TME.

2.4.5   Tumors become enriched in T effector cells by day 10 following OX40L-Fc treatment.

Based on our observation that maximal numbers of CXCR3$^+$ TDLN T cells occurred by day 7 after OX40L-Fc treatment, we hypothesized that these transport-competent T cells might then infiltrate the TME shortly thereafter. Although increased frequencies of CD4$^+$Foxp3$^-$ and CD8$^+$ T effector cells were detected in the TME throughout the observation period, a highly significant increase versus control mAb-treated animals was noted for CD4$^+$Foxp3$^-$ TIL at days 7 and 10 post-treatment and CD8$^+$ TIL at day 10 post-treatment ($P < 0.01$; Figure 4A). The change in percentages of T effector cells correlated with increases in the number of CD4$^+$Foxp3$^-$ and CD8$^+$ TIL per gram of tumor tissue (Appendix Figure 4). In order to distinguish between the recruitment of T effector cells and *in situ* T cell expansion within the TME, TIL were analyzed for their expression of Ki67. While Ki67 expression was up-regulated by T cells in the TDLN of OX40L-Fc-treated mice (Figure 3D), expression of this marker on TIL was not substantially altered (Figure 4B), suggesting that T effector cell accumulation in the TME of treated mice is most likely attributed to the enhanced recruitment of these cells, rather than to their expansion within tumor lesions.

Despite an elevated frequency of CD4$^+$Foxp3$^+$ T cells being consistently identified in the TDLN of OX40L-Fc-treated mice (Appendix Figure 5A), the frequency of these cells in the TME was reduced as early as day 3 post-treatment and this level remained low throughout the observation period (Appendix Figure 5B), consistent with a recent report (213). Additionally, a

43

decrease in cells exhibiting a myeloid-derived suppressor cell phenotype (CD11b$^+$Gr-1$^+$) was observed in the TME, along with a coordinate increase in F4/80$^+$ mature monocytes/macrophages between days 7 and 10 post-treatment (Appendix Figure 6).
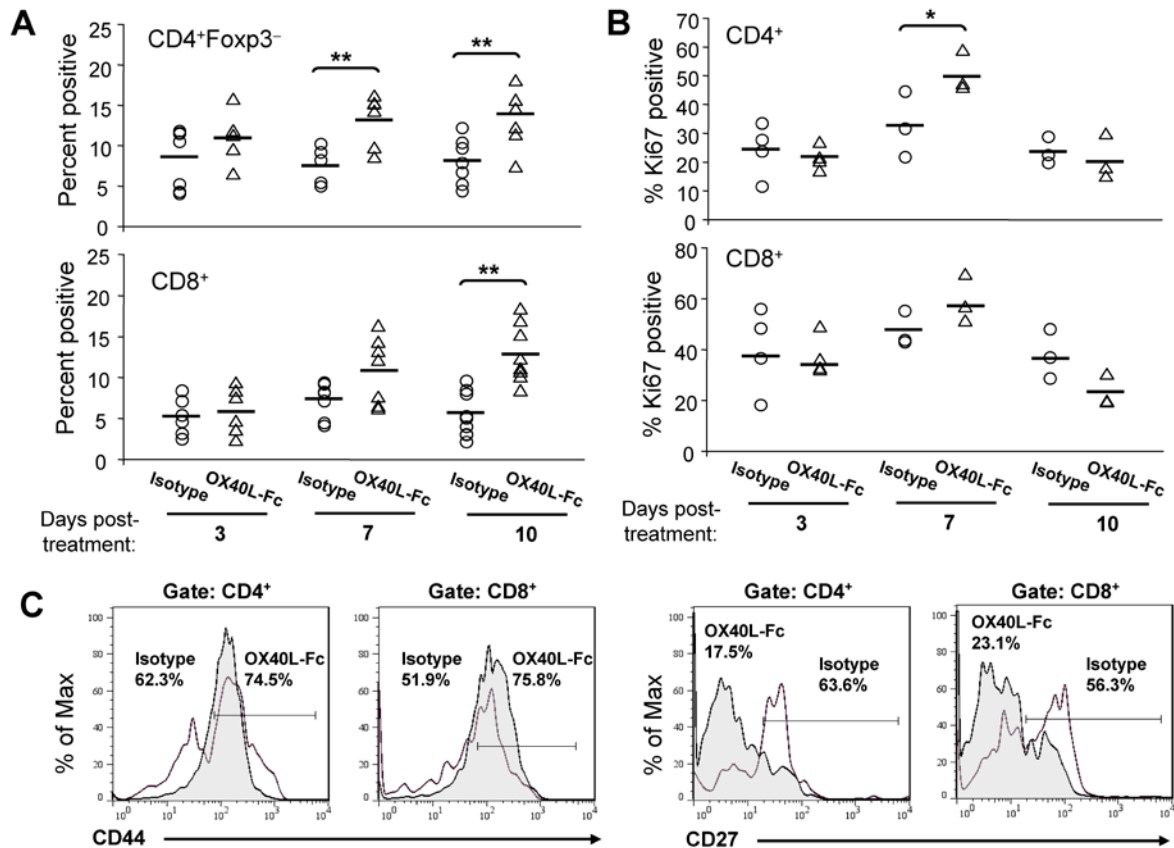
Figure 4. Accumulation of T effector cells in the TME of wild-type mice by day 10 following OX40L-Fc treatment. TME cells were isolated on days 3, 7, and 10 after treatment with isotype control antibody or OX40L-Fc. Graphs show percentages of CD4$^+$Foxp3$^-$ and CD8$^+$ T cells (A) and percentages of Ki67$^+$ T cells (B). Each symbol corresponds to one tumor-bearing mouse. The solid line represents the median value. (C) TIL were isolated on day 10 after treatment with isotype control antibody or OX40L-Fc. Percentages of CD44^{hi} of CD4$^+$ and CD44^{hi} of CD8$^+$ cells are indicated on representative histograms. CD27 was evaluated on gated CD4$^+$ and CD8$^+$ cells, as indicated (representative histograms are shown). Open histograms represent cells isolated from isotype control mAb-treated mice; filled histograms represent cells isolated from OX40L-Fc-treated mice. Similar data were obtained in two independent experiments performed. *, $P < 0.05$; **, $P < 0.01$.

2.4.6 Tumor infiltrating T cells exhibit a re-activated memory phenotype and are Type-1 polarized.

An analysis of the phenotype of TIL on day 10 after OX40L-Fc treatment, at which time T effector cell frequencies in the TME peaked, suggested no differential expression of CD25 or CD69 versus the control mAb-treated cohort (data not shown). However, the frequency of CD4$^+$ and CD8$^+$ TIL expressing high levels of CD44 (CD44^{hi}, antigen-experienced) and low levels of CD27 (CD27^{low}, recently-activated) was enriched at this time point (Figures 4C and Appendix Figure 7). These phenotypic analyses are consistent with a model in which OX40L-Fc-stimulated T cells are expanded in the TDLN by day 7 post-treatment and subsequently infiltrate the TME by day 10 post-treatment.

Because effective cancer immunotherapies have been largely associated with a state of Type-1 T cell polarization and an increased T effector cell-to-Treg ratio (214, 215), we next examined the polarization status of freshly-isolated TIL on days 3-10 following OX40L-Fc- versus control mAb-treatment. Using quantitative RT-PCR, factors associated with Type-1 T cell activity (i.e. T-bet and IFN-γ) and those associated with regulatory T cell activity (i.e. Foxp3 and IL-10) were assessed for their relative levels of expression. Although minimal alterations were observed in the expression of any of these four transcripts on days 3 and 7 post-treatment, by day 10 post-treatment, at a time when increased frequencies of TIL were observed, transcript levels for all 4 gene products were dramatically enhanced in the OX40L-Fc treatment group. (Figure 5A, upper panels). This is consistent with a recent report by Ruby and colleagues, who propose that while all T cell lineages are responsive to OX40 stimulation, the plasticity of the response is dependent on the local cytokine milieu (216). By considering the "balance" of polarized T cell responses based on a ratio of the effector-to-regulatory gene transcripts, however, we noted that

OX40L-Fc treatment skews the balance in favor of Type-1 T cell immunity at all time points analyzed (Figure 5A, lower panels). Similar alterations in these transcript ratios were observed in anti-CD3-stimulated TIL (Figure 5B). This suggests that although OX40 signaling may not be a polarizing event *per se*, a cytokine milieu appropriate for the preferential expansion of Type-1 versus regulatory-type immunity exists within the OX40L-Fc-treated TME.
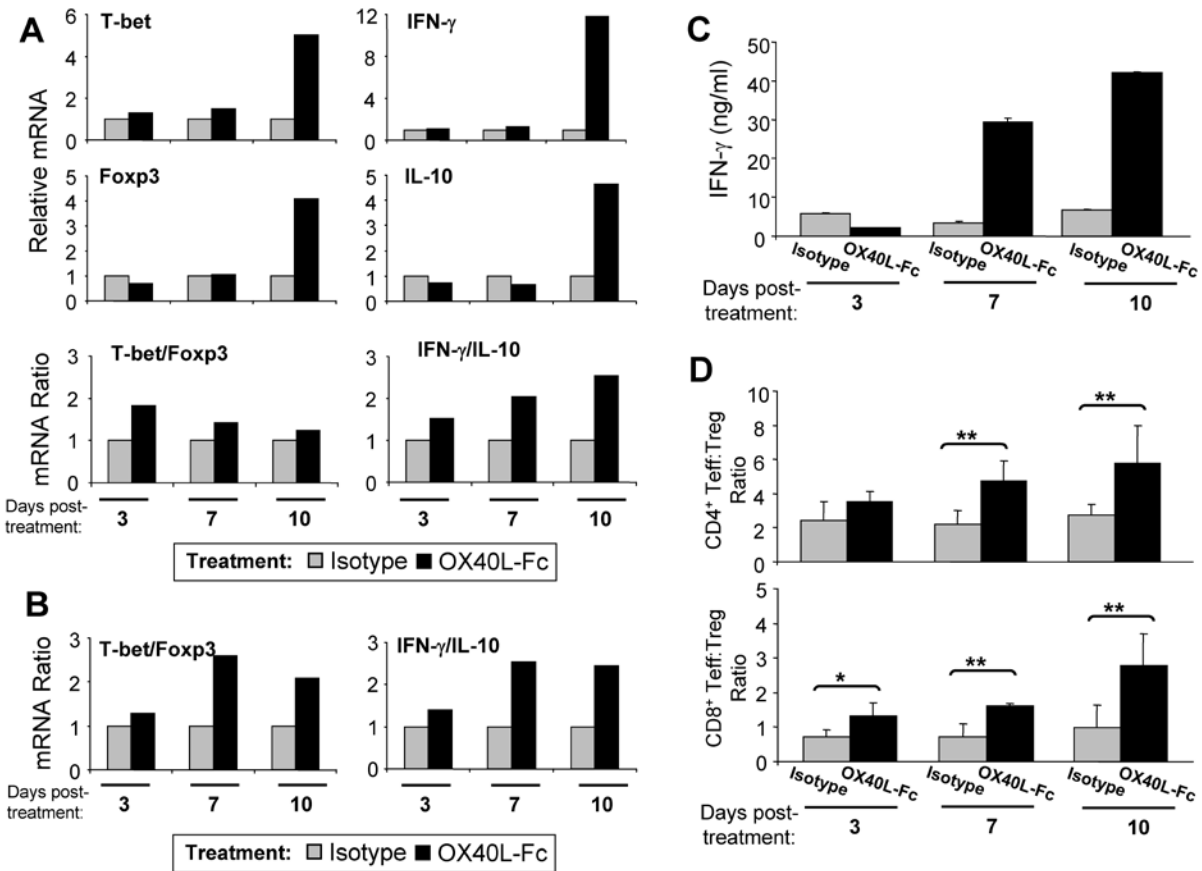
Figure 5. TIL exhibit a Type-1 polarized phenotype.

TIL were isolated from wild-type mice on days 3, 7, and 10 after treatment with isotype control antibody or OX40L-Fc. (A) Quantitative RT-PCR was performed on purified RNA ($n = 2$ per group, pooled) using primers specific for murine T-bet, Foxp3, IFN-γ, and IL-10. ΔΔCt were calculated to day 3 isotype treatment samples and relative RNA expression for each gene is depicted as $2^{\Delta\Delta Ct}$ (upper panels). Ratios of T-bet/Foxp3 and IFN-γ/IL-10 are also shown (lower panels). Similar data were obtained in two independent experiments performed. (B) TIL were stimulated with

anti-CD3 for 24 hours *in vitro* as outlined in Materials and Methods, with semi-quantitative RT-PCR performed on purified RNA ($n = 2$ per group, pooled) using primers specific for murine T-bet, Foxp3, IFN-γ, and IL-10. Similar data were obtained in two independent experiments performed. (C) Isolated TIL were re-stimulated *in vitro* with irradiated MCA205 cells for five days (as described in Materials and Methods). Recovered T cells were then stimulated with anti-CD3 for 72 hours and supernatants were assessed for levels of IFN-γ. Data are reported as the mean ± SD of duplicate determinations. Similar data were obtained in two independent experiments performed. (D) CD4$^+$Foxp3$^-$ and CD8$^+$ T effector-to-CD4$^+$Foxp3$^+$ Treg cell ratios were determined by flow cytometry ($n = 4$ per group). Data are representative of three independent experiments performed. *, $P < 0.05$; **, $P < 0.01$.

To ensure that alterations in IFN-γ RNA expression correlated with alterations at the protein level, TIL were isolated on days 3-10 post-treatment and stimulated *in vitro* prior to analysis of IFN-γ secretion levels by ELISA. Interestingly, TIL production of IFN-γ was not elevated, and perhaps even slightly reduced on day 3 after treatment with OX40L-Fc versus isotype mAb (Figure 5C). In contrast, TIL isolated 7 and 10 days after initiating OX40L-Fc-based therapy produced significantly higher levels of IFN-γ protein versus TIL harvested from control mAb-treated mice at these same time points. Moreover, when comparing the effector-to-regulatory balance at the cellular level within the TME, significant increases were observed in both the CD4$^+$Foxp3$^-$ and CD8$^+$ T effector versus Treg ratios at days 7 and 10 post-treatment ($P < 0.01$; Figure 5D).

2.4.7   OX40L-Fc treatment renders the TME permissive to Type-1 T cell infiltration via modulation of the tumor vasculature.

In parallel with an increased fraction of CXCR3$^+$ T cells in the TDLN of OX40L-Fc-treated mice, CXCL9 (a CXCR3 ligand) was dramatically up-regulated in the TME between days 7 and

10 post-treatment (Figure 6A, left panels), indicating that OX40L-Fc therapy redundantly promotes TIL trafficking by augmenting chemokine signals in both the periphery and the TME. We have also recently reported that effective recruitment of adoptively-transferred Type-1 polarized $CD8^+$ T cells into the TME requires tumor-associated VEC expression of VCAM-1 (217). Confocal immunofluorescence microscopy revealed that tumor-associated $CD31^+$ VEC rapidly up-regulate (i.e. by day 3) and maintain VCAM-1 expression through day 10 as a consequence of treatment with OX40L-Fc (Figure 6B, left panels), suggesting that Type-1 T effector cell recruitment into the TME might be further enhanced by OX40L-Fc via additional, chemokine-independent mechanisms. Importantly, treatment-associated enhancement of VCAM-1 and CXCL9 expression by $CD31^+$ VEC was recapitulated in $Rag^{-/-}$ mice (Figures 6A and B, right panels), suggesting the T cell-independent nature of these changes. In support of a direct effect of OX40L-Fc on VEC within the TME, we detected moderate levels of OX40 expression by a subset of $CD31^+CD11b^-$ VEC in untreated, progressor tumors (Appendix Figure 8). It is also important to note that Figure 6A data suggest that additional (non-VEC) stromal cells in the TME produce CXCL9 in wild-type, but not $Rag^{-/-}$ mice (most strikingly on day 7 post-treatment with OX40L-Fc). Hence, therapeutic production of CXCL9 in the TME appears to result from both T cell-dependent and T cell-independent processes.
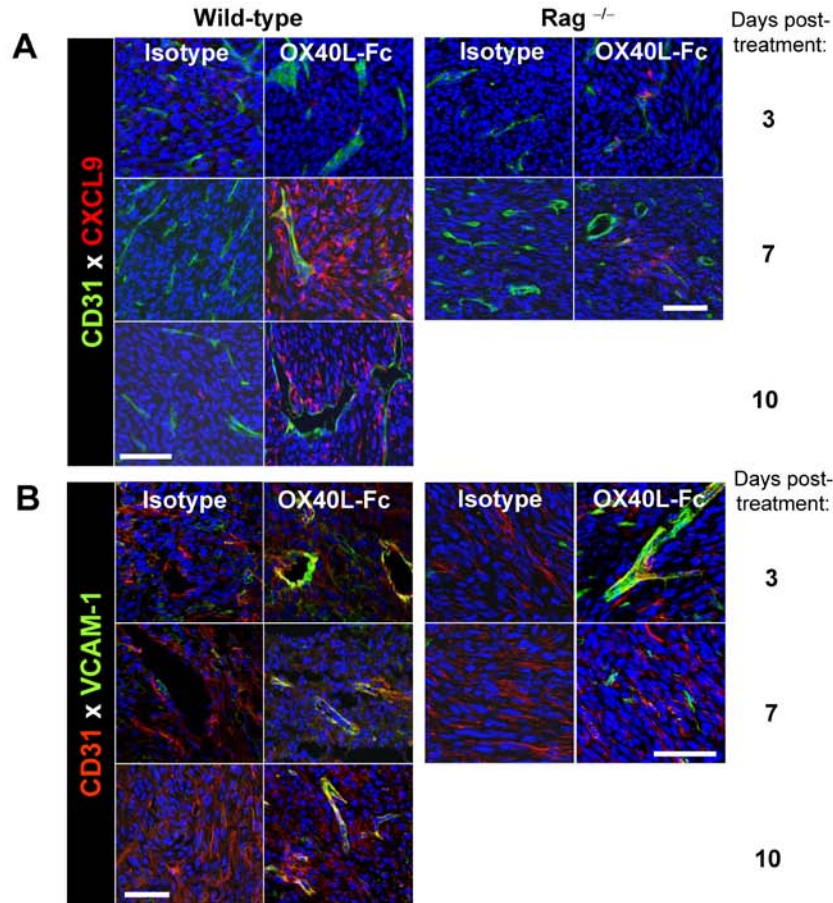
Figure 6. T cell-independent up-regulation of VEC-associated CXCL9 and VCAM-1 in the TME following OX40L-Fc treatment.

MCA205 tumors were isolated from wild-type (left panels) or Rag$^{-/-}$ (right panels) mice and analyzed by confocal fluorescence microscopy on the indicated days after treatment with isotype control antibody or OX40L-Fc. In A, expression of DAPI (blue), CXCL9/Mig (red), and CD31 (green) is depicted. In B, expression of DAPI (blue), CD31 (red) and VCAM-1 (green) is depicted. Bars, 50 μm.

We also observed a pronounced reorganization of the tumor vasculature after OX40L-Fc treatment, consistent with what has previously been described as a more "normalized" phenotype (111). While CD31$^+$ VEC density increased coordinately with disease progression in the tumors of isotype control mAb-treated mice, vessel density in OX40L-Fc-treated tumors was

significantly diminished by day 10 post-treatment (Appendix Figure 9A). These alterations in vascular density at day 10 post-treatment additionally correlated with a less tortuous and more organized (i.e. normalized) morphology of OX40L-Fc- versus control mAb-treated tumor vasculature (Appendix Figure 9B), consistent with a phenotype favorable for lymphocyte infiltration.

2.5   DISCUSSION

In this report, we describe multifaceted anti-tumor activities associated with a novel mOX40L-Fc fusion protein when applied in the therapeutic setting against well-established H-2^b and H-2^d sarcomas. When administered i.p. on days 17 and 20 post-tumor inoculation, OX40L-Fc treatment inhibited tumor growth, resulting in disease stabilization or complete regression in the majority of treated animals.

In the TDLN of mice bearing well-established MCA205 sarcomas, OX40 expression was restricted to CD4$^+$Foxp3$^+$ T cells, whereas CD4$^+$Foxp3$^-$ and CD8$^+$ T effector cells, as well as DC and potentially VEC, were observed to be OX40$^+$ in the TME. Expression of OX40 has also been reported to be up-regulated by T cells in primary tumors, but not in the tumor-free lymph nodes of human cancer patients (180). In alternative disease models, T cell up-regulation of OX40 has been observed at sites of inflammation during the onset of experimental autoimmune encephalomyelitis (218), and within the synovial fluid, but not the peripheral blood of patients with rheumatoid arthritis (219). This has been attributed to the influence of inflammatory cytokines, including IL-1 and TNF-α (220, 221). Such cytokines could also play a role in up-regulating the expression of OX40 by tumor-localized DC and VEC in our well-established

sarcoma models. Furthermore, 4-1BB, an alternate member of the costimulatory TNFR family with structural and functional similarities to OX40, can be expressed by activated DC and atherosclerotic endothelia under the appropriate conditions (222, 223).

Numerous studies have indicated that both $CD4^+$ and $CD8^+$ T effector cells play instrumental roles in anti-tumor immunity stimulated by OX40 agonists *in vivo* (178). Consistent with this notion, we observed significant expansion of $CXCR3^+$ TDLN T effector cells on day 7 after initiating OX40L-Fc-based therapy, followed on day 10 post-treatment by the accumulation of re-activated, Type-1 polarized $CD4^+Foxp3^-$ and $CD8^+$ T cells in the TME. Our data from $Rag^{-/-}$ models also now suggest the T cell-independent nature of OX40L-Fc-mediated events, including: i.) the rapid and sustained production of CXCL9 and expression of VCAM-1 on VEC in established tumors, and ii.) the conversion of $OX40^+$ TIDC into transport-competent APC (deduced from the subsequent enrichment of $CD11c^+CCR7^+$ myeloid DC in the TDLN by day 3 post-treatment). Although a recent study has demonstrated a similar enhancement in DC trafficking to the TDLN upon treatment with OX40 agonist mAb in an early-stage tumor model, this finding was attributed to therapy-mediated suppression of Treg function and to a corollary restoration in the migratory capacity of TIDC (172). Instead, based on the constitutive expression of OX40 by a sub-population of TIDC in the well-established TME and the preservation of DC alterations in $Rag^{-/-}$ mice following OX40L-Fc treatment, these alterations may occur via the direct engagement of OX40 on these cells. To unequivocally demonstrate a direct effect of OX40L-Fc on TIDC, prospective therapeutic models employing chimeric mice in which only DC are genetically deficient in expression of OX40 will be pursued.

The importance of manipulating the tumor vasculature to attract T cells has recently been demonstrated by Quezada and colleagues, who report ICAM and VCAM up-regulation in the

51

TME upon prophylactic Treg cell depletion as well as therapeutic vaccination (Gvax)/anti-CTLA-4 combination treatment (115), indicating that vascular activation may be achieved through several distinct mechanisms. Similar to our data, activation of the tumor vasculature in these models correlated with enhanced T cell infiltration, increased T effector-to-Treg cell ratios and improved therapeutic efficacy. Our data further suggest that therapy-associated induction of chemokines and adhesion molecules that render the TME more permissive to immune cell infiltration can be achieved in the absence of T cells. OX40L-Fc could conceivably mediate vascular activation in the TME of $Rag^{-/-}$ mice via: i.) direct stimulation of a subset of $OX40^+$ VEC, ii.) inflammatory cytokine/chemokine production by $OX40^+$ TIDC, or iii.) the participation of alternate inflammatory (i.e. NK among others) effector cells present in these mice. The initial effects of nonhematopoeietic and/or innate immune cell subsets in therapy-mediated vascular activation, however, are likely to synergize with the effects mediated by T cells in immune competent hosts. In our model, for example, initial secretion of inflammatory cytokines (i.e. TNF-α) by $OX40^+$ TIDC upon OX40L-Fc treatment may induce CXCL9 and VCAM-1 expression in the TME, allowing for the recruitment of Type-1 polarized T effector cells that produce IFN-γ (a potent inducer of CXCL9 and other angiostatic chemokines), resulting in further remodeling of the tumor vasculature and enhanced T cell infiltration. Future studies will investigate the validity of this paradigm.

Based on the tumor growth curves of OX40L-Fc- versus control mAb-treated mice, the impact of therapy only becomes apparent by 7-10 days after the initiation of therapy. This is consistent with the infiltration of a highly-reactive $CD27^{low}CD44^{hi}$ $CD8^+$ T effector cell population into the TME. As OX40 signaling has been previously shown to enhance recall responses and to preferentially expand $CD44^{hi}$ memory T cells upon antigen rechallenge (137,

224), this may suggest that OX40L-Fc treatment leads to the expansion of a tumor antigen-experienced, rather than naïve, T effector cell population in the TDLN, and subsequent trafficking of these T cells to the TME. Regardless, these infiltrating T cells appear competent to promote tumor regression or to regulate a state of tumor dormancy (i.e. stable disease) in the majority of OX40L-Fc-treated animals for a period of several weeks prior to the ultimate "escape" of progressor lesions. We are currently investigating whether this late progression event results from the erosion of protective anti-tumor T cell responses, the outgrowth of less-immunogenic tumor cell variants, and/or the reacquisition of aberrant vascular structures in the TME (63). If the former mechanism underlies the ultimate failure of OX40L-Fc to induce complete tumor rejection, we would anticipate the enhanced benefits of extending the number of treatment cycles involving OX40 agonists.

Overall, the therapeutic benefits demonstrated for OX40L-Fc in our well-established sarcoma models strongly supports the continued translation of OX40 agonists, particularly those based on a recombinant form of OX40L, into human clinical trials. Moving forward, it will be important to better delineate how the various OX40$^+$ target cell populations within the TME (and elsewhere) are impacted by OX40-mediated signals in order to select potential co-therapeutic agents and to define a strategically-rational schedule for the administration of each modality to yield maximal treatment benefit.

3.0   A GITRL-FC AGONIST EXHIBITS MODERATE THERAPEUTIC EFFICACY DESPITE INCREASING EFFECTOR-TO-REGULATORY T CELL RATIOS IN WELL-ESTABLISHED SARCOMAS

Angela D. Pardee[1], Sean Alber[2], Peisheng Hu[3], Alan L. Epstein[3] and Walter J. Storkus[1,4,5]

From the Departments of [1]Immunology, [2]Cell Biology and Physiology and [4]Dermatology, University of Pittsburgh School of Medicine, Pittsburgh, PA 15213, and the [3]Department of Pathology, Keck School of Medicine, University of Southern California, Los Angeles, CA 90033, and the [5]University of Pittsburgh Cancer Institute, Pittsburgh, PA 15213.

3.1   ABSTRACT

Agonistic modalities targeting the costimulatory molecule GITR (glucocorticoid-induced tumor necrosis factor receptor) have demonstrated therapeutic benefit in numerous murine tumor models. In some reports, anti-tumor efficacy has been attributed to the activation of conventional T cells, while in others the antagonism of CD4$^+$Foxp3$^+$ regulatory T cells (Treg) has played a more dominant role. Using a novel GITR ligand-Fc fusion protein (GITRL-Fc), we now show that GITR stimulation induces regression of well-established day 17 CMS4 (H-2^d), but not MCA205 (H-2^b) sarcomas, with comparable efficacy observed for treatment with an agonist anti-GITR mAb (DTA-1). To elucidate the reasons for therapeutic failure in the MCA205 model, we conducted a longitudinal analysis of cells isolated from the tumor-draining lymph nodes (TDLN) and the tumor microenvironment (TME) of GITRL-Fc-treated mice. By day 7 after treatment, a significant increase in expansion of both regulatory and effector T cells was observed in the TDLN, and by day 10 post-treatment, CD4$^+$Foxp3$^-$ and CD8$^+$ T effector cells had accumulated in tumors. Importantly, a corresponding decrease in Treg frequencies occurred in the TME, resulting in increased effector-to-regulatory T cell ratios. An incomplete activation phenotype (i.e. variable up-regulation of activation markers, inconsistent responses to *ex vivo* stimulation) was observed for T cells isolated from the TDLN and TME of GITRL-Fc-treated mice. These data suggest that at least in some tumor systems, single modality therapy using GITR agonists may prove suboptimal, and that combinational approaches may be warranted.

3.2   INTRODUCTION

Similar to other costimulatory members of the tumor necrosis factor receptor (TNFR) family, GITR (glucocorticoid-induced TNFR) is expressed at low levels on resting CD4$^+$Foxp3$^-$ and CD8$^+$ T cells, but is up-regulated shortly after T cell receptor (TCR) engagement on both naïve and antigen-experienced cells (5, 135). Particularly under conditions of low antigen dosing *in vivo*, signals contributed through GITR have been shown to enhance CD4$^+$ and CD8$^+$ T effector cell proliferation (225), activation marker expression (151), and production of IFN-γ and IL-10 upon *ex vivo* stimulation (226). Furthermore, an established state of T cell anergy can be reversed by direct ligation of GITR expressed by hyporesponsive T effector cells (227). CD4$^+$Foxp3$^+$ regulatory T cells (Treg) express higher levels of GITR than T effector cells under steady state conditions (127), and numerous studies have shown that GITR stimulation can inhibit the suppressor function of Tregs (208), or confer resistance of effector cells to Treg-mediated inhibition (154, 159).

Based on the ability of GITR agonists to simultaneously antagonize regulatory circuits and directly activate T cells, GITR represents an attractive target in cancer immunotherapy. Indeed, GITR-targeting therapeutics have demonstrated potent anti-tumor effects in numerous pre-clinical models (6, 165). Although an expanding literature supports the anti-tumor efficacy of GITR agonists, the mechanism(s) through which such reagents function has not been comprehensively studied. A number of studies suggest that both CD4$^+$ and CD8$^+$ T cell subsets play instrumental roles in productive anti-tumor immunity induced by GITR stimulation *in vivo*. CD4$^+$ T cell helper activity, which serves to "license" DC-mediated priming (29) and to support cytotoxic T lymphocyte (CTL) function via IFN-γ production (40), can be augmented by GITR-

targeted therapy (191). Furthermore, direct engagement of GITR enhances primary anti-tumor CD8$^+$ T cell responses (228), provides activation signals to hyporesponsive tumor-primed CTL (189), and renders effector T cells resistant to Treg-mediated inhibition (191, 229). Additional reports suggest that the therapeutic efficacy of GITR agonists is predicated primarily on the ability of such agents to mitigate Treg-sponsored immunosuppression (i.e. impairment of Treg infiltration into tumor sites and loss of Foxp3 expression by Treg following GITR engagement) (230).

A novel agonistic reagent directed against murine GITR (GITR ligand-Fc fusion protein; GITRL-Fc) was recently constructed and shown to effectively mediate tumor regression in mice bearing day 6 Colon 26 (H-2^d) tumors to a degree that was comparable to that observed for treatment with agonist anti-GITR mAb (DTA-1) (192). To more rigorously assess the translational potential of this reagent in a more advanced disease setting, we allowed MCA205 (H-2^b) sarcomas to establish and grow progressively until day 17, at which point a short course of systemic GITRL-Fc therapy was initiated. Although CD4$^+$Foxp3$^-$ and CD8$^+$ T effector cell expansion in the TDLN and increased effector-to-regulatory T cell ratios in the TME were induced by GITRL-Fc versus isotype mAb control treatment, complete regression of these well-established MCA205 tumors occurred in only a minority of treated animals. Interestingly, T cells isolated from the TDLN and TME of treated mice did not appear to be fully activated by GITRL-Fc administration, as determined by an analysis of cell phenotype and *ex vivo* functionality. Based on these data, we believe that therapies based on GITR agonists alone may provide only limited clinical benefit in the advanced cancer setting.

3.3   MATERIALS AND METHODS

Mice. Six to ten week old female C57BL/6 (H-2^b) and BALB/cJ (H-2^d) mice were purchased from The Jackson Laboratory and maintained in the pathogen-free animal facility in the Biomedical Sciences Tower at the University of Pittsburgh. All animal work was done in accordance with a protocol approved by the Institutional Animal Care and Use Committee.

Tumor Establishment. The MCA205 (H-2^b) sarcoma cell line was purchased from the American Type Culture Collection (ATCC). The CMS4 (H-2^d) sarcoma has been described in detail previously (209). Cell lines were cultured in complete media (CM; RPMI-1640 supplemented with 100 U/ml penicillin, 100 μg/ml streptomycin, 10 mM L-glutamine and 10% heat-inactivated fetal bovine serum (all reagents from Life Technologies) in a humidified incubator at 37° C and 5% CO$_2$. All cell lines were negative for known mouse pathogens. Tumors were established by injection of 5 x 10^5 tumor cells s.c. into the right flanks of syngeneic mice, with tumor size assessed every 3 to 4 days and recorded in mm^2 (as the product of orthogonal diameters). Mice were sacrificed when tumors became ulcerated or reached a maximum size of 400 mm^2.

Costimulatory Therapy. Tumor-bearing mice were injected i.p. with 100 μg of rat IgG isotype control antibody (Sigma-Aldrich), mGITRL-Fc, or rat anti-GITR mAb (DTA-1) in a total volume of 100 μl PBS on days 17 and 20 post-tumor inoculation when tumors were approximately 30-50 mm^2 in size. The agonist anti-GITR mAb and the GITRL-Fc fusion protein (192) have been previously described.

Isolation of Tumor, LN and Spleen cells. Single cell suspensions were obtained from spleen and TDLN as previously described (209). For tumor-infiltrating lymphocytes (TIL),

tumors were enzymatically digested with 0.1% w/v collagenase, 1% w/v hyaluronidase, and 0.1% w/v DNase (all from Sigma), with lymphocytes isolated as buoyant cells after discontinuous density centrifugation as previously described (210).

In Vitro Stimulation (IVS) of T cells. Bulk cells isolated from the TDLN or TME of isotype mAb- or GITRL-Fc-treated mice were stimulated *ex vivo* with 5μg/ml anti-CD3 (BioLegend) in CM with 20 U/ml recombinant human IL-2 for 72 hours. Cell-free supernatants were then harvested and assessed for levels of mIFN-γ using a specific OptEIA ELISA set (BD Biosciences) according to the manufacturer's instructions. This assay had a lower detection limit of 32.5 pg/ml. Data are reported as the mean ± SD of duplicate determinations.

RT-PCR. Total RNA was isolated from TIL on days 3, 7, and 10 after the initial treatment (day 17 post-tumor inoculation), as indicated, using RNeasy Micro kit (Qiagen), according to the manufacturer's instructions. For quantitative RT-PCR, reverse transcription and PCR amplification was performed by the University of Pittsburgh's Genomics and Proteomics Core Laboratories (a shared resource). For quantitative analysis of T-bet, IFN-γ, and control β-actin, previously published primer pairs were used (211), and cDNA was amplified using SYBR® Green PCR Master Mix (Applied Biosystems). For quantitative analysis of Foxp3, IL-10, and control β-actin, RT^2 qPCR Primer Assays (SABiosciences) were used and cDNA was amplified using RT^2 SYBR Green qPCR Master Mix (SABiosciences). For each sample, the cycle threshold (Ct) values for the control β-actin gene were determined for normalization purposes and the ΔCt between β-actin and T-bet, Foxp3, IFN-γ and IL-10 were calculated. ΔΔCt were calculated to isotype treatment samples. Relative RNA expression was determined for each gene ($2^{ΔΔCt}$) and ratios of T-bet/Foxp3 and IFN-γ/IL-10 expression are reported.

Confocal Immunofluorescence Staining and Imaging. Tumor tissue was processed and sectioned as previously reported (209), followed by immunofluorescence staining and confocal microscopy. For analysis of GITR expression by T cell subsets, sections were incubated with rat anti-mouse CD4 or CD8α (both BD Biosciences), in combination with goat anti-mouse GITR (Santa Cruz Biotechnology). After washing, sections were incubated with donkey anti-rat Alexa Fluor 488 and donkey anti-goat Cy3 (both Jackson ImmunoResearch). For analysis of GITR expression by Foxp3$^+$ T cells, sections were treated with Alexa Fluor 488-conjugated rat anti-mouse Foxp3 (eBioscience), in combination with goat anti-mouse GITR, followed after washing by staining with donkey anti-goat Cy3. All sections were briefly incubated with DAPI (Sigma) and then mounted. Images were acquired using an Olympus Fluoview 1000 confocal microscope (Olympus). Isotype control and specific antibody images were taken using the same level of exposure on the channel settings.

Flow Cytometry. Before all stainings, cells were Fc-blocked with anti-CD16/CD32 (BD). Single-cell suspensions were stained using the following antibodies: PerCP-, FITC-, PE- and APC-conjugated CD4 and CD8α (all BD), PE-conjugated GITR and CD25 (both eBioscience), or appropriate-matched, fluorochrome-labeled isotype control mAb. For Ki67 intracellular staining, T cells were surface stained as described above, fixed, and incubated with PerCP-Cy5.5-conjugated Ki67 (BD), according to the manufacturer's instructions. For Foxp3 intracellular staining, CD4$^+$ T cells were surface stained as described above and then further processed using an APC-conjugated anti-mouse/rat Foxp3 Staining kit (eBioscience) according to the manufacturer's instructions. Cells were analyzed using an LSR II flow cytometer (Beckman Coulter), with corollary data assessed using FlowJo software (version 7.6.1; Tree Star, Inc.).

Statistical Analysis. All comparisons of inter-group means were performed using a two-tailed Student's *t* test, with *P* values < 0.05 considered significant.

3.4   RESULTS

3.4.1   GITRL-Fc is marginally effective against well-established tumors.

Hu and colleagues generated two different GITRL-Fc constructs (#175-2 and #178-14) that vary by five amino acids (192). From pilot studies, it was determined that construct #175-2 demonstrated greater *in vivo* activity than construct #178-14 in our sarcoma models (data not shown). As a result, GITRL-Fc construct #178-14 was not used in any further therapeutic experiments. We treated C57BL/6 mice bearing day 17 MCA205 sarcomas via i.p. injection of 100 µg of GITRL-Fc (construct #175-2), agonist anti-GITR mAb (DTA-1) or control rat IgG. A second identical dose was provided three days later. When compared to the control mAb treatment cohort, GITRL-Fc- and DTA-1-treated mice exhibited a moderate delay in tumor progression, with complete tumor regression observed in a small minority of cases (Figure 7A). Overall, long-term tumor-free survivors were observed in only 17% of cases treated with GITRL-Fc (Figure 7B).
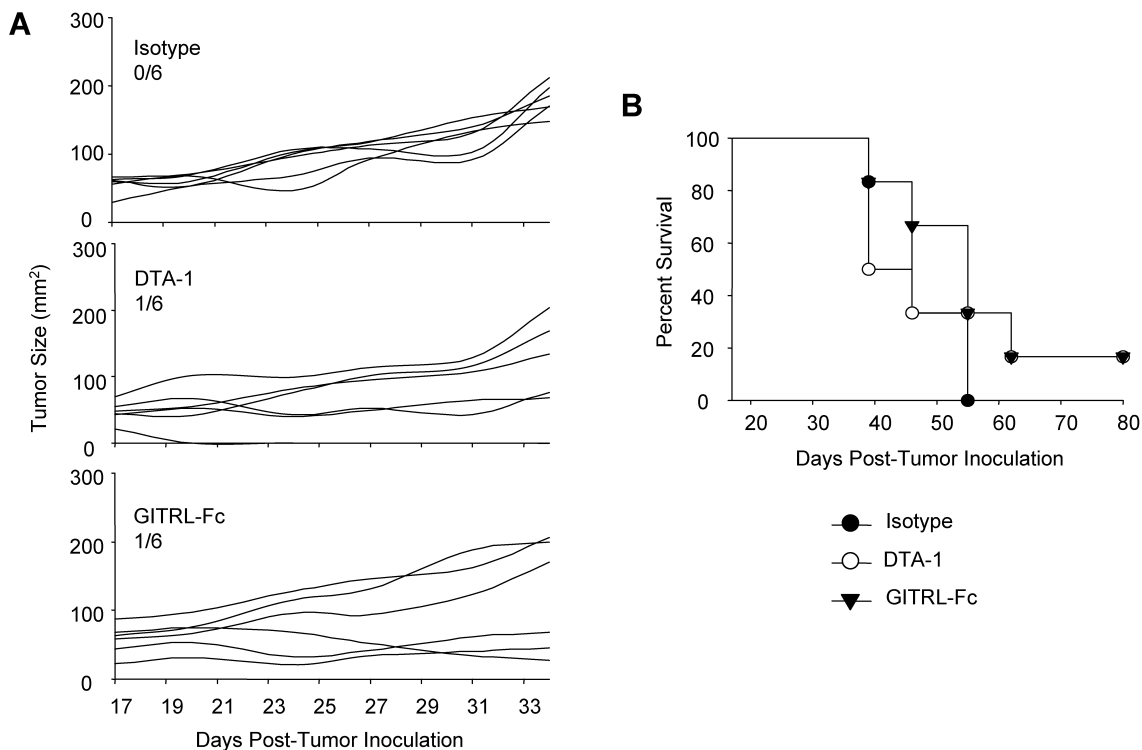
Figure 7. Limited therapeutic efficacy of GITRL-Fc against well-established tumors. (A) MCA205 sarcomas ($n = 6$ per group) were injected s.c. into the right flank of C57BL/6 mice. Mice bearing established day 17 tumors (~30 to 50 mm^2 in area) were treated i.p. with 100 μg of rat IgG isotype control mAb, agonist GITR mAb (DTA-1) or GITRL-Fc, as indicated. Treatment was repeated on day 20 after tumor inoculation. Tumor areas (mm^2) were calculated every 3 days, with the data for individual animals reported. The number of tumor-free mice at day 80 of the total treated mice is indicated. (B) Data from Figure 7A are presented in a Kaplan-Meier plot. Data are representative of two independent experiments performed.

To assess the therapeutic benefits of GITRL-Fc in an alternative sarcoma model, BALB/c mice bearing established CMS4 tumors were treated on days 17 and 20 post-tumor inoculation with isotype mAb control, DTA-1, or GITRL-Fc. In contrast to the minimal anti-tumor efficacy demonstrated by both GITR agonists in the MCA205 tumor model, DTA-1- or GITRL-Fc-based

62

therapies resulted in tumor eradication (Figure 8A) and prolonged survival (Figure 8B) in 80% and 100% of treated animals, respectively. When taken together, these data indicate that the therapeutic activity of GITR agonists against established sarcomas may be recipient strain- and/or tumor cell line-specific.
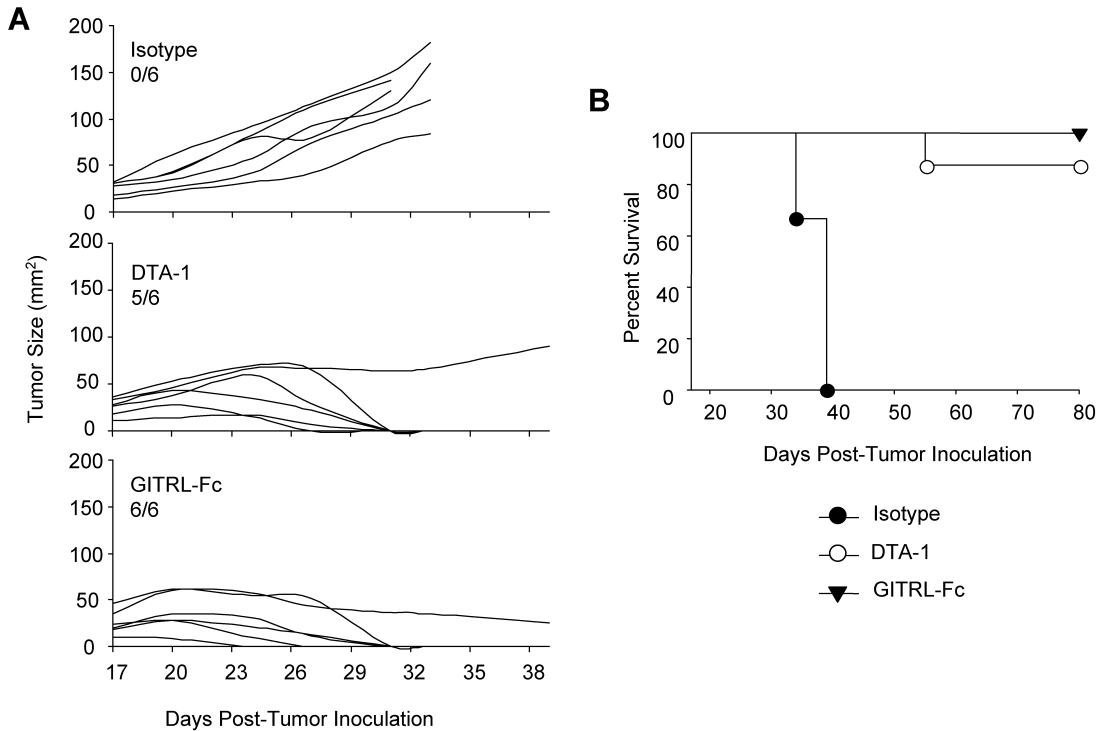
Figure 8. Tumor rejection induced by GITRL-Fc in an alternative sarcoma model.

(A) BALB/c mice bearing day 17 CMS4 sarcomas ($n = 6$ per group) were treated as in Figure 7. Tumor areas (mm^2) were calculated every 3 days, with the data for individual animals reported. The number of tumor-free mice at day 80 out of the number of treated mice is indicated. (B) Data from Figure 8A are presented in a Kaplan-Meier plot. Data are representative of two independent experiments performed.

3.4.2 GITR is constitutively expressed by Tregs, but up-regulated by TIL.

GITR has been reported to be expressed at low levels on resting T effector cells and at high levels by Tregs and activated T effector cells (5). Indeed, bulk $CD4^+$ T cells from naïve C57BL/6 mice can either express low or high levels of GITR (Figure 9A), and upon further analysis, $CD4^+GITR^{hi}$ cells from these naïve mice were also $Foxp3^+$ (data not shown). We next assessed frequencies of $GITR^{hi}$ T cells within the TDLN and the TME of untreated MCA205 tumor-bearing mice between days 17 and 20 post-tumor inoculation, as these cells may represent primary cellular targets of GITRL-Fc-based therapy. Nearly 100% of $CD4^+Foxp3^+$ T cells from the TDLN of tumor-bearing mice express high levels of GITR, while only very low frequencies of $CD4^+Foxp3^-$ and $CD8^+$ T cells were $GITR^{hi}$ (Figure 9B). Because the TME provides a large depot of antigen that can be presented to TIL by both professional and non-professional APCs (231), we hypothesized that antigen-dependent up-regulation of GITR on T cells is likely to be most profound within progressing tumors. Although $CD4^+Foxp3^+$ T cells from the TDLN and TME expressed comparably high levels of GITR, GITR expression was slightly up-regulated on $CD8^+$ T cells and substantially up-regulated on $CD4^+Foxp3^-$ T cells, including a median of over 10% of $CD8^+$ T cells and over 40% of $CD4^+Foxp3^-$ T cells that were $GITR^{hi}$ (Figure 9B). GITR was also detected on $CD4^+Foxp3^-$ and $CD4^+Foxp3^+$ T cells in established MCA205 tumors via confocal immunofluorescence microscopy (Figure 9C). These results suggest that $CD4^+Foxp3^+GITR^{hi}$ T cells in the TDLN and TME, in addition to $CD4^+Foxp3^-GITR^{hi}$ and $CD8^+GITR^{hi}$ T cells in the TME, likely represent principal targets of GITRL-Fc in the tumor-bearing host.
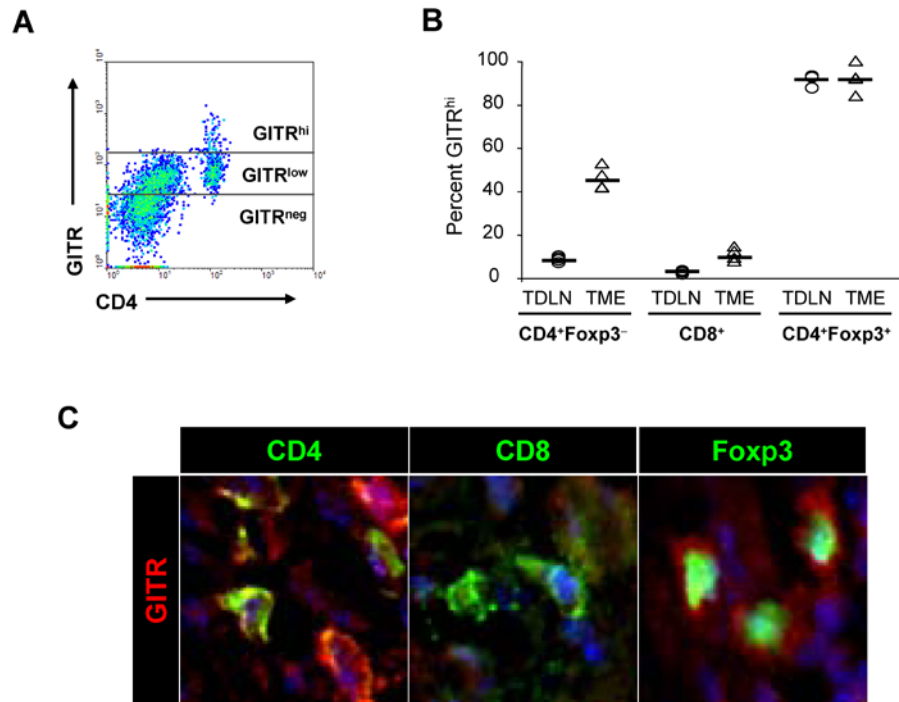
Figure 9. Differential GITR expression patterns by T cells in TDLN and tumors.

(A) Representative GITR staining on CD4^{+} T cells isolated from the spleens of naïve mice. GITR^{+} cells are divided into GITR^{hi} and GITR^{low} populations, as indicated. (B) Single-cell suspensions ($n = 4$) were prepared from untreated MCA205 tumors (TME) and tumor-draining lymph nodes (TDLN) isolated between days 17 and 20 post-tumor inoculation. Percentages of GITR^{hi} T cells among the indicated gated cell populations are shown. Each symbol corresponds to an individual tumor-bearing mouse (bar = median value). (C) Untreated MCA205 tumors were isolated between days 17 and 20 post-tumor inoculation, then sectioned, stained and analyzed by confocal fluorescence microscopy as described in Materials and Methods. Representative staining of DAPI (blue), GITR (red), and either CD4, CD8 or Foxp3 (all in green) is shown, with CD4^{+}GITR^{+} cells appearing yellow due to co-staining overlays. Experiments were repeated two times with similar results obtained in each instance.

3.4.3 GITRL-Fc administration induces the expansion of both effector and regulatory T cells in the TDLN.

To evaluate treatment-dependent alterations in the TDLN T cell compartment of tumor-bearing mice, C57BL/6 mice bearing established MCA205 sarcomas were treated with isotype mAb control or GITRL-Fc as in Figure 7. TDLN from these mice were then harvested on days 3, 7, and 10 after initiating treatment. Despite low expression of GITR by T effector cells in the TDLN (Figure 9B), absolute numbers of both $CD4^+Foxp3^-$ and $CD8^+$ T cells increased significantly by day 7 after GITRL-Fc treatment initiation, with a median of 17.1 ($\pm$ 3.9) x 10^5 $CD4^+Foxp3^-$ and 25.7 ($\pm$ 9.8) x 10^5 $CD8^+$ TDLN cells were observed in GITRL-Fc-treated mice versus 10.9 ($\pm$4.4) x 10^5 $CD4^+Foxp3^-$ and 9.9 ($\pm$ 2.7) x 10^5 $CD8^+$ TDLN cells in control mAb-treated animals (Figure 10A). To determine whether this expanded T effector cell population in the TDLN of GITRL-Fc-treated mice was a result of *in situ* proliferation or influx from peripheral tissues, expression of the proliferation marker Ki67 was assessed in $CD4^+CD25^-$ and $CD8^+$ T cells. Since a strong correlation between CD25 and Foxp3 expression was consistently observed (data not shown), CD25 served as a surrogate marker in some experiments to distinguish between effector and regulatory $CD4^+$ T cell phenotypes. At day 7 post-treatment, Ki67 was up-regulated by both $CD4^+CD25^-$ and $CD8^+$ T cells in the TDLN of GITRL-Fc-treated mice versus isotype mAb-treated controls (Figure 10B), suggesting that T effector cells expand within the TDLN in response to GITRL-Fc treatment.
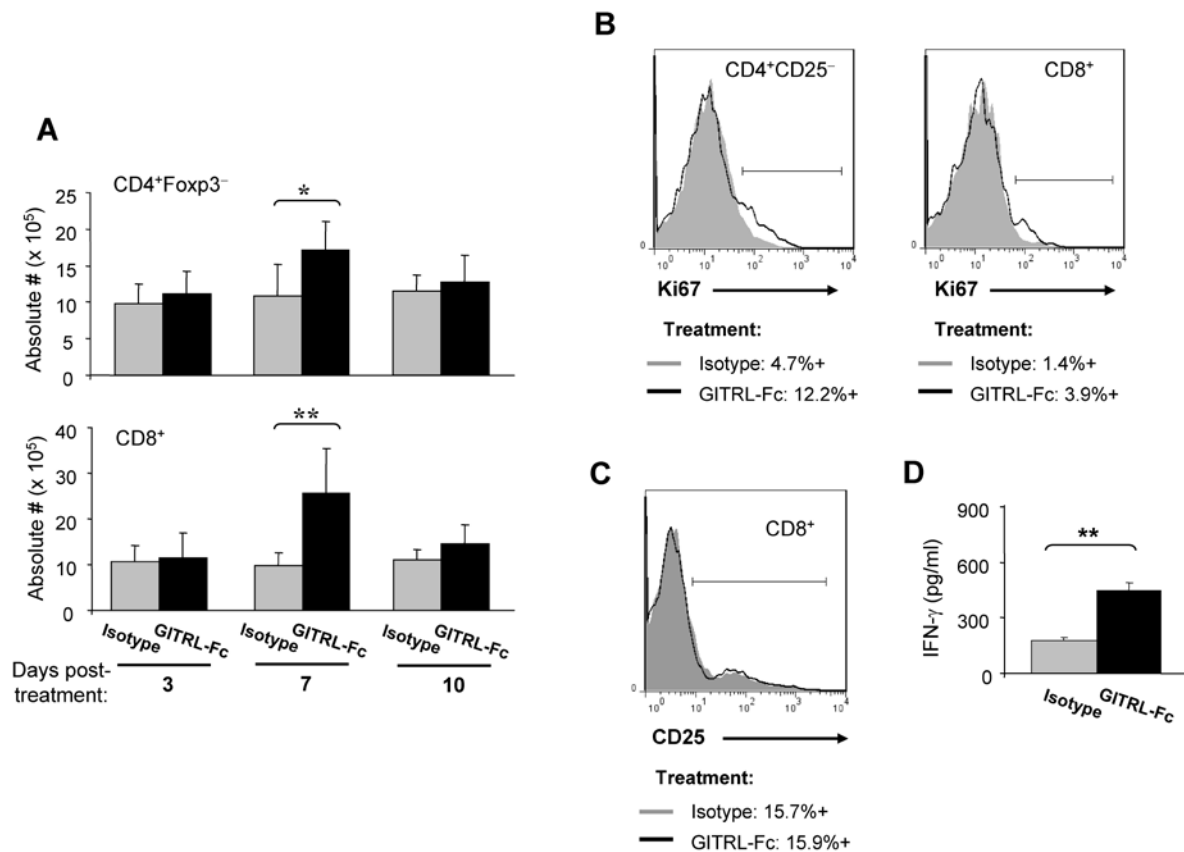
Figure 10. Expansion of T effector cells in the TDLN peaking at day 7 following GITRL-Fc treatment.

MCA205 tumor-bearing mice were treated as in Figure 7. (A) TDLN cells were isolated on days 3, 7, and 10 after treatment initiation with isotype control antibody or GITRL-Fc (n = 3-6 per group). Absolute numbers (x 10^5) of CD4$^+$Foxp3$^-$ and CD8$^+$ T cells are reported as the mean ± SD. For panels B and C, TDLN cells were isolated on day 7 after treatment with isotype control antibody or GITRL-Fc. Ki67 was evaluated on gated CD4$^+$CD25$^-$ and CD8$^+$ cells (B) and CD25 was evaluated on gated CD8$^+$ cells (C). Representative histograms are shown. Filled histograms represent cells isolated from isotype control mAb-treated mice; open histograms represent cells isolated from GITRL-Fc-treated mice. Percentages of Ki67$^+$ or CD25$^+$ cells per treatment are indicated. (D) TDLN cells were isolated on day 7 after treatment with isotype control antibody or GITRL-Fc and stimulated with anti-CD3 for 72 hours. Supernatants were then assessed for levels of IFN-γ, with data reported as the mean ± SD of duplicate determinations. Values correspond to one animal (representative of two total) per group. Data are representative of results obtained in 2 independent experiments in each case. *, $P < 0.05$; **, $P < 0.01$.

Given that GITRL-Fc administration was able to induce proliferation of TDLN T cells, we assessed these cells for additional indicators of cell activation, including enhanced cytokine secretion (151, 226, 232). Unexpectedly, neither CD4$^+$Foxp3$^-$ (data not shown) or CD8$^+$ T cells (Figure 10C) in the TDLN expressed elevated levels of the activation marker CD25 after treatment with GITRL-Fc versus isotype mAb. Similarly, these T cells did not exhibit alterations in control level expression of CD69, CD44, or CD27 (data not shown). In contrast, *in vitro* stimulation of TDLN cells isolated from GITRL-Fc-treated mice resulted in enhanced IFN-γ production compared to isotype mAb-treated controls (Figure 10D). This suggests that although T effector cells expanded in the TDLN upon GITRL-Fc treatment, comprehensive activation of T cells under these conditions did not occur.

Consistent with previous reports using the agonist mAb DTA-1 (189, 191), highly-significant increases in CD4$^+$Foxp3$^+$ T cell frequencies were identified in the TDLN of GITRL-Fc-treated mice ($P < 0.01$; Figure 11A). Increased frequencies of CD4$^+$CD25$^+$ T cells were associated with elevated Ki67 expression (Figure 11B), indicating that these cells were actively proliferating within the TDLN as a consequence of GITRL-Fc treatment. Moreover, when comparing effector-to-regulatory T cell ratios within the TDLN, GITRL-Fc-mediated decreases were observed in both the CD4$^+$Foxp3$^-$ and CD8$^+$ T effector versus Treg ratios throughout the observation period (Figure 11C). As a consequence, despite the capacity of GITRL-Fc to promote proliferation of CD4$^+$Foxp3$^-$ and CD8$^+$ T effector cells, our data suggest these conditions result in the preferential expansion of Tregs (and suboptimal anti-tumor immunity) in the TDLN of tumor-bearing mice.
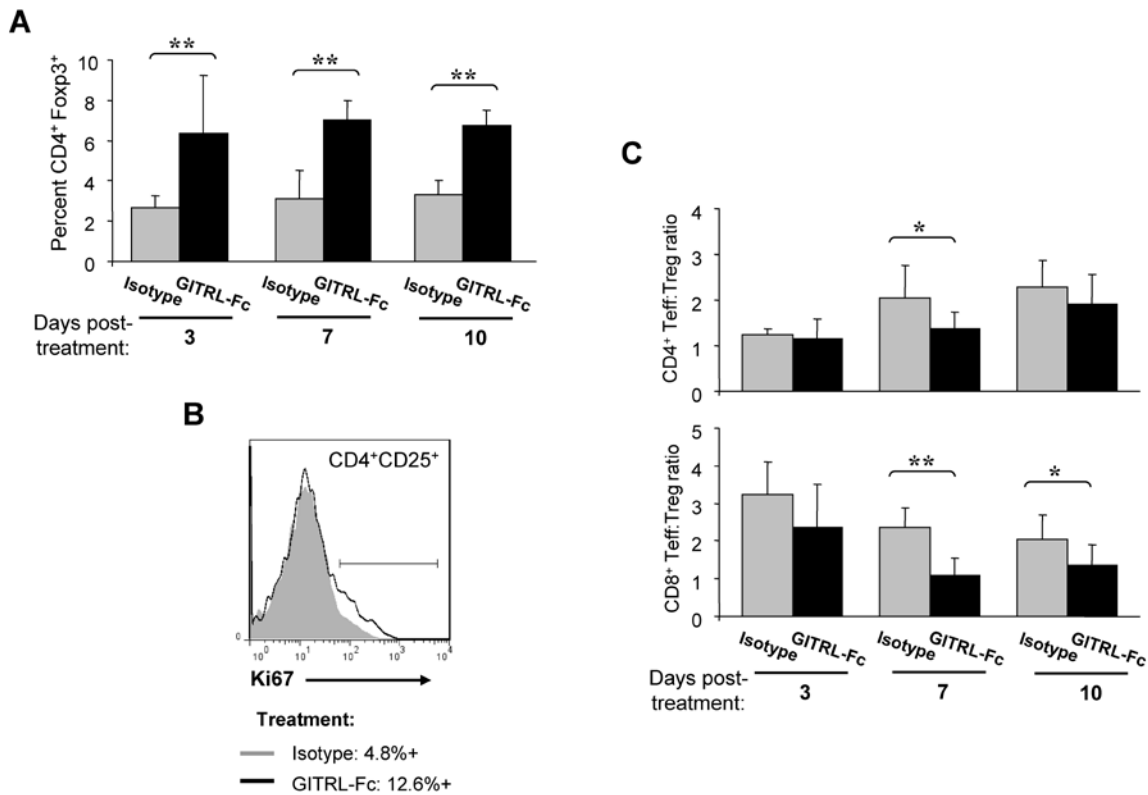
Figure 11. Rapid and sustained proliferation of regulatory T cells in the TDLN upon GITRL-Fc treatment.

(A) TDLN cells were isolated on days 3, 7, and 10 after treatment with isotype control antibody or GITRL-Fc ($n = $ 3-6 per group). Percentages of CD4$^+$Foxp3$^+$ T cells among gated live cells are reported as the mean ± SD. (B) Ki67 was evaluated on gated CD4$^+$CD25$^+$ cells isolated from the TDLN on day 7 after treatment (representative histogram is shown). Filled histogram represents cells isolated from isotype control mAb-treated mice; open histogram represents cells isolated from GITRL-Fc-treated mice. Percentages of Ki67$^+$ cells per treatment are indicated. (C) TDLN cells were isolated on days 3, 7, and 10 after treatment with isotype control antibody or GITRL-Fc. CD4$^+$Foxp3$^−$ and CD8$^+$ T effector-to-CD4$^+$Foxp3$^+$ Treg cell ratios were determined by flow cytometry. Similar data were obtained in two independent experiments performed. *, $P < 0.05$; **, $P < 0.01$.

3.4.4 Incompletely-activated T effector cells accumulate in the TME by day 10 following GITRL-Fc treatment.

Given these data, we next hypothesized that T effector cell expansion in the TDLN upon GITRL-Fc treatment would correlate with increased frequencies of these cells in the TME, particularly since GITR was highly-expressed by $CD4^+Foxp3^-$ and $CD8^+$ TIL (Figure 9B). Notable increases in T effector cell frequencies versus control mAb-treated animals, however, were only detected in the TME at day 10 post-treatment, with highly-significant increases identified in the $CD8^+$ T cell subset (9.6 ± 2.7% versus 5.6 ± 1.8%, respectively; $P < 0.01$; Figure 12A). Upon further examination, Ki67 expression was unaltered in $CD4^+CD25^-$ and $CD8^+$ TIL isolated from GITRL-Fc- versus isotype mAb-treated mice (data not shown), suggesting that T effector cell accumulation in the TME of treated mice is most likely a result of enhanced recruitment of these cells, rather than TIL expansion *in situ*. The cumulative data from our longitudinal analyses are consistent with a model in which T effector cells expand in the TDLN, peaking at day 7 after GITRL-Fc treatment (Figure 10A), followed shortly thereafter (i.e. day 10 post-treatment) by infiltration/recruitment of these cells into the TME (Figure 12A).

Similar to the unique activation phenotype we observed in the TDLN following GITRL-Fc therapy, $CD4^+Foxp3^-$ (data not shown) and $CD8^+$ T cells (Figure 12B) in the TME of GITRL-Fc-treated animals up-regulated the activation marker CD25, but failed to secrete elevated levels of IFN-γ upon *in vitro* stimulation (Figure 12C). Additionally, no substantial alterations in CD69, CD44, or CD27 expression were observed (data not shown). Although the activation phenotypes were not identical in the TDLN and TME (unchanged CD25 expression but enhanced IFN-γ production in the former, enhanced CD25 expression but unchanged IFN-γ production in the

latter), T cells isolated from either the TDLN or TME of treated mice did not appear to be fully activated as a consequence of GITRL-Fc-based therapy.
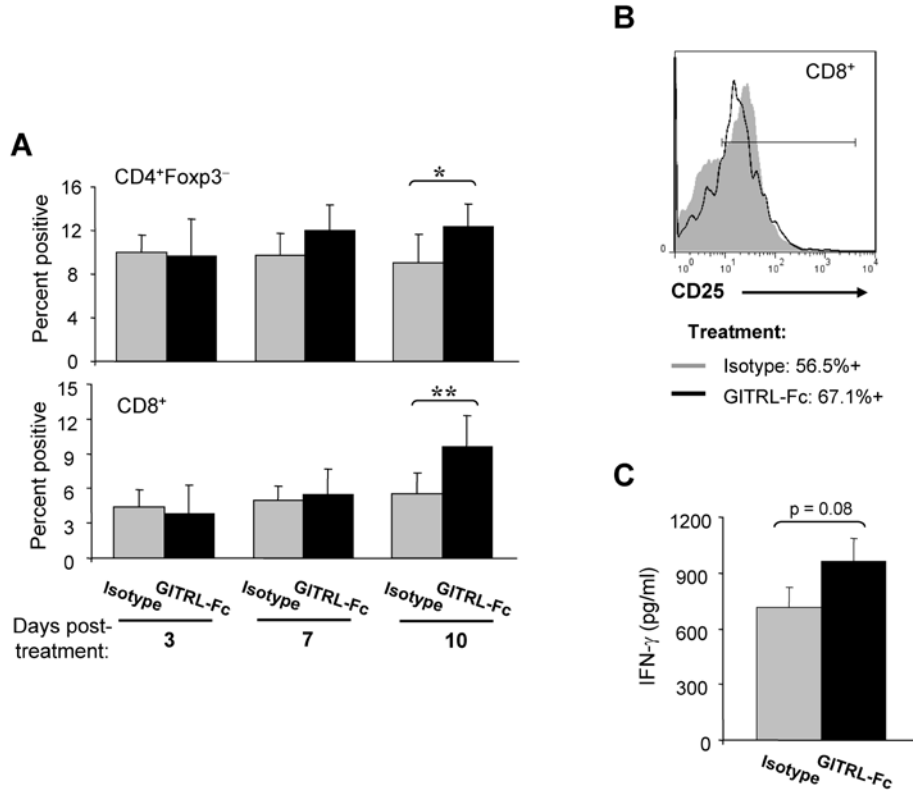
Figure 12. Accumulation of incompletely-activated T effector cells in the TME by day 10 following GITRL-Fc treatment.

(A) TME cells were isolated on days 3, 7, and 10 after treatment with isotype control antibody or GITRL-Fc ($n = 3$-6 per group). Percentages of CD4$^+$Foxp3$^-$ and CD8$^+$ T cells among gated live cells are reported as the mean $\pm$ SD. (B) CD25 was evaluated on gated CD8$^+$ cells isolated from the TME on day 10 after treatment (representative histogram is shown). Filled histogram represents cells isolated from isotype control mAb-treated mice; open histogram represents cells isolated from GITRL-Fc-treated mice. Percentages of CD25$^+$ cells per treatment are indicated. (C) TME cells were isolated on day 10 after treatment with isotype control antibody or GITRL-Fc and stimulated with anti-CD3 for 72 hours. Supernatants were then assessed for levels of IFN-γ, with data reported as the mean $\pm$ SD of duplicate determinations. Values correspond to one animal (representative of two total) per group. Data are representative of results obtained in 2 independent experiments in each case. *, $P < 0.05$; **, $P < 0.01$.

3.4.5 Decreased Treg frequencies results in an elevated effector-to-regulatory T cell ratio in the TME following GITRL-Fc treatment.

In accordance with two recent reports (230, 232), the frequency of $CD4^+Foxp3^+$ T cells in the TME of GITRL-Fc-treated mice was reduced as early as day 3 post-treatment, and remained low throughout the observation period (Figure 13A), despite elevated frequencies of these cells observed in the TDLN (Figure 11A). Simultaneous increases in $CD4^+Foxp3^-$ and $CD8^+$ TIL frequencies and decreases in $CD4^+Foxp3^+$ T cell frequencies after GITRL-Fc treatment resulted in enhanced effector-to-regulatory T cell ratios in the TME (Figure 13B). This observation is of particular therapeutic importance, as effective cancer immunotherapies have been largely associated with enhanced intratumoral T effector cell-to-Treg ratios (215). To ensure that alterations in the effector-to-regulatory balance at the cellular level correlated with alterations at the RNA level, factors associated with Type-1 T cell activity (i.e. T-bet and IFN-γ) and those associated with regulatory T cell activity (i.e. Foxp3 and IL-10) were assessed for their relative levels of expression in TIL isolated on days 3-10 following GITRL-Fc- versus control mAb-treatment. Using quantitative RT-PCR, moderate increases in the effector-to-regulatory gene transcript ratios were observed for both transcription factors (T-bet/Foxp3) and cytokines (IFN-γ/IL-10) (Figure 13C). Together, these data indicate that GITRL-Fc treatment skews the balance between the effector and regulatory arms of immunity within the TME in favor of Type-1 T cell immunity at both the cellular and molecular level.
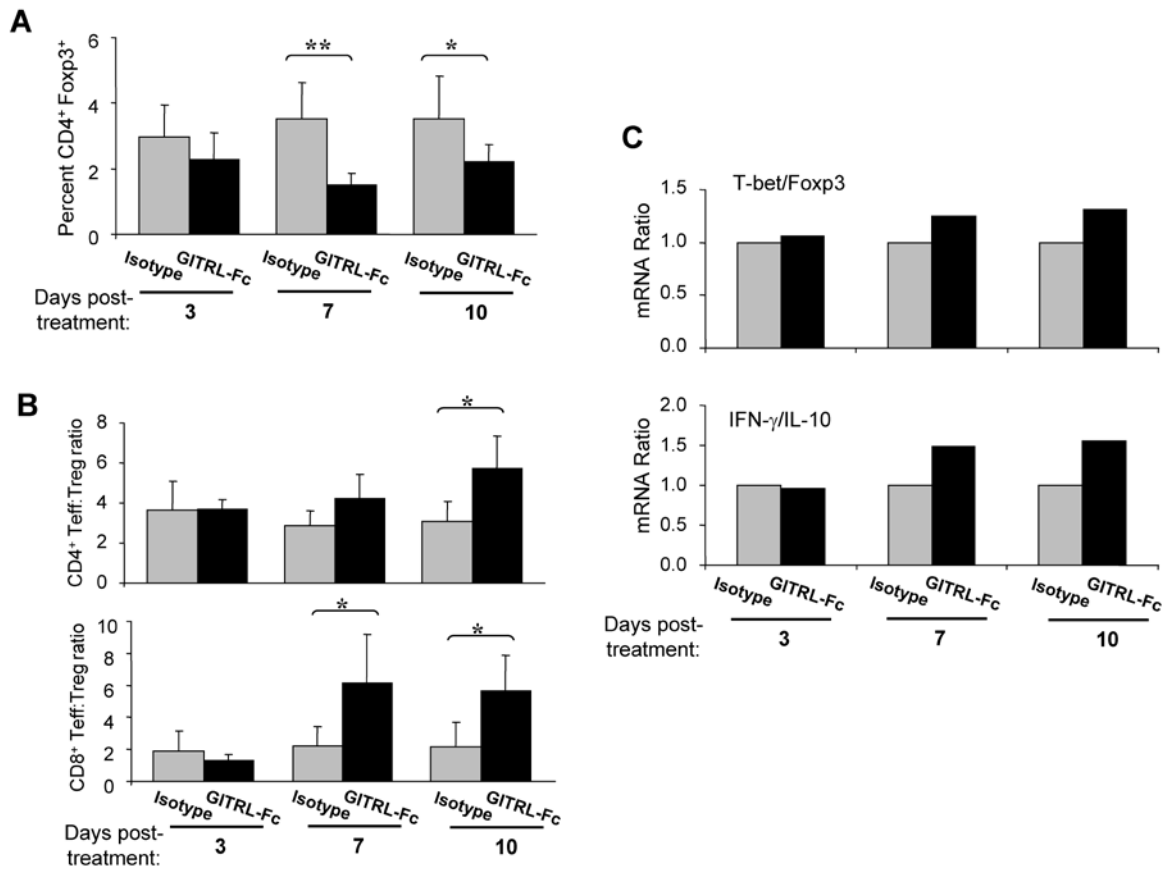
Figure 13. Increased effector-to-regulatory T cell ratios in the TME following GITRL-Fc treatment.

TME cells were isolated on days 3, 7, and 10 after treatment with isotype control antibody or GITRL-Fc. (A) Percentages of CD4$^+$Foxp3$^+$ T cells among gated live cells are reported as the mean ± SD (n = 3-6 per group). Data are representative of two independent experiments performed. (B) CD4$^+$Foxp3$^-$ and CD8$^+$ T effector-to-CD4$^+$Foxp3$^+$ Treg cell ratios were determined by flow cytometry. Similar data were obtained in two independent experiments performed. (C) Quantitative RT-PCR was performed on purified RNA (n = 2 per group, pooled) using primers specific for murine T-bet, Foxp3, IFN-γ, and IL-10. Relative RNA expression was determined for each gene ($2^{ΔΔCt}$) and ratios of T-bet/Foxp3 and IFN-γ/IL-10 expression, normalized to isotype control treatment, are depicted. *, $P < 0.05$; **, $P < 0.01$.

3.5   DISCUSSION

The anti-tumor efficacy of GITR agonists, particularly the anti-GITR mAb DTA-1, has already been widely explored in numerous murine tumor models (190, 232-234), although the vast majority of these treatment regimens were initiated within the first week following tumor cell inoculation. Due to the well-recognized failure of many immunotherapies that demonstrated safety and efficacy in the pre-clinical setting to bridge the gap between mice and men (163, 201), a priority of this study was to utilize an animal model with enhanced translational relevance. Schreiber and colleagues have described that tumor cell inoculation causes coagulation necrosis and acute inflammation during the first 10 days, creating the illusion of an established, palpable tumor (202). Only by about 2 weeks post-tumor inoculation have such artifacts been replaced by a mature tumor stroma, making these tumors indistinguishable from non-transplanted primary tumors. Following these recommendations, we began a short course of GITRL-Fc or DTA-1 therapy at day 17 post-tumor inoculation, when MCA205 tumors were approximately 50 mm^2 in size.

These tumors contained aberrant vascular structures, a hallmark of solid tumors (111), and high frequencies of mature (F4/80$^+$CD11b$^+$) and immature (Gr-1$^+$CD11b$^+$) myeloid cells (typically 15% and 20% of total TME cells, respectively) (data not shown). Using this salient disease model, we were able to show that both GITRL-Fc and DTA-1 therapy can induce the regression of well-established day 17 CMS4 (H-2^d), but not MCA205 (H-2^b) sarcomas. Two potential explanations exist for this discrepancy. First, despite injection of equivalent numbers of either MCA205 or CMS4 tumor cells, MCA205 tumors were approximately 50 mm^2 in size at the time of treatment initiation, whereas CMS4 tumors were slightly smaller (30 mm^2), indicating that MCA205 grows more aggressively and may be inherently more difficult to treat

than CMS4. In this regard, the TME of MCA205 and CMS4 may also be differential with regard to the balance of protective versus suppressive immunity, mechanisms by which these immune cell populations mediate their functions, and general responsiveness to immunotherapy. However, our recent results employing an OX40 agonist-based therapy, which successfully treated both day 17 MCA205 and CMS4 models (235), would argue against this latter point. Second, given the appreciated immune polarization differences between C57BL/6 (more Type-1 biased) and BALB/c (more Type-2 biased) strains of mice (236), the mechanism of action for therapeutic GITR agonists could be somewhat different when comparing the MCA205 versus CMS4 models. In order to identify the factors underlying strain-specific responsiveness to GITR-based therapy, we are currently investigating the molecular and cellular alterations associated with GITRL-Fc treatment in greater detail in the CMS4 model.

A longitudinal analysis was conducted to address the consequences of GITRL-Fc therapy on T cell subsets in the TDLN. Based on the observation that $CD4^+Foxp3^+$ T cells in the TDLN express high levels of GITR, it was not unexpected that these cells exhibited rapid and sustained proliferation in response to GITRL-Fc treatment. Previous studies have found that Tregs expanded *in vitro* as a result of GITR stimulation lose their suppressor activity (208), suggesting that expanded $CD4^+Foxp3^+$ TDLN T cells in our model may be functionally silenced by GITRL-Fc treatment. Although T effector cells in the TDLN were primarily $GITR^{low}$ in phenotype, by day 7 following GITRL-Fc treatment we observed significant increases in the absolute numbers of both $CD4^+Foxp3^-$ and $CD8^+$ T cells that express elevated levels of Ki67. Because $CD4^+Foxp3^+$ T cells are the only plausible target for GITRL-Fc in the TDLN, T effector cell expansion at this site is most likely attributable to GITR-mediated inactivation of Treg function

and subsequent restoration of the proliferative capacity of TDLN T effector cells. This hypothesis is being tested in ongoing studies.

Notably higher frequencies of CD4$^+$Foxp3$^-$ and CD8$^+$ T effector cells exhibited a GITR^{hi} phenotype within MCA205 tumor lesions when compared to the TDLN, and GITRL-Fc treatment resulted in elevated frequencies of these cells by day 10 post-treatment. This did not correlate with an up-regulation of Ki67 expression in T cells, however, suggesting that T cell accumulation in the tumors of treated mice is principally the result of enhanced recruitment—presumably from the TDLN—and not proliferation of these T cells within TME. In contrast, CD4$^+$Foxp3$^+$ T cell frequencies were significantly diminished in the TME of GITRL-Fc-treated mice, consistent with the recent observations of Cohen and colleagues in a B16 melanoma model (230). Through adoptive transfer experiments and the utilization of Foxp3-GFP transgenic mice, they were able to convincingly show that DTA-1 treatment both inhibits Treg recruitment into tumors and down-regulates Foxp3 expression in tumor-localized Treg. One or both of these mechanisms likely plays a role in the GITRL-Fc-induced decrease in CD4$^+$Foxp3$^+$ TIL observed in our sarcoma model.

It has been previously shown in murine tumor and autoimmune disease models that GITR stimulation is sufficient to support T cell activation and the development of T effector function *in vivo* (151, 191, 226, 232), whether as a result of direct engagement of GITR on these cells or via the inactivation of bystander Tregs. Surprisingly, we found that T cells isolated from the TDLN and TME of GITRL-Fc- versus control mAb-treated animals were not activated to the extent that would be expected from these previous reports. Differences between experimental models, such as variations in GITR agonist dosing schedules and routes of administration, may be responsible for these seemingly contrasting findings. Furthermore, one must also consider that previous

studies have primarily used the agonist mAb DTA-1, while we have employed a recombinant version of the natural GITR ligand, which may convey at least slightly different signals into GITR^{hi} target cells.

Importantly, in contrast to many former models, GITR-based therapy in our study was not initiated until tumors became well-established, in accordance with the stringent definition established by Schreiber *et al.* (202). Particularly in the setting of progressive disease, numerous regulatory mechanisms are responsible for maintaining immune tolerance in the tumor-bearing host. First, tumor-specific T cells can be rendered anergic or hyporesponsive if priming occurs under suboptimal conditions in the TDLN (74, 76). Moreover, efficiently-primed T cells can lose effector function upon infiltration of tumor lesions as a result of defective TCR signaling (81). In addition to these T cell-intrinsic mechanisms of suppression, T effector cell activity can also be inhibited extrinsically by Tregs and myeloid-derived suppressor cells (MDSC), both of which can be found at high frequencies in the TDLN and TME (102, 104, 237). Perhaps it is not surprising then if GITRL-Fc as a monotherapy, at least in the MCA205 tumor model, is unable to counteract this plethora of immunosuppressive factors in order to elicit robust T cell activation.

Overall, the apparent heterogeneous efficacy of single modality GITR agonist treatment in our tumor models suggests that uniform therapy benefits may be best observed using combinational treatment regimens. Reagents that allow complete T cell activation, such as T cell checkpoint blockade inhibitors (i.e. anti-CTLA-4 and anti-PD-1), represent logical co-therapies for combination with GITR agonists (238-240). Indeed, a recent report showed that anti-CTLA-4/anti-GITR mAb combination treatment provides improved benefits, such as the regression of 150 mm^2 s.c. CT26 colon carcinomas. However, treatment was initiated at day 4 day post-tumor

inoculation in this study, at which point a mature TME would not be in place (232). We are

currently evaluating such treatment options in our day 17 sarcoma models.

4.0   SUMMARY & INTERPRETATIONS

4.1   PROPOSED MODEL

Despite similarities in the structure, surface expression, and downstream signaling pathways of the T cell costimulatory molecules OX40 and GITR (5), our findings demonstrate that OX40 and GITR agonists exhibit variable therapeutic efficacy in the setting of established tumors and function through subtly distinct immunologic mechanisms. While a short course of OX40L-Fc or GITRL-Fc therapy elicited potent anti-tumor immunity against day 17 CMS4 (H-2^d) sarcomas, resulting in over 80% tumor-free survival, treatment with either of these costimulatory agonists was only able to induce MCA205 (H-2^b) tumor rejection in less than 10% of treated mice. Notably, though, 50% of OX40L-Fc-treated mice exhibited small, barely palpable lesions that remained "dormant" for more than 6 weeks, before eventually progressing, while animals that didn't initially reject their tumors upon GITRL-Fc treatment (approximately 80%) succumbed to progressive disease by day 50 post-tumor inoculation. Therefore, although overall survival against MCA205 tumors was equivalent in OX40L-Fc- and GITRL-Fc-treated animals, progression-free survival was considerably enhanced by the OX40 agonist.

Similar expression patterns of OX40 and GITR were observed on T cells isolated from untreated tumor-bearing mice. Consistent with the existing literature, CD4$^+$Foxp3$^+$ Tregs were observed to constitutively express both costimulatory molecules (127), while CD4$^+$Foxp3$^-$ and

79

CD8^{+} T effector cells within tumor lesions, but not the TDLN, were found to up-regulate OX40 and GITR expression. Unexpectedly, however, OX40 was highly up-regulated on CD11c^{+}CD11b^{+}ClassII^{hi} tumor-infiltrating DC (TIDC). Although DC expression of OX40 had not been previously described, 4-1BB, an additional member of the costimulatory TNFR family, can be expressed by activated DC (223). In our preliminary studies, GITR did not appear to be up-regulated by TIDC (unpublished data). Since an exhaustive characterization of OX40 and GITR expressing cells in tumor-bearing mice was not conducted, we cannot rule out the possibility that alternative cell subsets represent additional targets of OX40- and GITR-based therapies.

Through our longitudinal evaluation of OX40L-Fc-dependent alterations in the TDLN and TME of wild-type and T cell-deficient mice (Rag^{−/−}), we were able to characterize a series of sequential cellular and molecular events that likely contribute to the potent anti-tumor efficacy displayed by this reagent (Figure 14A). As early as day 3 post-treatment, accumulation of mature, CCR7^{+} DC was observed in the TDLN, in addition to coordinate up-regulation of chemokine and adhesion molecule expression by endothelial cells (VEC) in the TME. Both of these events occurred in a T cell-independent manner and are likely a direct result of OX40 ligation on these cells, as DC, and potentially VEC, were observed to be OX40^{+} in the TME. The secondary phase of this response, starting approximately 7 days after treatment, involved profound expansion of CXCR3^{+}CD44^{hi} T effector cells, which may be a consequence of: i.) enhanced cross-priming by activated, TDLN-infiltrating DC, ii.) direct engagement of OX40 on these cells, and/or iii.) inactivation of TDLN CD4^{+}Foxp3^{+} Treg (see discussion below). Finally, by day 10 post-treatment, Type-1 polarized T cells that secrete high levels of IFN-γ and exhibit a re-activated memory phenotype had accumulated in the tumors.
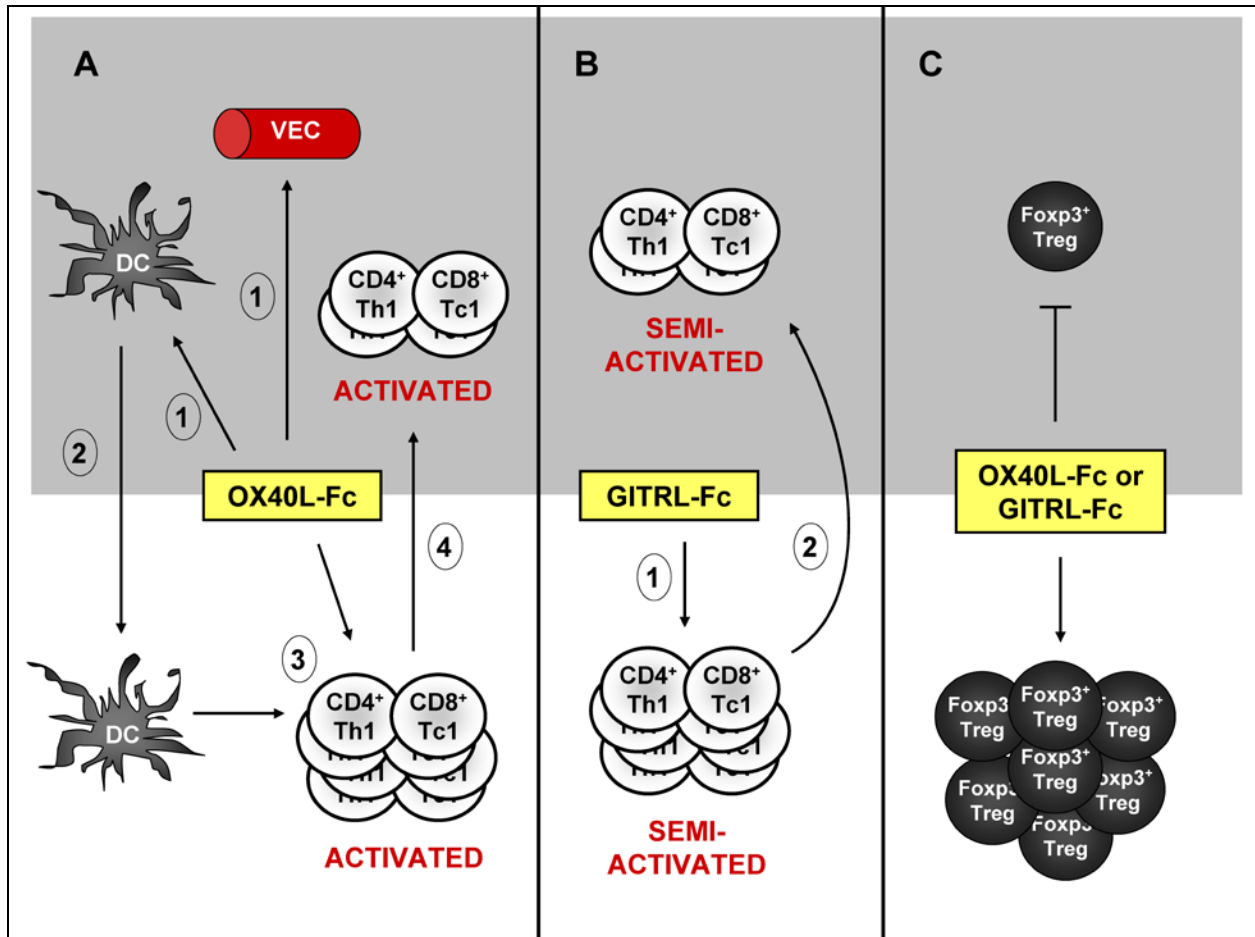
Figure 14. Pleiotropic and sequential effects of OX40L-Fc and GITRL-Fc treatment in tumor-bearing mice. Shaded upper area represents the tumor microenvironment, unshaded lower area represents the TDLN. (A) OX40L-Fc transmits maturation and migration signals into OX40$^+$ DC and, independently of T cells, induces CXCL9 and VCAM-1 expression by OX40$^+$ VEC (1). Myeloid DC accumulate in the TDLN and express elevated levels of CD80 and CCR7 in a T cell-independent manner (2). CXCR3$^+$CD44^{hi} T effector cells proliferate within the TDLN (3). Activated T effector cells are recruited to and infiltrate the TME, facilitated by treatment-dependent CXCL9 and VCAM-1 up-regulation and vascular normalization (4). (B) T effector cells proliferate within the TDLN, but exhibit a partially activated phenotype (1). Incompletely-activated T effector cells are recruited to and infiltrate the TME (2). (C) Either OX40L-Fc or GITRL-Fc treatment induces rapid and sustained proliferation of CD4$^+$Foxp3$^+$ Tregs in the TDLN, while diminished frequencies of these cells in the TME were observed throughout the observation period following treatment with either of the costimulatory agonists.

Similar to OX40L-Fc treatment, T effector cells expanded within the TDLN of GITRL-Fc-treated mice at day 7 post-treatment (Figure 14B). Contrary to *in vivo* OX40 stimulation, however, GITR signaling was unable to fully activate these cells. Some indicators of activation were present (i.e. enhanced IFN-γ production versus isotype-treated controls upon *ex vivo* stimulation), whereas others were not (i.e. no changes in CD69, CD44, or CD27 expression). As in the OX40L-Fc treatment model, T effector cells expressing low levels of Ki67 accumulated in the TME by day 10 following GITRL-Fc treatment, suggesting that this event is most likely attributed to the enhanced recruitment of these cells, rather than to their expansion within tumor lesions. As in the TDLN of these animals, however, suboptimal activation of TIL was observed in response to GITRL-Fc administration. At this point, it is not clear why OX40L-Fc is capable of inducing more robust T cell activation compared to GITRL-Fc, although it could easily be hypothesized that the ability or inability of these reagents, respectively, to stimulate DC plays an important role. In other words, by stimulating DCs to migrate from the TME to the TDLN, OX40L-Fc treatment provides both signals 1 and 2 to TDLN T cells, while in the GITRL-Fc treatment model, the amount of tumor antigen being presented to TDLN T cells at the time of GITR costimulation is insufficient to allow complete T cell activation. Although preliminary, these comparative results suggest that the most therapeutically efficacious costimulatory agonists will be capable of harnessing both innate and adaptive arms of the immune system.

Given the low levels of OX40 and GITR expression on CD4$^+$Foxp3$^-$ and CD8$^+$ TDLN T effector cells, the observation that these cells proliferate profoundly in the TDLN of both OX40L-Fc- and GITRL-Fc-treated mice was slightly unexpected. In the OX40L-Fc treatment model, it could be postulated that TCR stimulation by TDLN-infiltrating DC at day 3 post-treatment induces OX40 up-regulation on T cells by day 7, at which point they can respond to

OX40L-Fc stimulation and proliferate accordingly. This is consistent with the observation that OX40 expression by T cells peaks approximately 3 days following TCR engagement (5). However, GITRL-Fc therapy induced similar levels of TDLN T effector cell expansion (without the corresponding DC alterations), suggesting that DC stimulation may be necessary for costimulatory therapy-mediated activation, but not proliferation, of T effector cells.

An alternative, and more plausible, explanation is that T cell expansion in the TDLN of treated mice is a consequence of OX40L-Fc- and GITRL-Fc-mediated disruption of the regulatory T cell compartment. Indeed, a common effect of both OX40- and GITR-based therapies was rapid and sustained proliferation of Tregs in the TDLN (Figure 14C). This was not surprising, though, based on the observation that $CD4^+Foxp3^+$ T cells in the TDLN express high levels of OX40 and GITR. It has been previously demonstrated that *in vitro* stimulation of Tregs, which are naturally anergic, induces proliferation of these cells, but also abrogates their suppressor activity (241), suggesting that expanded $CD4^+Foxp3^+$ TDLN T cells in our model may be functionally silenced by both OX40L-Fc and GITRL-Fc treatment. This impairment of Treg functionality would hypothetically restore the proliferative capacity of TDLN T effector cells. Future studies should address the suppressive activity of $CD4^+Foxp3^+$ TDLN T cells isolated from treated mice.

Interestingly, despite profound expansion of $CD4^+Foxp3^+$ T cells in the TDLN of animals treated with either OX40 or GITR agonists, the frequency of these cells in the TME was reduced as early as day 3 post-treatment and this level remained low throughout the observation period (Figure 14C). Although the reason(s) for these contradictory effects of costimulatory treatment on $CD4^+Foxp3^+$ T cells in the TDLN versus the TME are presently undefined, this remains an active area of investigation. In both OX40L-Fc and GITRL-Fc treatment models, however, the

coordinate increase of T effector cells and decrease in Tregs in the TME resulted in skewing of the intratumor balance between the effector and regulatory arms of immunity in favor of Type-1 T cell immunity, at both the cellular and molecular (i.e. mRNA) level. Importantly, elevated intratumoral T effector cell-to-Treg ratios are associated with favorable prognosis in both mice and humans (215, 242).

4.2   COSTIMULATORY COMBINATIONS

Based on our observation that T cells isolated from the TDLN and TME of OX40L-Fc-treated mice up-regulated CD44 expression and produced significantly higher levels of IFN-γ upon *in vitro* stimulation versus cells harvested from control mAb-treated mice (235), we hypothesized that addition of OX40L-Fc to our GITRL-Fc treatment regimen would overcome the limitations of GITRL-Fc monotherapy (i.e. impaired T cell activation) and elicit synergistic anti-tumor effects. In a pilot study, C57BL/6 mice bearing established MCA205 sarcomas were treated on days 17 and 20 post-tumor inoculation with isotype mAb control, GITRL-Fc, OX40L-Fc, or the combination of GITRL-Fc/OX40L-Fc. Upon assessment of progression-free survival, OX40L-Fc, with or without GITRL-Fc, as compared with GITRL-Fc alone, demonstrated marginally improved therapeutic benefit. Although preliminary, these data suggest that the efficacy of OX40L-Fc was not improved by the addition of GITRL-Fc. As hypothesized, however, the addition of OX40L-Fc moderately enhanced the anti-tumor efficacy of GITRL-Fc. This may be attributable to superior DC and/or T cell activation mediated by OX40L-Fc, but not GITRL-Fc, therapy. Future experiments will explore the molecular and cellular alterations associated with GITRL-Fc/OX40L-Fc combination therapy. To our knowledge, OX40 and GITR dual

costimulation has not previously been studied *in vitro* or as a therapy regimen in preclinical tumor models. Therefore, the therapeutic potential of combinational OX40L-Fc/GITRL-Fc treatment should not yet be dismissed, as the lack of synergistic activity observed in this pilot study may be specific to our tumor model and/or dosing schedule.

Despite these results, alternative combinations of costimulatory signals, most notably OX40/4-1BB dual costimulation, have been shown by other groups to elicit synergistic T cell activity. Combinations of 4-1BB and OX40 agonists have been investigated in pre-clinical tumor models by numerous groups (243, 244). In one case, all mice bearing late-stage hepatic metastases died within 50 days post-tumor inoculation following treatment with either 4-1BB or OX40 monotherapies, whereas a 21.4% survival rate at day 180 was observed in the two agent-based design (173). More recently, Dubrot and colleagues demonstrated that subcutaneous injection of hybridomas that secrete both anti-4-1BB and anti-OX40 mAbs were therapeutically superior to treatments using hybridomas that produced only one of these antibodies (245). Upon evaluation of the mechanism underlying such synergistic effects, it was determined that *in vitro* 4-1BB costimulation was sufficient to drive clonal expansion of $CD8^+$ T cells, but that acquisition of full Tc1 effector function required coordinate 4-1BB & OX40 triggering (138). Although it is tempting to draw comparisons between these data and our own (i.e. GITR signals, potentially akin to 4-1BB signals, induce T cell proliferation, but OX40 stimulation is necessary for optimal activation), further analysis of the mechanisms supporting superior efficacy of dual OX40/GITR costimulation is clearly warranted. Cumulatively, however, these data indicate that approaches integrating multiple costimulatory agonists, particularly those incorporating activators of the 4-1BB and OX40 costimulatory pathways, hold significant potential in the treatment of malignant disease.

4.3 COSTIMULATORY AGONISTS IN THE ADJUVANT SETTING

In accordance with our findings that OX40L-Fc enhances the immunostimulatory capacity of TIDC, one would hypothesize that certain combinational strategies would further exploit the beneficial role of DC in OX40-based therapy. Indeed, a synergistic relationship between soluble OX40L and GM-CSF, an important DC mobilization factor, has been previously demonstrated (169). Furthermore, provision of Toll-like receptor agonists that support DC maturation and function may also prove beneficial when administered in parallel with OX40 agonists. In support of this notion, intratumoral injection of CpG oligodeoxynucleotides, which bind TLR9 expressed by DC and other APC, was found to elicit synergistic anti-tumor immunity upon combinational treatment with an agonist OX40 mAb (246).

Since the immune-stimulating properties of costimulatory TNFR agonists, including those targeting OX40, GITR, and 4-1BB, are short-lived and rely on the pre-existence of tumor-primed T cells in the tumor-bearing host, the therapeutic benefit of these treatment modalities will likely be optimized when used in combination with alternate forms of cancer therapy (6). For example, addition of recombinant IL-12 or IL-12 gene therapy to TNFR regimens has proven to be an effective combination, likely via its coordinate promotion of both innate and adaptive Type-1 immune responses. Several reports suggest that 4-1BB-mediated therapy is synergistically enhanced when combined with IL-12 gene therapy (247-250). It has been proposed that IL-12 initially activates NK cells to secrete IFN-γ, inducing DC to up-regulate 4-1BB and mature into efficient antigen presenting cells upon administration of 4-1BB agonist co-therapy (248). If NK cell-produced IFN-γ is also capable of inducing OX40 up-regulation by DC, it is highly likely that combinational OX40L-Fc and IL-12 therapy will demonstrate

86

synergistic anti-tumor efficacy. Recombinant IL-12 was recently found to enhance OX40 agonist therapy in a T cell-intrinsic manner, although additional therapeutic contributions from innate immune cells were not assessed in this study (251). Novel combinational regimens incorporating alternative cytokines that promote T effector cell survival and function is also highly recommended based on the cumulative data from our lab and others. As an example, IL-15 has recently been shown to up-regulate GITR expression on $CD8^+$ T cells, while IL-7-mediated up-regulation of OX40 was observed in $CD4^+$ T cells, leading in both cases to an expanded T cell memory pool (135). However, to our knowledge the combination of GITR agonists and IL-15 or OX40 agonists and IL-7 has not been studied as a therapy regimen in pre-clinical tumor models.

One could also readily postulate combinational costimulatory agonist protocols that would improve the efficacy of adoptively transferred (i.e. *ex vivo* expanded or TCR-engineered) anti-tumor T cells into the TME. A unique strategy employed by Carl June and colleagues consists of genetically engineering T cells to express antibody-based external receptors and cytosolic regions that contain TCR and CD28 intracellular signaling domains. These "chimeric antigen receptors," or CARs, bind molecules expressed on the surface of tumor cells in an MHC-unrestricted manner. Notably, CAR-expressing T cells modified to contain the 4-1BB signaling domain displayed prolonged survival *in vivo* and superior therapeutic efficacy compared to cells lacking the 4-1BB signaling component (252). Furthermore, as numerous studies suggest that tumor-specific T cells are rendered non-responsive upon infiltration of the tumor microenvironment (206), a reasonable approach to re-activate such T cells would be to conjugate costimulatory agonists to tumor-targeting antibodies. For example, Zhang *et al*. demonstrated that 4-1BBL conjugated to TNT-3, a nuclear antigen present in necrotic tumor cell debris,

prolongs survival of tumor-bearing mice versus animals treated with an untargeted 4-1BBL construct (253).

Since TNFR engagement occurs in an antigen-independent manner, provision of signal 1 (tumor antigen) by vaccination would allow therapeutic costimulation to preferentially enhance the development of specific anti-tumor T cells. In other words, by integrating both passive and active immunotherapeutic strategies, perhaps coadministration of costimulatory agonists and cancer vaccines represents the combinational approach with greatest therapeutic potential. Two independent groups effectively treated tumor-bearing mice with vaccines consisting of tumor cells transduced to express the Fv fragment of agonistic 4-1BB mAb, leading to enhanced tumor-specific immunity as a result of the coordinate provision of cognate antigen and costimulation by these engineered APC (254, 255). In addition, GM-CSF-transduced tumor cell vaccines can synergize with OX40 stimulation by preferentially enhancing the development of tumor-specific immunity (175). Moreover, B16 tumor-bearing mice treated with a control TRP-2-presenting DC vaccine succumbed to progressive tumor growth by day 50, whereas vaccination with similar DC that were engineered to secrete an agonist GITR mAb resulted in 60% survival by day 100 (256). An alternative approach that is conceptually similar to active vaccination involves the promotion of "immunogenic" tumor cell death by chemotherapy, radiotherapy, or engagement of the apoptotic TNFR family member DR5 (TRAIL receptor) on tumor cells. Indeed, these cytotoxic regimens appear to yield synergistic benefits when combined with 4-1BB (257-259), OX40 (260), and GITR (261) agonist therapies. In a recent study with particular relevance to our OX40L-Fc treatment model, it was reported that conjugation of tumor antigen to 4-1BBL allowed specific targeting of 4-1BB-expressing DC, resulting in enhanced tumor antigen uptake and cross-presentation (262). Therefore, manipulation of our OX40L-Fc reagent to serve as a

vehicle for tumor antigen delivery to OX40$^+$ TIDC would, at least in theory, simultaneously provide tumor antigen and OX40-mediated activation signals to these DC. The cumulative data presented here and by others indicate that TNFR-targeting therapeutics, administered as a monotherapy or in combinational regimens, possess high potential for the treatment of cancer, and it is anticipated that these modalities will shape the design of cancer immunotherapies in the coming years.
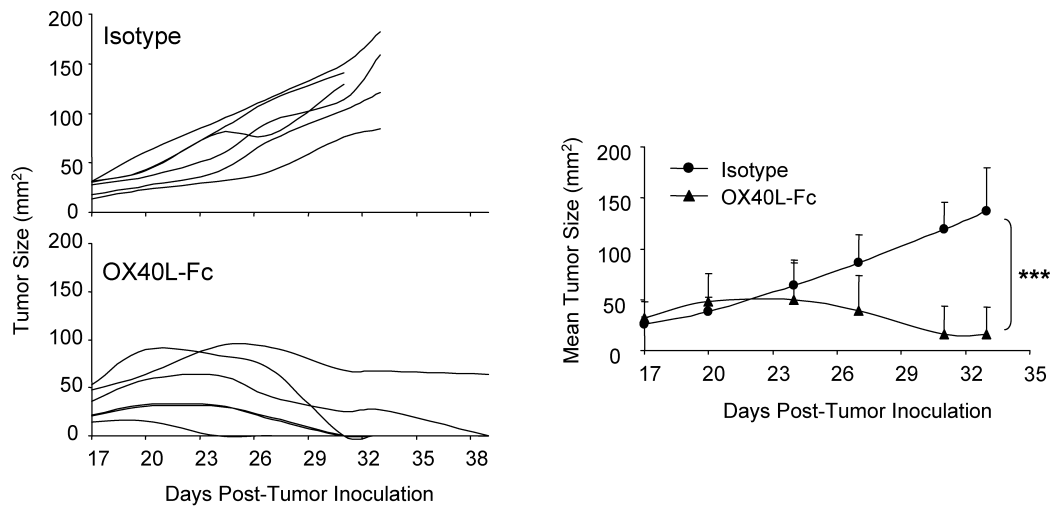
Appendix Figure 1. Systemic OX40L-Fc treatment: CMS4 tumor model.

CMS4 BALB/c sarcomas (n = 6 per group) were injected s.c. into the right flank. Mice bearing established day 17 tumors (~30 to 50 mm^2 in area) were treated i.p. with 100 μg of rat IgG isotype control antibody or OX40L-Fc, as indicated. Treatment was repeated on day 20 after tumor inoculation. Tumor areas (mm^2) were calculated every 3 days, with the data for individual animals (left panels) and mean tumor areas ± SD (right panel) depicted. Data are representative of two independent experiments performed. ***, $P < 0.001$.
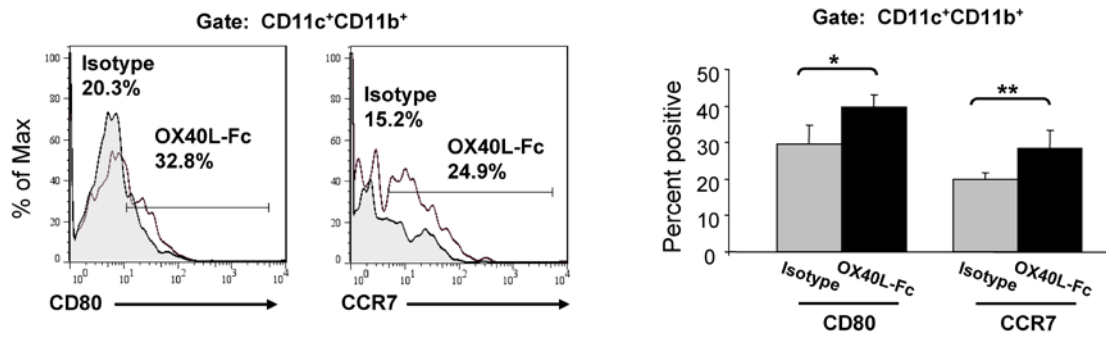
Appendix Figure 2. Up-regulation of CD80 and CCR7 expression on DC in the TDLN upon OX40L-Fc treatment. MCA205 tumor-bearing mice were treated on day 17 after tumor inoculation with isotype control antibody or OX40L-Fc and TDLN cells were isolated on day 3 after treatment. CD80 and CCR7 expression were evaluated on gated CD11c$^+$CD11b$^+$ DC. Representative histograms (right panel) and quantification (left panel) are shown. Filled histograms represent cells isolated from isotype control mAb-treated mice; open histograms represent cells isolated from OX40L-Fc-treated mice. One representative out of two independent experiments is depicted. *, $P < 0.05$; **, $P < 0.01$.
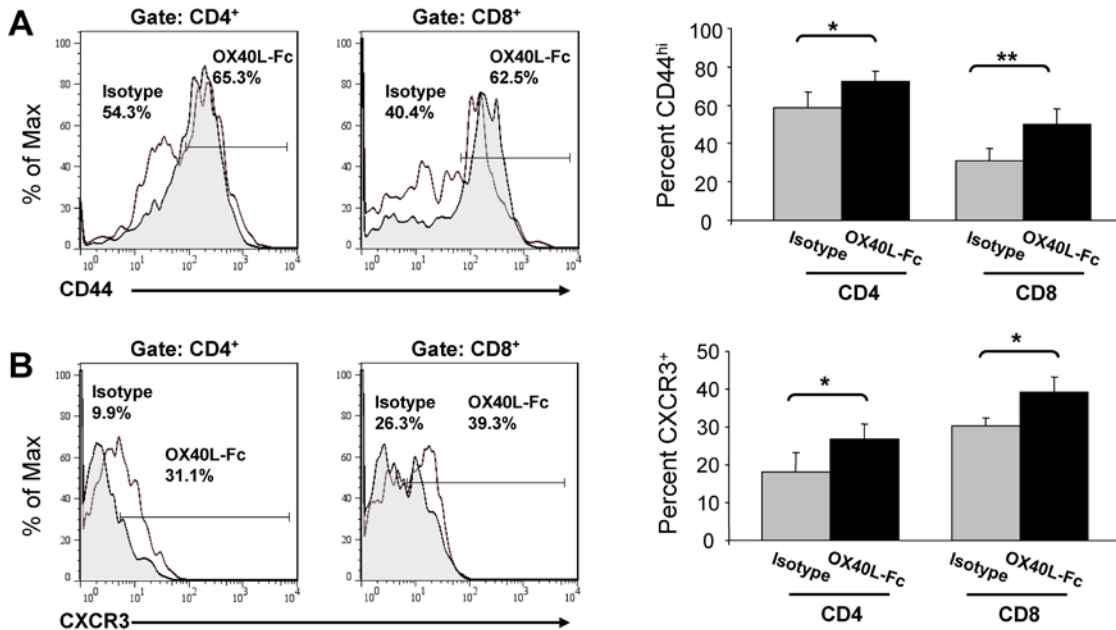
Appendix Figure 3. Phenotype of TDLN T cells on day 7 following OX40L-Fc treatment.

(A and B) TDLN cells were isolated on day 7 after treatment with isotype control antibody or OX40L-Fc. (A) Representative histograms (right panel) and quantification (left panel) of CD44^{hi} (A) and CXCR3^{+} (B) T cells are shown. (A) Open histograms represent cells isolated from isotype control mAb-treated mice; filled histograms represent cells isolated from OX40L-Fc-treated mice. (B) Filled histograms represent cells isolated from isotype control mAb-treated mice; open histograms represent cells isolated from OX40L-Fc-treated mice. Data are representative of two independent experiments performed. *, $P < 0.05$; **, $P < 0.01$.
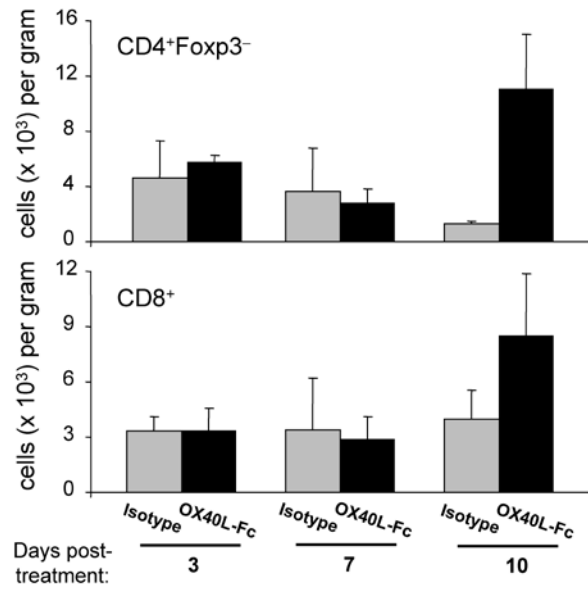
Appendix Figure 4. Longitudinal analysis of T effector cell numbers in the TME upon OX40L-Fc treatment.

TME cells were isolated on days 3, 7, and 10 after treatment with isotype control antibody or OX40L-Fc. Absolute

numbers (x 10^3) of CD4$^+$Foxp3$^-$ and CD8$^+$ TIL per gram of tumor are shown.
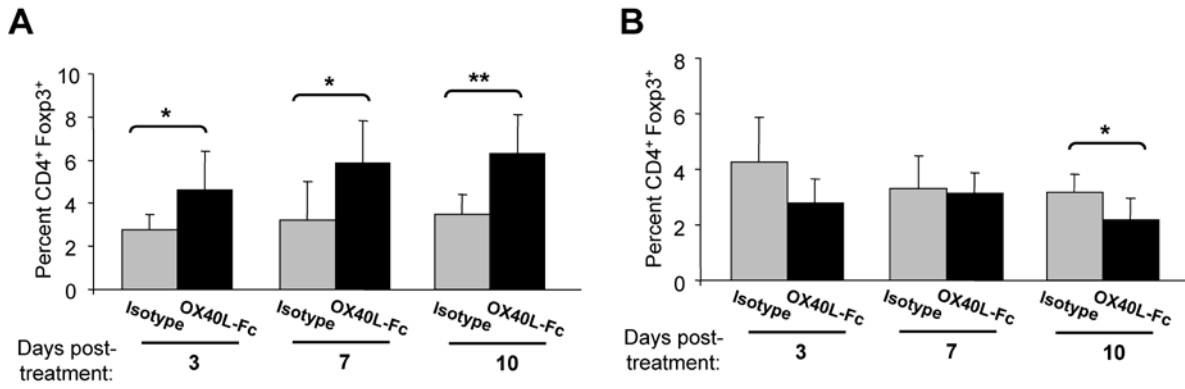
Appendix Figure 5. Longitudinal analysis of CD4$^+$Foxp3$^+$ T cell frequencies upon OX40L-Fc treatment.

(A) TDLN and (B) TME cells were isolated on days 3, 7, and 10 after treatment with isotype control antibody or OX40L-Fc. Percentages of CD4$^+$Foxp3$^+$ T cells among gated live cells are shown. Data are representative of three independent experiments performed. *, $P < 0.05$; **, $P < 0.01$.
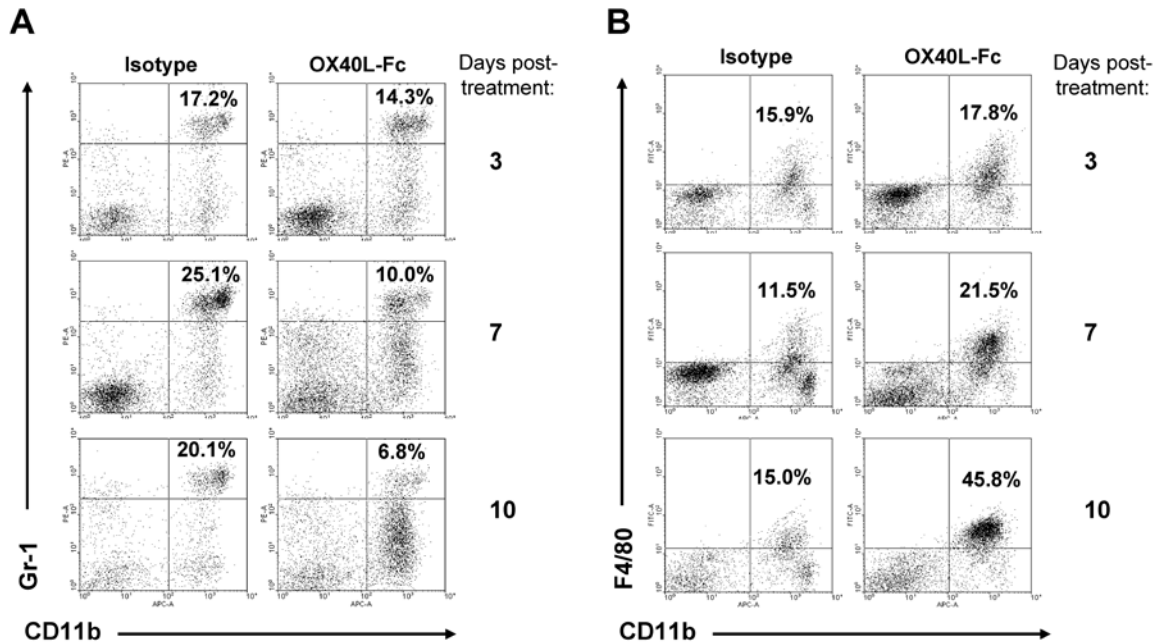
Appendix Figure 6. Alterations in CD11b^{+} monocyte populations following OX40L-Fc treatment.

TME cells were isolated on days 3, 7, and 10 after treatment with isotype control antibody or OX40L-Fc. (A) Representative staining of CD11b and Gr-1 on gated live cells is shown along with percentages of CD11b^{+}Gr-1^{+} cells. (B) Representative staining of CD11b and F4/80 on gated live cells is shown along with percentages of CD11b^{+}F4/80^{+} cells. The experiment was repeated two times with similar results.
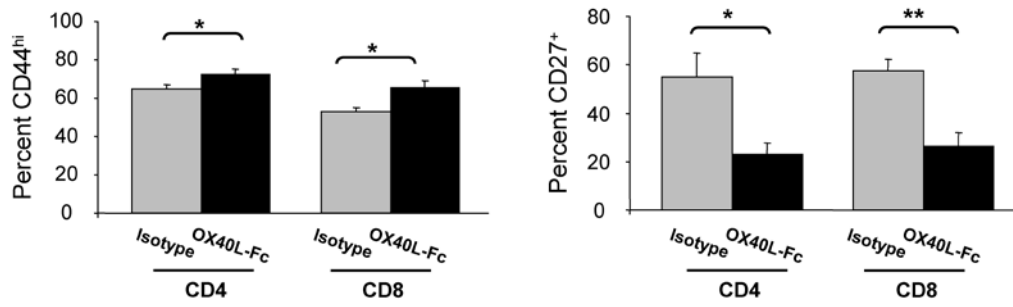
Appendix Figure 7. Phenotype of TIL on day 10 following OX40L-Fc treatment.

TME cells were isolated on day 10 after treatment with isotype control antibody or OX40L-Fc. Percentages of CD44^{hi} and CD27^{+} T cells are shown. Data are representative of two independent experiments performed. *, $P < 0.05$; **, $P < 0.01$.

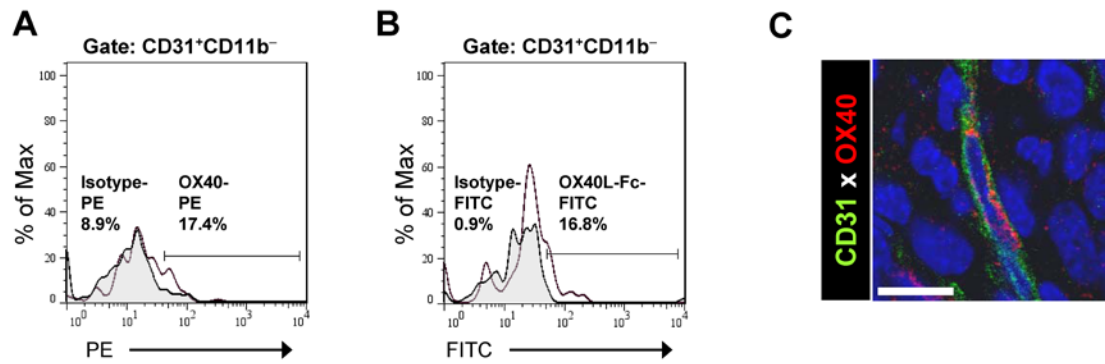**Appendix Figure 8.** Moderate OX40 expression by CD31$^+$CD11b$^-$ vascular endothelial cells in the TME.

(A and B) Single-cell suspensions were prepared from untreated MCA205 tumors (TME) resected between days 17 and 20 post-tumor inoculation. (A) Representative staining of OX40 on gated CD31$^+$CD11b$^-$ endothelial cells. Filled histogram represents control isotype staining. Percentages of OX40$^+$ cells are indicated. The experiment was repeated two times with similar results. (B) Representative staining of gated CD31$^+$CD11b$^-$ endothelial cells with FITC-labeled OX40L-Fc. Filled histogram represents control isotype staining. Percentages of OX40L-Fc$^+$ cells are indicated. The experiment was repeated two times with similar results. (C) Untreated MCA205 tumors were sectioned, stained and analyzed by confocal microscopy (as described in Materials and Methods). Representative staining of DAPI (blue), OX40 (red), and CD31 (green) is shown. Samples were analyzed by confocal microscopy with a 60x objective. Bar, 10 μm.
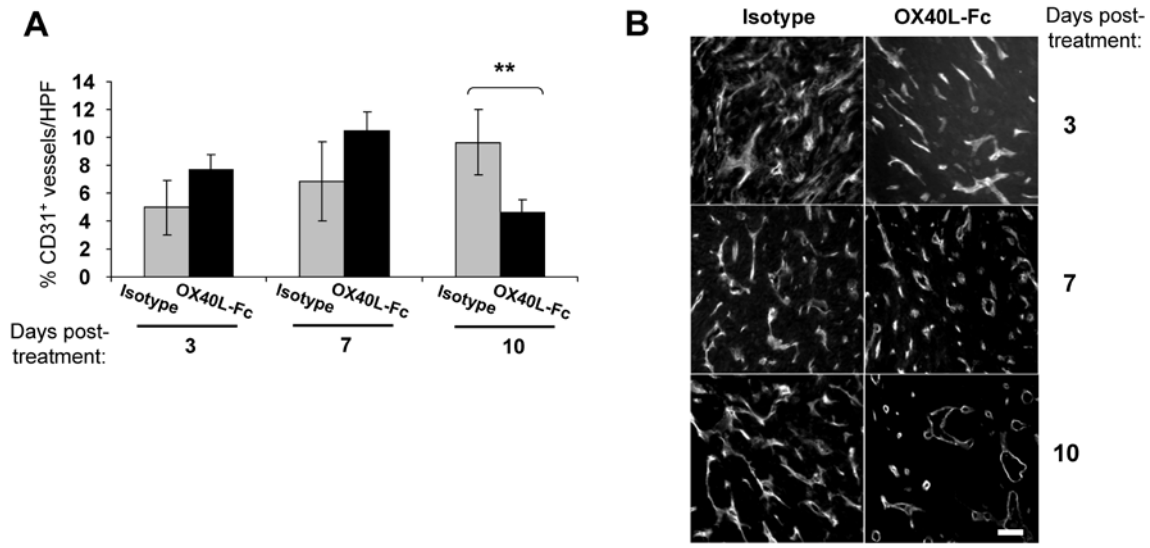
Appendix Figure 9. Normalized phenotype of tumor vasculature upon OX40L-Fc treatment.

MCA205 tumors were sectioned, stained and analyzed by immunofluorescence microscopy on days 3, 7, and 10 after treatment with isotype control antibody or OX40L-Fc. (A) The percentage of CD31$^+$ vessels per high-power field (HPF) within a representative tumor was quantified by Metamorph software. For each tissue section, 10 images were captured from non-overlapping image field areas. The percentage of CD31$^+$ cells was calculated as follows: (CD31$^+$ pixels per field / total pixels per field) x 100. **, $P < 0.0001$. (B) Tumor sections were single-stained for CD31. Samples were analyzed by immunofluorescence microscopy with a 20x objective and black and white images were acquired. Bar, 50 μm.

BIBLIOGRAPHY

1.   Dunn GP, Old LJ, Schreiber RD. The three Es of cancer immunoediting. Annu Rev Immunol 2004; 22: 329-60.

2.   Gajewski TF, Meng Y, Blank C, et al. Immune resistance orchestrated by the tumor microenvironment. Immunol Rev 2006; 213: 131-45.

3.   Kantoff PW, Higano CS, Shore ND, et al. Sipuleucel-T immunotherapy for castration-resistant prostate cancer. N Engl J Med 2010; 363: 411-22.

4.   Hodi FS, O'Day SJ, McDermott DF, et al. Improved survival with ipilimumab in patients with metastatic melanoma. N Engl J Med 2010; 363: 711-23.

5.   Watts TH. TNF/TNFR family members in costimulation of T cell responses. Annu Rev Immunol 2005; 23: 23-68.

6.   Pardee AD, Wesa AK, Storkus WJ. Integrating costimulatory agonists to optimize immune-based cancer therapies. Immunotherapy 2009; 1: 249-64.

7.   Cheever MA. Twelve immunotherapy drugs that could cure cancers. Immunol Rev 2008; 222: 357-68.

8.   Burnet FM. The concept of immunological surveillance. Prog Exp Tumor Res 1970; 13: 1-27.

9.   Stutman O. Tumor development after 3-methylcholanthrene in immunologically deficient athymic-nude mice. Science 1974; 183: 534-6.

10.   Dighe AS, Richards E, Old LJ, Schreiber RD. Enhanced in vivo growth and resistance to rejection of tumor cells expressing dominant negative IFN gamma receptors. Immunity 1994; 1: 447-56.

11.   Street SE, Trapani JA, MacGregor D, Smyth MJ. Suppression of lymphoma and epithelial malignancies effected by interferon gamma. J Exp Med 2002; 196: 129-34.

12.   Smyth MJ, Crowe NY, Godfrey DI. NK cells and NKT cells collaborate in host protection from methylcholanthrene-induced fibrosarcoma. Int Immunol 2001; 13: 459-63.

13. Shankaran V, Ikeda H, Bruce AT, et al. IFNgamma and lymphocytes prevent primary tumour development and shape tumour immunogenicity. Nature 2001; 410: 1107-11.

14. Roithmaier S, Haydon AM, Loi S, et al. Incidence of malignancies in heart and/or lung transplant recipients: a single-institution experience. J Heart Lung Transplant 2007; 26: 845-9.

15. Galon J, Costes A, Sanchez-Cabo F, et al. Type, density, and location of immune cells within human colorectal tumors predict clinical outcome. Science 2006; 313: 1960-4.

16. Sharma P, Shen Y, Wen S, et al. CD8 tumor-infiltrating lymphocytes are predictive of survival in muscle-invasive urothelial carcinoma. Proc Natl Acad Sci U S A 2007; 104: 3967-72.

17. Zhang L, Conejo-Garcia JR, Katsaros D, et al. Intratumoral T cells, recurrence, and survival in epithelial ovarian cancer. N Engl J Med 2003; 348: 203-13.

18. Mantovani A, Romero P, Palucka AK, Marincola FM. Tumour immunity: effector response to tumour and role of the microenvironment. Lancet 2008; 371: 771-83.

19. Matzinger P. The danger model: a renewed sense of self. Science 2002; 296: 301-5.

20. Apetoh L, Ghiringhelli F, Tesniere A, et al. Toll-like receptor 4-dependent contribution of the immune system to anticancer chemotherapy and radiotherapy. Nat Med 2007; 13: 1050-9.

21. Hodge-Dufour J, Noble PW, Horton MR, et al. Induction of IL-12 and chemokines by hyaluronan requires adhesion-dependent priming of resident but not elicited macrophages. J Immunol 1997; 159: 2492-500.

22. Chan CW, Crafton E, Fan HN, et al. Interferon-producing killer dendritic cells provide a link between innate and adaptive immunity. Nat Med 2006; 12: 207-13.

23. Dunn GP, Bruce AT, Sheehan KC, et al. A critical function for type I interferons in cancer immunoediting. Nat Immunol 2005; 6: 722-9.

24. Albert ML, Sauter B, Bhardwaj N. Dendritic cells acquire antigen from apoptotic cells and induce class I-restricted CTLs. Nature 1998; 392: 86-9.

25. Sozzani S, Allavena P, D'Amico G, et al. Differential regulation of chemokine receptors during dendritic cell maturation: a model for their trafficking properties. J Immunol 1998; 161: 1083-6.

26. Banchereau J, Briere F, Caux C, et al. Immunobiology of dendritic cells. Annu Rev Immunol 2000; 18: 767-811.

27.   Cresswell P, Ackerman AL, Giodini A, Peaper DR, Wearsch PA. Mechanisms of MHC class I-restricted antigen processing and cross-presentation. Immunol Rev 2005; 207: 145-57.

28.   Itano AA, Jenkins MK. Antigen presentation to naive CD4 T cells in the lymph node. Nat Immunol 2003; 4: 733-9.

29.   Pardoll DM, Topalian SL. The role of CD4+ T cell responses in antitumor immunity. Curr Opin Immunol 1998; 10: 588-94.

30.   Chamoto K, Wakita D, Narita Y, et al. An essential role of antigen-presenting cell/T-helper type 1 cell-cell interactions in draining lymph node during complete eradication of class II-negative tumor tissue by T-helper type 1 cell therapy. Cancer Res 2006; 66: 1809-17.

31.   Kalinski P, Hilkens CM, Wierenga EA, Kapsenberg ML. T-cell priming by type-1 and type-2 polarized dendritic cells: the concept of a third signal. Immunol Today 1999; 20: 561-7.

32.   Murphy KM, Stockinger B. Effector T cell plasticity: flexibility in the face of changing circumstances. Nat Immunol 2010; 11: 674-80.

33.   Nishimura F, Dusak JE, Eguchi J, et al. Adoptive transfer of type 1 CTL mediates effective anti-central nervous system tumor response: critical roles of IFN-inducible protein-10. Cancer Res 2006; 66: 4478-87.

34.   Kunz M, Toksoy A, Goebeler M, Engelhardt E, Brocker E, Gillitzer R. Strong expression of the lymphoattractant C-X-C chemokine Mig is associated with heavy infiltration of T cells in human malignant melanoma. J Pathol 1999; 189: 552-8.

35.   Bromberg JF, Horvath CM, Wen Z, Schreiber RD, Darnell JE, Jr. Transcriptionally active Stat1 is required for the antiproliferative effects of both interferon alpha and interferon gamma. Proc Natl Acad Sci U S A 1996; 93: 7673-8.

36.   Qin Z, Schwartzkopff J, Pradera F, et al. A critical requirement of interferon gamma-mediated angiostasis for tumor rejection by CD8+ T cells. Cancer Res 2003; 63: 4095-100.

37.   Ibe S, Qin Z, Schuler T, Preiss S, Blankenstein T. Tumor rejection by disturbing tumor stroma cell interactions. J Exp Med 2001; 194: 1549-59.

38.   Arenberg DA, Kunkel SL, Polverini PJ, et al. Interferon-gamma-inducible protein 10 (IP-10) is an angiostatic factor that inhibits human non-small cell lung cancer (NSCLC) tumorigenesis and spontaneous metastases. J Exp Med 1996; 184: 981-92.

39.   Smyth MJ, Cretney E, Kershaw MH, Hayakawa Y. Cytokines in cancer immunity and immunotherapy. Immunol Rev 2004; 202: 275-93.

40.   Fallarino F, Gajewski TF. Cutting edge: differentiation of antitumor CTL in vivo requires host expression of Stat1. J Immunol 1999; 163: 4109-13.

41.   Wang E, Miller LD, Ohnmacht GA, et al. Prospective molecular profiling of melanoma metastases suggests classifiers of immune responsiveness. Cancer Res 2002; 62: 3581-6.

42.   Wang Z, Cao Y, Albino AP, Zeff RA, Houghton A, Ferrone S. Lack of HLA class I antigen expression by melanoma cells SK-MEL-33 caused by a reading frameshift in beta 2-microglobulin messenger RNA. J Clin Invest 1993; 91: 684-92.

43.   Jinushi M, Takehara T, Tatsumi T, et al. Expression and role of MICA and MICB in human hepatocellular carcinomas and their regulation by retinoic acid. Int J Cancer 2003; 104: 354-61.

44.   Wallace ME, Smyth MJ. The role of natural killer cells in tumor control--effectors and regulators of adaptive immunity. Springer Semin Immunopathol 2005; 27: 49-64.

45.   Russell JH, Ley TJ. Lymphocyte-mediated cytotoxicity. Annu Rev Immunol 2002; 20: 323-70.

46.   Hanson HL, Donermeyer DL, Ikeda H, et al. Eradication of established tumors by CD8+ T cell adoptive immunotherapy. Immunity 2000; 13: 265-76.

47.   Smyth MJ, Thia KY, Street SE, MacGregor D, Godfrey DI, Trapani JA. Perforin-mediated cytotoxicity is critical for surveillance of spontaneous lymphoma. J Exp Med 2000; 192: 755-60.

48.   Overwijk WW, Theoret MR, Finkelstein SE, et al. Tumor regression and autoimmunity after reversal of a functionally tolerant state of self-reactive CD8+ T cells. J Exp Med 2003; 198: 569-80.

49.   Wahlin BE, Sander B, Christensson B, Kimby E. CD8+ T-cell content in diagnostic lymph nodes measured by flow cytometry is a predictor of survival in follicular lymphoma. Clin Cancer Res 2007; 13: 388-97.

50.   Melief CJ, Vasmel WL, Offringa R, et al. Immunosurveillance of virus-induced tumors. Cold Spring Harb Symp Quant Biol 1989; 54 Pt 1: 597-603.

51.   Finn OJ. Cancer immunology. N Engl J Med 2008; 358: 2704-15.

52.   Knuth A, Danowski B, Oettgen HF, Old LJ. T-cell-mediated cytotoxicity against autologous malignant melanoma: analysis with interleukin 2-dependent T-cell cultures. Proc Natl Acad Sci U S A 1984; 81: 3511-5.

53.   van der Bruggen P, Traversari C, Chomez P, et al. A gene encoding an antigen recognized by cytolytic T lymphocytes on a human melanoma. Science 1991; 254: 1643-7.

54. Renkvist N, Castelli C, Robbins PF, Parmiani G. A listing of human tumor antigens recognized by T cells. Cancer Immunol Immunother 2001; 50: 3-15.

55. Hanahan D, Weinberg RA. The hallmarks of cancer. Cell 2000; 100: 57-70.

56. Yu P, Rowley DA, Fu YX, Schreiber H. The role of stroma in immune recognition and destruction of well-established solid tumors. Curr Opin Immunol 2006; 18: 226-31.

57. van Kempen LC, Ruiter DJ, van Muijen GN, Coussens LM. The tumor microenvironment: a critical determinant of neoplastic evolution. Eur J Cell Biol 2003; 82: 539-48.

58. Komita H, Zhao X, Taylor JL, et al. CD8+ T-cell responses against hemoglobin-beta prevent solid tumor growth. Cancer Res 2008; 68: 8076-84.

59. Lee J, Fassnacht M, Nair S, Boczkowski D, Gilboa E. Tumor immunotherapy targeting fibroblast activation protein, a product expressed in tumor-associated fibroblasts. Cancer Res 2005; 65: 11156-63.

60. Niethammer AG, Xiang R, Becker JC, et al. A DNA vaccine against VEGF receptor 2 prevents effective angiogenesis and inhibits tumor growth. Nat Med 2002; 8: 1369-75.

61. Spiotto MT, Rowley DA, Schreiber H. Bystander elimination of antigen loss variants in established tumors. Nat Med 2004; 10: 294-8.

62. Rabinovich GA, Gabrilovich D, Sotomayor EM. Immunosuppressive strategies that are mediated by tumor cells. Annu Rev Immunol 2007; 25: 267-96.

63. Teng MW, Swann JB, Koebel CM, Schreiber RD, Smyth MJ. Immune-mediated dormancy: an equilibrium with cancer. J Leukoc Biol 2008; 84: 988-93.

64. Herrlinger U, Hebart H, Kanz L, Dichgans J, Weller M. Relapse of primary CNS lymphoma after more than 10 years in complete remission. J Neurol 2005; 252: 1409-10.

65. Karrison TG, Ferguson DJ, Meier P. Dormancy of mammary carcinoma after mastectomy. J Natl Cancer Inst 1999; 91: 80-5.

66. MacKie RM, Reid R, Junor B. Fatal melanoma transferred in a donated kidney 16 years after melanoma surgery. N Engl J Med 2003; 348: 567-8.

67. Koebel CM, Vermi W, Swann JB, et al. Adaptive immunity maintains occult cancer in an equilibrium state. Nature 2007; 450: 903-7.

68. Seliger B. Molecular mechanisms of MHC class I abnormalities and APM components in human tumors. Cancer Immunol Immunother 2008; 57: 1719-26.

69.   Kaplan DH, Shankaran V, Dighe AS, et al. Demonstration of an interferon gamma-dependent tumor surveillance system in immunocompetent mice. Proc Natl Acad Sci U S A 1998; 95: 7556-61.

70.   Kaiser BK, Yim D, Chow IT, et al. Disulphide-isomerase-enabled shedding of tumour-associated NKG2D ligands. Nature 2007; 447: 482-6.

71.   Schwartz RH. T cell anergy. Annu Rev Immunol 2003; 21: 305-34.

72.   Staveley-O'Carroll K, Sotomayor E, Montgomery J, et al. Induction of antigen-specific T cell anergy: An early event in the course of tumor progression. Proc Natl Acad Sci U S A 1998; 95: 1178-83.

73.   Huang AY, Golumbek P, Ahmadzadeh M, Jaffee E, Pardoll D, Levitsky H. Role of bone marrow-derived cells in presenting MHC class I-restricted tumor antigens. Science 1994; 264: 961-5.

74.   Hargadon KM, Brinkman CC, Sheasley-O'neill S L, Nichols LA, Bullock TN, Engelhard VH. Incomplete differentiation of antigen-specific CD8 T cells in tumor-draining lymph nodes. J Immunol 2006; 177: 6081-90.

75.   Morelli AE, Thomson AW. Tolerogenic dendritic cells and the quest for transplant tolerance. Nat Rev Immunol 2007; 7: 610-21.

76.   Munn DH, Mellor AL. The tumor-draining lymph node as an immune-privileged site. Immunol Rev 2006; 213: 146-58.

77.   Vicari AP, Chiodoni C, Vaure C, et al. Reversal of tumor-induced dendritic cell paralysis by CpG immunostimulatory oligonucleotide and anti-interleukin 10 receptor antibody. J Exp Med 2002; 196: 541-9.

78.   Kiertscher SM, Luo J, Dubinett SM, Roth MD. Tumors promote altered maturation and early apoptosis of monocyte-derived dendritic cells. J Immunol 2000; 164: 1269-76.

79.   Munn DH, Sharma MD, Baban B, et al. GCN2 kinase in T cells mediates proliferative arrest and anergy induction in response to indoleamine 2,3-dioxygenase. Immunity 2005; 22: 633-42.

80.   Frey AB, Monu N. Effector-phase tolerance: another mechanism of how cancer escapes antitumor immune response. J Leukoc Biol 2006; 79: 652-62.

81.   Monu N, Frey AB. Suppression of proximal T cell receptor signaling and lytic function in CD8+ tumor-infiltrating T cells. Cancer Res 2007; 67: 11447-54.

82.   Radoja S, Saio M, Schaer D, Koneru M, Vukmanovic S, Frey AB. CD8(+) tumor-infiltrating T cells are deficient in perforin-mediated cytolytic activity due to defective microtubule-organizing center mobilization and lytic granule exocytosis. J Immunol 2001; 167: 5042-51.

83. Blohm U, Roth E, Brommer K, Dumrese T, Rosenthal FM, Pircher H. Lack of effector cell function and altered tetramer binding of tumor-infiltrating lymphocytes. J Immunol 2002; 169: 5522-30.

84. Tran KQ, Zhou J, Durflinger KH, et al. Minimally cultured tumor-infiltrating lymphocytes display optimal characteristics for adoptive cell therapy. J Immunother 2008; 31: 742-51.

85. Zou W, Chen L. Inhibitory B7-family molecules in the tumour microenvironment. Nat Rev Immunol 2008; 8: 467-77.

86. Blank C, Gajewski TF, Mackensen A. Interaction of PD-L1 on tumor cells with PD-1 on tumor-specific T cells as a mechanism of immune evasion: implications for tumor immunotherapy. Cancer Immunol Immunother 2005; 54: 307-14.

87. Salceda S, Tang T, Kmet M, et al. The immunomodulatory protein B7-H4 is overexpressed in breast and ovarian cancers and promotes epithelial cell transformation. Exp Cell Res 2005; 306: 128-41.

88. Thompson RH, Kuntz SM, Leibovich BC, et al. Tumor B7-H1 is associated with poor prognosis in renal cell carcinoma patients with long-term follow-up. Cancer Res 2006; 66: 3381-5.

89. Wittke F, Hoffmann R, Buer J, et al. Interleukin 10 (IL-10): an immunosuppressive factor and independent predictor in patients with metastatic renal cell carcinoma. Br J Cancer 1999; 79: 1182-4.

90. Thomas DA, Massague J. TGF-beta directly targets cytotoxic T cell functions during tumor evasion of immune surveillance. Cancer Cell 2005; 8: 369-80.

91. Teicher BA. Transforming growth factor-beta and the immune response to malignant disease. Clin Cancer Res 2007; 13: 6247-51.

92. Fontenot JD, Gavin MA, Rudensky AY. Foxp3 programs the development and function of CD4+CD25+ regulatory T cells. Nat Immunol 2003; 4: 330-6.

93. Suri-Payer E, Amar AZ, Thornton AM, Shevach EM. CD4+CD25+ T cells inhibit both the induction and effector function of autoreactive T cells and represent a unique lineage of immunoregulatory cells. J Immunol 1998; 160: 1212-8.

94. Thornton AM, Shevach EM. Suppressor effector function of CD4+CD25+ immunoregulatory T cells is antigen nonspecific. J Immunol 2000; 164: 183-90.

95. Nakamura K, Kitani A, Strober W. Cell contact-dependent immunosuppression by CD4(+)CD25(+) regulatory T cells is mediated by cell surface-bound transforming growth factor beta. J Exp Med 2001; 194: 629-44.

96.   Jonuleit H, Schmitt E, Schuler G, Knop J, Enk AH. Induction of interleukin 10-producing, nonproliferating CD4(+) T cells with regulatory properties by repetitive stimulation with allogeneic immature human dendritic cells. J Exp Med 2000; 192: 1213-22.

97.   Yamagiwa S, Gray JD, Hashimoto S, Horwitz DA. A role for TGF-beta in the generation and expansion of CD4+CD25+ regulatory T cells from human peripheral blood. J Immunol 2001; 166: 7282-9.

98.   Asseman C, Mauze S, Leach MW, Coffman RL, Powrie F. An essential role for interleukin 10 in the function of regulatory T cells that inhibit intestinal inflammation. J Exp Med 1999; 190: 995-1004.

99.   Tanaka H, Tanaka J, Kjaergaard J, Shu S. Depletion of CD4+ CD25+ regulatory cells augments the generation of specific immune T cells in tumor-draining lymph nodes. J Immunother 2002; 25: 207-17.

100.   Hiura T, Kagamu H, Miura S, et al. Both regulatory T cells and antitumor effector T cells are primed in the same draining lymph nodes during tumor progression. J Immunol 2005; 175: 5058-66.

101.   Liyanage UK, Moore TT, Joo HG, et al. Prevalence of regulatory T cells is increased in peripheral blood and tumor microenvironment of patients with pancreas or breast adenocarcinoma. J Immunol 2002; 169: 2756-61.

102.   Curiel TJ, Coukos G, Zou L, et al. Specific recruitment of regulatory T cells in ovarian carcinoma fosters immune privilege and predicts reduced survival. Nat Med 2004; 10: 942-9.

103.   Zou W. Regulatory T cells, tumour immunity and immunotherapy. Nat Rev Immunol 2006; 6: 295-307.

104.   Sica A, Bronte V. Altered macrophage differentiation and immune dysfunction in tumor development. J Clin Invest 2007; 117: 1155-66.

105.   Gabrilovich DI, Bronte V, Chen SH, et al. The terminology issue for myeloid-derived suppressor cells. Cancer Res 2007; 67: 425.

106.   Gallina G, Dolcetti L, Serafini P, et al. Tumors induce a subset of inflammatory monocytes with immunosuppressive activity on CD8+ T cells. J Clin Invest 2006; 116: 2777-90.

107.   Rodriguez PC, Quiceno DG, Zabaleta J, et al. Arginase I production in the tumor microenvironment by mature myeloid cells inhibits T-cell receptor expression and antigen-specific T-cell responses. Cancer Res 2004; 64: 5839-49.

108. Zea AH, Rodriguez PC, Atkins MB, et al. Arginase-producing myeloid suppressor cells in renal cell carcinoma patients: a mechanism of tumor evasion. Cancer Res 2005; 65: 3044-8.

109. Buckanovich RJ, Facciabene A, Kim S, et al. Endothelin B receptor mediates the endothelial barrier to T cell homing to tumors and disables immune therapy. Nat Med 2008; 14: 28-36.

110. Carlos TM, Harlan JM. Leukocyte-endothelial adhesion molecules. Blood 1994; 84: 2068-101.

111. Jain RK. Normalization of tumor vasculature: an emerging concept in antiangiogenic therapy. Science 2005; 307: 58-62.

112. Sato E, Fujimoto J, Toyoki H, et al. Expression of IP-10 related to angiogenesis in uterine cervical cancers. Br J Cancer 2007; 96: 1735-9.

113. Ganss R, Ryschich E, Klar E, Arnold B, Hammerling GJ. Combination of T-cell therapy and trigger of inflammation induces remodeling of the vasculature and tumor eradication. Cancer Res 2002; 62: 1462-70.

114. Garbi N, Arnold B, Gordon S, Hammerling GJ, Ganss R. CpG motifs as proinflammatory factors render autochthonous tumors permissive for infiltration and destruction. J Immunol 2004; 172: 5861-9.

115. Quezada SA, Peggs KS, Simpson TR, Shen Y, Littman DR, Allison JP. Limited tumor infiltration by activated T effector cells restricts the therapeutic activity of regulatory T cell depletion against established melanoma. J Exp Med 2008; 205: 2125-38.

116. Dougan M, Dranoff G. Immune therapy for cancer. Annu Rev Immunol 2009; 27: 83-117.

117. Komita H, Zhao X, Katakam AK, et al. Conditional interleukin-12 gene therapy promotes safe and effective antitumor immunity. Cancer Gene Ther 2009; 16: 883-91.

118. Berger R, Rotem-Yehudar R, Slama G, et al. Phase I safety and pharmacokinetic study of CT-011, a humanized antibody interacting with PD-1, in patients with advanced hematologic malignancies. Clin Cancer Res 2008; 14: 3044-51.

119. Mahnke K, Schonfeld K, Fondel S, et al. Depletion of CD4+CD25+ human regulatory T cells in vivo: kinetics of Treg depletion and alterations in immune functions in vivo and in vitro. Int J Cancer 2007; 120: 2723-33.

120. Goldman B, DeFrancesco L. The cancer vaccine roller coaster. Nat Biotechnol 2009; 27: 129-39.

121. Jaffee EM, Hruban RH, Biedrzycki B, et al. Novel allogeneic granulocyte-macrophage colony-stimulating factor-secreting tumor vaccine for pancreatic cancer: a phase I trial of safety and immune activation. J Clin Oncol 2001; 19: 145-56.

122. Valmori D, Souleimanian NE, Tosello V, et al. Vaccination with NY-ESO-1 protein and CpG in Montanide induces integrated antibody/Th1 responses and CD8 T cells through cross-priming. Proc Natl Acad Sci U S A 2007; 104: 8947-52.

123. Bretscher P, Cohn M. A theory of self-nonself discrimination. Science 1970; 169: 1042-9.

124. Jenkins MK, Schwartz RH. Antigen presentation by chemically modified splenocytes induces antigen-specific T cell unresponsiveness in vitro and in vivo. J Exp Med 1987; 165: 302-19.

125. Chattopadhyay K, Ramagopal UA, Brenowitz M, Nathenson SG, Almo SC. Evolution of GITRL immune function: murine GITRL exhibits unique structural and biochemical properties within the TNF superfamily. Proc Natl Acad Sci U S A 2008; 105: 635-40.

126. Zhou Z, Song X, Berezov A, et al. Human glucocorticoid-induced TNF receptor ligand regulates its signaling activity through multiple oligomerization states. Proc Natl Acad Sci U S A 2008; 105: 5465-70.

127. McHugh RS, Whitters MJ, Piccirillo CA, et al. CD4(+)CD25(+) immunoregulatory T cells: gene expression analysis reveals a functional role for the glucocorticoid-induced TNF receptor. Immunity 2002; 16: 311-23.

128. Taraban VY, Rowley TF, O'Brien L, et al. Expression and costimulatory effects of the TNF receptor superfamily members CD134 (OX40) and CD137 (4-1BB), and their role in the generation of anti-tumor immune responses. Eur J Immunol 2002; 32: 3617-27.

129. Gramaglia I, Jember A, Pippig SD, Weinberg AD, Killeen N, Croft M. The OX40 costimulatory receptor determines the development of CD4 memory by regulating primary clonal expansion. J Immunol 2000; 165: 3043-50.

130. Evans DE, Prell RA, Thalhofer CJ, Hurwitz AA, Weinberg AD. Engagement of OX40 enhances antigen-specific CD4(+) T cell mobilization/memory development and humoral immunity: comparison of alphaOX-40 with alphaCTLA-4. J Immunol 2001; 167: 6804-11.

131. Bansal-Pakala P, Halteman BS, Cheng MH, Croft M. Costimulation of CD8 T cell responses by OX40. J Immunol 2004; 172: 4821-5.

132. Prell RA, Evans DE, Thalhofer C, Shi T, Funatake C, Weinberg AD. OX40-mediated memory T cell generation is TNF receptor-associated factor 2 dependent. J Immunol 2003; 171: 5997-6005.

133. Bansal-Pakala P, Jember AG, Croft M. Signaling through OX40 (CD134) breaks peripheral T-cell tolerance. Nat Med 2001; 7: 907-12.

134. Graham DS, Graham RR, Manku H, et al. Polymorphism at the TNF superfamily gene TNFSF4 confers susceptibility to systemic lupus erythematosus. Nat Genet 2008; 40: 83-9.

135. Sabbagh L, Snell LM, Watts TH. TNF family ligands define niches for T cell memory. Trends Immunol 2007; 28: 333-9.

136. Song J, Salek-Ardakani S, Rogers PR, Cheng M, Van Parijs L, Croft M. The costimulation-regulated duration of PKB activation controls T cell longevity. Nat Immunol 2004; 5: 150-8.

137. Ruby CE, Redmond WL, Haley D, Weinberg AD. Anti-OX40 stimulation in vivo enhances CD8+ memory T cell survival and significantly increases recall responses. Eur J Immunol 2007; 37: 157-66.

138. Lee SJ, Rossi RJ, Lee SK, et al. CD134 costimulation couples the CD137 pathway to induce production of supereffector CD8 T cells that become IL-7 dependent. J Immunol 2007; 179: 2203-14.

139. Mousavi SF, Soroosh P, Takahashi T, et al. OX40 costimulatory signals potentiate the memory commitment of effector CD8+ T cells. J Immunol 2008; 181: 5990-6001.

140. Soroosh P, Ine S, Sugamura K, Ishii N. Differential requirements for OX40 signals on generation of effector and central memory CD4+ T cells. J Immunol 2007; 179: 5014-23.

141. So T, Lee SW, Croft M. Immune regulation and control of regulatory T cells by OX40 and 4-1BB. Cytokine Growth Factor Rev 2008; 19: 253-62.

142. Vu MD, Xiao X, Gao W, et al. OX40 costimulation turns off Foxp3+ Tregs. Blood 2007; 110: 2501-10.

143. Takeda I, Ine S, Killeen N, et al. Distinct roles for the OX40-OX40 ligand interaction in regulatory and nonregulatory T cells. J Immunol 2004; 172: 3580-9.

144. So T, Croft M. Cutting edge: OX40 inhibits TGF-beta- and antigen-driven conversion of naive CD4 T cells into CD25+Foxp3+ T cells. J Immunol 2007; 179: 1427-30.

145. Ito T, Wang YH, Duramad O, et al. OX40 ligand shuts down IL-10-producing regulatory T cells. Proc Natl Acad Sci U S A 2006; 103: 13138-43.

146. Shimizu J, Yamazaki S, Takahashi T, Ishida Y, Sakaguchi S. Stimulation of CD25(+)CD4(+) regulatory T cells through GITR breaks immunological self-tolerance. Nat Immunol 2002; 3: 135-42.

147. Wu Y, Borde M, Heissmeyer V, et al. FOXP3 controls regulatory T cell function through cooperation with NFAT. Cell 2006; 126: 375-87.

148. Zhan Y, Gerondakis S, Coghill E, et al. Glucocorticoid-induced TNF receptor expression by T cells is reciprocally regulated by NF-kappaB and NFAT. J Immunol 2008; 181: 5405-13.

149. Kanamaru F, Youngnak P, Hashiguchi M, et al. Costimulation via glucocorticoid-induced TNF receptor in both conventional and CD25+ regulatory CD4+ T cells. J Immunol 2004; 172: 7306-14.

150. Ronchetti S, Zollo O, Bruscoli S, et al. GITR, a member of the TNF receptor superfamily, is costimulatory to mouse T lymphocyte subpopulations. Eur J Immunol 2004; 34: 613-22.

151. Kohm AP, Williams JS, Miller SD. Cutting edge: ligation of the glucocorticoid-induced TNF receptor enhances autoreactive CD4+ T cell activation and experimental autoimmune encephalomyelitis. J Immunol 2004; 172: 4686-90.

152. Esparza EM, Arch RH. Glucocorticoid-induced TNF receptor functions as a costimulatory receptor that promotes survival in early phases of T cell activation. J Immunol 2005; 174: 7869-74.

153. Ronchetti S, Nocentini G, Riccardi C, Pandolfi PP. Role of GITR in activation response of T lymphocytes. Blood 2002; 100: 350-2.

154. Stephens GL, McHugh RS, Whitters MJ, et al. Engagement of glucocorticoid-induced TNFR family-related receptor on effector T cells by its ligand mediates resistance to suppression by CD4+CD25+ T cells. J Immunol 2004; 173: 5008-20.

155. Ji HB, Liao G, Faubion WA, et al. Cutting edge: the natural ligand for glucocorticoid-induced TNF receptor-related protein abrogates regulatory T cell suppression. J Immunol 2004; 172: 5823-7.

156. Igarashi H, Cao Y, Iwai H, et al. GITR ligand-costimulation activates effector and regulatory functions of CD4+ T cells. Biochem Biophys Res Commun 2008; 369: 1134-8.

157. Tuyaerts S, Van Meirvenne S, Bonehill A, et al. Expression of human GITRL on myeloid dendritic cells enhances their immunostimulatory function but does not abrogate the suppressive effect of CD4+CD25+ regulatory T cells. J Leukoc Biol 2007; 82: 93-105.

158. Wang L, Pino-Lagos K, de Vries VC, Guleria I, Sayegh MH, Noelle RJ. Programmed death 1 ligand signaling regulates the generation of adaptive Foxp3+CD4+ regulatory T cells. Proc Natl Acad Sci U S A 2008; 105: 9331-6.

159. Shevach EM, Stephens GL. The GITR-GITRL interaction: co-stimulation or contrasuppression of regulatory activity? Nat Rev Immunol 2006; 6: 613-8.

160.	Liu B, Li Z, Mahesh SP, et al. Glucocorticoid-induced tumor necrosis factor receptor negatively regulates activation of human primary natural killer (NK) cells by blocking proliferative signals and increasing NK cell apoptosis. J Biol Chem 2008; 283: 8202-10.

161.	Hanabuchi S, Watanabe N, Wang YH, et al. Human plasmacytoid predendritic cells activate NK cells through glucocorticoid-induced tumor necrosis factor receptor-ligand (GITRL). Blood 2006; 107: 3617-23.

162.	Kim HJ, Kim HY, Kim BK, Kim S, Chung DH. Engagement of glucocorticoid-induced TNF receptor costimulates NKT cell activation in vitro and in vivo. J Immunol 2006; 176: 3507-15.

163.	Schraven B, Kalinke U. CD28 superagonists: what makes the difference in humans? Immunity 2008; 28: 591-5.

164.	Blansfield JA, Beck KE, Tran K, et al. Cytotoxic T-lymphocyte-associated antigen-4 blockage can induce autoimmune hypophysitis in patients with metastatic melanoma and renal cancer. J Immunother 2005; 28: 593-8.

165.	Melero I, Hervas-Stubbs S, Glennie M, Pardoll DM, Chen L. Immunostimulatory monoclonal antibodies for cancer therapy. Nat Rev Cancer 2007; 7: 95-106.

166.	Kjaergaard J, Tanaka J, Kim JA, Rothchild K, Weinberg A, Shu S. Therapeutic efficacy of OX-40 receptor antibody depends on tumor immunogenicity and anatomic site of tumor growth. Cancer Res 2000; 60: 5514-21.

167.	Kjaergaard J, Peng L, Cohen PA, Drazba JA, Weinberg AD, Shu S. Augmentation versus inhibition: effects of conjunctional OX-40 receptor monoclonal antibody and IL-2 treatment on adoptive immunotherapy of advanced tumor. J Immunol 2001; 167: 6669-77.

168.	Andarini S, Kikuchi T, Nukiwa M, et al. Adenovirus vector-mediated in vivo gene transfer of OX40 ligand to tumor cells enhances antitumor immunity of tumor-bearing hosts. Cancer Res 2004; 64: 3281-7.

169.	Ali SA, Ahmad M, Lynam J, et al. Anti-tumour therapeutic efficacy of OX40L in murine tumour model. Vaccine 2004; 22: 3585-94.

170.	Zaini J, Andarini S, Tahara M, et al. OX40 ligand expressed by DCs costimulates NKT and CD4+ Th cell antitumor immunity in mice. J Clin Invest 2007; 117: 3330-8.

171.	Sadun RE, Hsu WE, Zhang N, et al. Fc-mOX40L fusion protein produces complete remission and enhanced survival in 2 murine tumor models. J Immunother 2008; 31: 235-45.

172.	Piconese S, Valzasina B, Colombo MP. OX40 triggering blocks suppression by regulatory T cells and facilitates tumor rejection. J Exp Med 2008; 205: 825-39.

173. Pan PY, Zang Y, Weber K, Meseck ML, Chen SH. OX40 ligation enhances primary and memory cytotoxic T lymphocyte responses in an immunotherapy for hepatic colon metastases. Mol Ther 2002; 6: 528-36.

174. Song A, Song J, Tang X, Croft M. Cooperation between CD4 and CD8 T cells for anti-tumor activity is enhanced by OX40 signals. Eur J Immunol 2007; 37: 1224-32.

175. Murata S, Ladle BH, Kim PS, et al. OX40 costimulation synergizes with GM-CSF whole-cell vaccination to overcome established CD8+ T cell tolerance to an endogenous tumor antigen. J Immunol 2006; 176: 974-83.

176. Kalinski P, Giermasz A, Nakamura Y, et al. Helper role of NK cells during the induction of anticancer responses by dendritic cells. Mol Immunol 2005; 42: 535-9.

177. Nakajima C, Uekusa Y, Iwasaki M, et al. A role of Interferon-gamma (IFN-gamma) in tumor immunity: T cells with the capacity to reject tumor cells are generated but fail to migrate to tumor sites in IFN-gamma-deficient mice. Cancer Res 2001; 61: 3399-405.

178. Gough MJ, Ruby CE, Redmond WL, Dhungel B, Brown A, Weinberg AD. OX40 agonist therapy enhances CD8 infiltration and decreases immune suppression in the tumor. Cancer Res 2008; 68: 5206-15.

179. Morris A, Vetto JT, Ramstad T, et al. Induction of anti-mammary cancer immunity by engaging the OX-40 receptor in vivo. Breast Cancer Res Treat 2001; 67: 71-80.

180. Weinberg AD, Rivera MM, Prell R, et al. Engagement of the OX-40 receptor in vivo enhances antitumor immunity. J Immunol 2000; 164: 2160-9.

181. Ramstad T, Lawnicki L, Vetto J, Weinberg A. Immunohistochemical analysis of primary breast tumors and tumor-draining lymph nodes by means of the T-cell costimulatory molecule OX-40. Am J Surg 2000; 179: 400-6.

182. Imura A, Hori T, Imada K, et al. OX40 expressed on fresh leukemic cells from adult T-cell leukemia patients mediates cell adhesion to vascular endothelial cells: implication for the possible involvement of OX40 in leukemic cell infiltration. Blood 1997; 89: 2951-8.

183. Vetto JT, Lum S, Morris A, et al. Presence of the T-cell activation marker OX-40 on tumor infiltrating lymphocytes and draining lymph node cells from patients with melanoma and head and neck cancers. Am J Surg 1997; 174: 258-65.

184. Petty JK, He K, Corless CL, Vetto JT, Weinberg AD. Survival in human colorectal cancer correlates with expression of the T-cell costimulatory molecule OX-40 (CD134). Am J Surg 2002; 183: 512-8.

185. Ladanyi A, Somlai B, Gilde K, Fejos Z, Gaudi I, Timar J. T-cell activation marker expression on tumor-infiltrating lymphocytes as prognostic factor in cutaneous malignant melanoma. Clin Cancer Res 2004; 10: 521-30.

186.   Weinberg AD, Thalhofer C, Morris N, et al. Anti-OX40 (CD134) administration to nonhuman primates: immunostimulatory effects and toxicokinetic study. J Immunother 2006; 29: 575-85.

187.   Morris NP, Peters C, Montler R, et al. Development and characterization of recombinant human Fc:OX40L fusion protein linked via a coiled-coil trimerization domain. Mol Immunol 2007; 44: 3112-21.

188.   Wolchok JD, Yang AS, Weber JS. Immune regulatory antibodies: are they the next advance? Cancer J 2010; 16: 311-7.

189.   Ramirez-Montagut T, Chow A, Hirschhorn-Cymerman D, et al. Glucocorticoid-induced TNF receptor family related gene activation overcomes tolerance/ignorance to melanoma differentiation antigens and enhances antitumor immunity. J Immunol 2006; 176: 6434-42.

190.   Ko K, Yamazaki S, Nakamura K, et al. Treatment of advanced tumors with agonistic anti-GITR mAb and its effects on tumor-infiltrating Foxp3+CD25+CD4+ regulatory T cells. J Exp Med 2005; 202: 885-91.

191.   Zhou P, L'Italien L, Hodges D, Schebye XM. Pivotal roles of CD4+ effector T cells in mediating agonistic anti-GITR mAb-induced-immune activation and tumor immunity in CT26 tumors. J Immunol 2007; 179: 7365-75.

192.   Hu P, Arias RS, Sadun RE, et al. Construction and preclinical characterization of Fc-mGITRL for the immunotherapy of cancer. Clin Cancer Res 2008; 14: 579-88.

193.   Calmels B, Paul S, Futin N, Ledoux C, Stoeckel F, Acres B. Bypassing tumor-associated immune suppression with recombinant adenovirus constructs expressing membrane bound or secreted GITR-L. Cancer Gene Ther 2005; 12: 198-205.

194.   Strauss L, Bergmann C, Szczepanski M, Gooding W, Johnson JT, Whiteside TL. A unique subset of CD4+CD25highFoxp3+ T cells secreting interleukin-10 and transforming growth factor-beta1 mediates suppression in the tumor microenvironment. Clin Cancer Res 2007; 13: 4345-54.

195.   Whiteside TL. Immune suppression in cancer: effects on immune cells, mechanisms and future therapeutic intervention. Semin Cancer Biol 2006; 16: 3-15.

196.   Salih HR, Schmetzer HM, Burke C, et al. Soluble CD137 (4-1BB) ligand is released following leukocyte activation and is found in sera of patients with hematological malignancies. J Immunol 2001; 167: 4059-66.

197.   Kim YS, Jung HW, Choi J, et al. Expression of AITR and AITR ligand in breast cancer patients. Oncol Rep 2007; 18: 1189-94.

198.   Baltz KM, Krusch M, Baessler T, et al. Neutralization of tumor-derived soluble glucocorticoid-induced TNFR-related protein ligand increases NK cell anti-tumor reactivity. Blood 2008; 112: 3735-43.

199.   Baltz KM, Krusch M, Bringmann A, et al. Cancer immunoediting by GITR (glucocorticoid-induced TNF-related protein) ligand in humans: NK cell/tumor cell interactions. FASEB J 2007; 21: 2442-54.

200.   Ponte JF, Ponath P, Gulati R, et al. Enhancement of humoral and cellular immunity with an anti-glucocorticoid-induced tumour necrosis factor receptor monoclonal antibody. Immunology 2010; 130: 231-42.

201.   Eggermont AM. Immunotherapy: Vaccine trials in melanoma -- time for reflection. Nat Rev Clin Oncol 2009; 6: 256-8.

202.   Schreiber K, Rowley DA, Riethmuller G, Schreiber H. Cancer immunotherapy and preclinical studies: why we are not wasting our time with animal experiments. Hematol Oncol Clin North Am 2006; 20: 567-84.

203.   Suntharalingam G, Perry MR, Ward S, et al. Cytokine storm in a phase 1 trial of the anti-CD28 monoclonal antibody TGN1412. N Engl J Med 2006; 355: 1018-28.

204.   Hamzah J, Jugold M, Kiessling F, et al. Vascular normalization in Rgs5-deficient tumours promotes immune destruction. Nature 2008; 453: 410-4.

205.   Zou W. Immunosuppressive networks in the tumour environment and their therapeutic relevance. Nat Rev Cancer 2005; 5: 263-74.

206.   Zippelius A, Batard P, Rubio-Godoy V, et al. Effector function of human tumor-specific CD8 T cells in melanoma lesions: a state of local functional tolerance. Cancer Res 2004; 64: 2865-73.

207.   Yu P, Lee Y, Liu W, et al. Intratumor depletion of CD4+ cells unmasks tumor immunogenicity leading to the rejection of late-stage tumors. J Exp Med 2005; 201: 779-91.

208.   Valzasina B, Guiducci C, Dislich H, Killeen N, Weinberg AD, Colombo MP. Triggering of OX40 (CD134) on CD4(+)CD25+ T cells blocks their inhibitory activity: a novel regulatory role for OX40 and its comparison with GITR. Blood 2005; 105: 2845-51.

209.   Berhanu A, Huang J, Alber SM, Watkins SC, Storkus WJ. Combinational FLt3 ligand and granulocyte macrophage colony-stimulating factor treatment promotes enhanced tumor infiltration by dendritic cells and antitumor CD8(+) T-cell cross-priming but is ineffective as a therapy. Cancer Res 2006; 66: 4895-903.

210.   Sasaki K, Pardee AD, Qu Y, et al. IL-4 suppresses very late antigen-4 expression which is required for therapeutic Th1 T-cell trafficking into tumors. J Immunother 2009; 32: 793-802.

211. Tayade C, Fang Y, Black GP, V AP, Jr., Erlebacher A, Croy BA. Differential transcription of Eomes and T-bet during maturation of mouse uterine natural killer cells. J Leukoc Biol 2005; 78: 1347-55.

212. Liu C, Lou Y, Lizee G, et al. Plasmacytoid dendritic cells induce NK cell-dependent, tumor antigen-specific T cell cross-priming and tumor regression in mice. J Clin Invest 2008; 118: 1165-75.

213. Hirschhorn-Cymerman D, Rizzuto GA, Merghoub T, et al. OX40 engagement and chemotherapy combination provides potent antitumor immunity with concomitant regulatory T cell apoptosis. J Exp Med 2009; 206: 1103-16.

214. Kemp RA, Ronchese F. Tumor-specific Tc1, but not Tc2, cells deliver protective antitumor immunity. J Immunol 2001; 167: 6497-502.

215. Quezada SA, Peggs KS, Curran MA, Allison JP. CTLA4 blockade and GM-CSF combination immunotherapy alters the intratumor balance of effector and regulatory T cells. J Clin Invest 2006; 116: 1935-45.

216. Ruby CE, Yates MA, Hirschhorn-Cymerman D, et al. Cutting Edge: OX40 agonists can drive regulatory T cell expansion if the cytokine milieu is right. J Immunol 2009; 183: 4853-7.

217. Sasaki K, Zhu X, Vasquez C, et al. Preferential expression of very late antigen-4 on type 1 CTL cells plays a critical role in trafficking into central nervous system tumors. Cancer Res 2007; 67: 6451-8.

218. Weinberg AD, Bourdette DN, Sullivan TJ, et al. Selective depletion of myelin-reactive T cells with the anti-OX-40 antibody ameliorates autoimmune encephalomyelitis. Nat Med 1996; 2: 183-9.

219. Giacomelli R, Passacantando A, Perricone R, et al. T lymphocytes in the synovial fluid of patients with active rheumatoid arthritis display CD134-OX40 surface antigen. Clin Exp Rheumatol 2001; 19: 317-20.

220. Horai R, Nakajima A, Habiro K, et al. TNF-alpha is crucial for the development of autoimmune arthritis in IL-1 receptor antagonist-deficient mice. J Clin Invest 2004; 114: 1603-11.

221. Nakae S, Asano M, Horai R, Sakaguchi N, Iwakura Y. IL-1 enhances T cell-dependent antibody production through induction of CD40 ligand and OX40 on T cells. J Immunol 2001; 167: 90-7.

222. Olofsson PS, Soderstrom LA, Wagsater D, et al. CD137 is expressed in human atherosclerosis and promotes development of plaque inflammation in hypercholesterolemic mice. Circulation 2008; 117: 1292-301.

223. Wilcox RA, Chapoval AI, Gorski KS, et al. Cutting edge: Expression of functional CD137 receptor by dendritic cells. J Immunol 2002; 168: 4262-7.

224. Salek-Ardakani S, Song J, Halteman BS, et al. OX40 (CD134) controls memory T helper 2 cells that drive lung inflammation. J Exp Med 2003; 198: 315-24.

225. Muriglan SJ, Ramirez-Montagut T, Alpdogan O, et al. GITR activation induces an opposite effect on alloreactive CD4(+) and CD8(+) T cells in graft-versus-host disease. J Exp Med 2004; 200: 149-57.

226. van Olffen RW, Koning N, van Gisbergen KP, et al. GITR triggering induces expansion of both effector and regulatory CD4+ T cells in vivo. J Immunol 2009; 182: 7490-500.

227. Kim J, Choi WS, Kang H, et al. Conversion of alloantigen-specific CD8+ T cell anergy to CD8+ T cell priming through in vivo ligation of glucocorticoid-induced TNF receptor. J Immunol 2006; 176: 5223-31.

228. Cohen AD, Diab A, Perales MA, et al. Agonist anti-GITR antibody enhances vaccine-induced CD8(+) T-cell responses and tumor immunity. Cancer Res 2006; 66: 4904-12.

229. Nishikawa H, Kato T, Hirayama M, et al. Regulatory T cell-resistant CD8+ T cells induced by glucocorticoid-induced tumor necrosis factor receptor signaling. Cancer Res 2008; 68: 5948-54.

230. Cohen AD, Schaer DA, Liu C, et al. Agonist anti-GITR monoclonal antibody induces melanoma tumor immunity in mice by altering regulatory T cell stability and intra-tumor accumulation. PLoS One 2010; 5: e10436.

231. Balkwill F, Mantovani A. Inflammation and cancer: back to Virchow? Lancet 2001; 357: 539-45.

232. Mitsui J, Nishikawa H, Muraoka D, et al. Two distinct mechanisms of augmented antitumor activity by modulation of immunostimulatory/inhibitory signals. Clin Cancer Res 2010; 16: 2781-91.

233. Chen L, Huang TG, Meseck M, Mandeli J, Fallon J, Woo SL. Rejection of metastatic 4T1 breast cancer by attenuation of Treg cells in combination with immune stimulation. Mol Ther 2007; 15: 2194-202.

234. Coe D, Begom S, Addey C, White M, Dyson J, Chai JG. Depletion of regulatory T cells by anti-GITR mAb as a novel mechanism for cancer immunotherapy. Cancer Immunol Immunother 2010; 59: 1367-77.

235. Pardee AD, McCurry D, Alber S, Hu P, Epstein AL, Storkus WJ. A therapeutic OX40 agonist dynamically alters dendritic, endothelial and T cell subsets within the established tumor microenvironment. Cancer Res In Press 2010.

236. Heinzel FP, Sadick MD, Holaday BJ, Coffman RL, Locksley RM. Reciprocal expression of interferon gamma or interleukin 4 during the resolution or progression of murine leishmaniasis. Evidence for expansion of distinct helper T cell subsets. J Exp Med 1989; 169: 59-72.

237. Tien AH, Xu L, Helgason CD. Altered immunity accompanies disease progression in a mouse model of prostate dysplasia. Cancer Res 2005; 65: 2947-55.

238. Maker AV, Attia P, Rosenberg SA. Analysis of the cellular mechanism of antitumor responses and autoimmunity in patients treated with CTLA-4 blockade. J Immunol 2005; 175: 7746-54.

239. Peggs KS, Quezada SA, Chambers CA, Korman AJ, Allison JP. Blockade of CTLA-4 on both effector and regulatory T cell compartments contributes to the antitumor activity of anti-CTLA-4 antibodies. J Exp Med 2009; 206: 1717-25.

240. Hirano F, Kaneko K, Tamura H, et al. Blockade of B7-H1 and PD-1 by monoclonal antibodies potentiates cancer therapeutic immunity. Cancer Res 2005; 65: 1089-96.

241. Takahashi T, Kuniyasu Y, Toda M, et al. Immunologic self-tolerance maintained by CD25+CD4+ naturally anergic and suppressive T cells: induction of autoimmune disease by breaking their anergic/suppressive state. Int Immunol 1998; 10: 1969-80.

242. Sato E, Olson SH, Ahn J, et al. Intraepithelial CD8+ tumor-infiltrating lymphocytes and a high CD8+/regulatory T cell ratio are associated with favorable prognosis in ovarian cancer. Proc Natl Acad Sci U S A 2005; 102: 18538-43.

243. Lee SJ, Myers L, Muralimohan G, et al. 4-1BB and OX40 dual costimulation synergistically stimulate primary specific CD8 T cells for robust effector function. J Immunol 2004; 173: 3002-12.

244. Cuadros C, Dominguez AL, Lollini PL, et al. Vaccination with dendritic cells pulsed with apoptotic tumors in combination with anti-OX40 and anti-4-1BB monoclonal antibodies induces T cell-mediated protective immunity in Her-2/neu transgenic mice. Int J Cancer 2005; 116: 934-43.

245. Dubrot J, Portero A, Orive G, et al. Delivery of immunostimulatory monoclonal antibodies by encapsulated hybridoma cells. Cancer Immunol Immunother 2010; 59: 1621-31.

246. Houot R, Levy R. T cell modulation combined with intratumoral CpG cures lymphoma in a mouse model without the need for chemotherapy. Blood 2008; 113: 3546-52.

247. Chen SH, Pham-Nguyen KB, Martinet O, et al. Rejection of disseminated metastases of colon carcinoma by synergism of IL-12 gene therapy and 4-1BB costimulation. Mol Ther 2000; 2: 39-46.

248. Pan PY, Gu P, Li Q, Xu D, Weber K, Chen SH. Regulation of dendritic cell function by NK cells: mechanisms underlying the synergism in the combination therapy of IL-12 and 4-1BB activation. J Immunol 2004; 172: 4779-89.

249. Xu D, Gu P, Pan PY, Li Q, Sato AI, Chen SH. NK and CD8+ T cell-mediated eradication of poorly immunogenic B16-F10 melanoma by the combined action of IL-12 gene therapy and 4-1BB costimulation. Int J Cancer 2004; 109: 499-506.

250. Tirapu I, Arina A, Mazzolini G, et al. Improving efficacy of interleukin-12-transfected dendritic cells injected into murine colon cancer with anti-CD137 monoclonal antibodies and alloantigens. Int J Cancer 2004; 110: 51-60.

251. Ruby CE, Montler R, Zheng R, Shu S, Weinberg AD. IL-12 is required for anti-OX40-mediated CD4 T cell survival. J Immunol 2008; 180: 2140-8.

252. Milone MC, Fish JD, Carpenito C, et al. Chimeric receptors containing CD137 signal transduction domains mediate enhanced survival of T cells and increased antileukemic efficacy in vivo. Mol Ther 2009; 17: 1453-64.

253. Zhang N, Sadun RE, Arias RS, et al. Targeted and untargeted CD137L fusion proteins for the immunotherapy of experimental solid tumors. Clin Cancer Res 2007; 13: 2758-67.

254. Ye Z, Hellstrom I, Hayden-Ledbetter M, Dahlin A, Ledbetter JA, Hellstrom KE. Gene therapy for cancer using single-chain Fv fragments specific for 4-1BB. Nat Med 2002; 8: 343-8.

255. Yang S, Yang Y, Raycraft J, et al. Melanoma cells transfected to express CD83 induce antitumor immunity that can be increased by also engaging CD137. Proc Natl Acad Sci U S A 2004; 101: 4990-5.

256. Boczkowski D, Lee J, Pruitt S, Nair S. Dendritic cells engineered to secrete anti-GITR antibodies are effective adjuvants to dendritic cell-based immunotherapy. Cancer Gene Ther 2009; 16: 900-11.

257. Shi W, Siemann DW. Augmented antitumor effects of radiation therapy by 4-1BB antibody (BMS-469492) treatment. Anticancer Res 2006; 26: 3445-53.

258. Kim YH, Choi BK, Kim KH, Kang SW, Kwon BS. Combination therapy with cisplatin and anti-4-1BB: synergistic anticancer effects and amelioration of cisplatin-induced nephrotoxicity. Cancer Res 2008; 68: 7264-9.

259. Takeda K, Kojima Y, Uno T, et al. Combination therapy of established tumors by antibodies targeting immune activating and suppressing molecules. J Immunol 2010; 184: 5493-501.

260. Yokouchi H, Yamazaki K, Chamoto K, et al. Anti-OX40 monoclonal antibody therapy in combination with radiotherapy results in therapeutic antitumor immunity to murine lung cancer. Cancer Sci 2008; 99: 361-7.

261.   Ko HJ, Kim YJ, Kim YS, et al. A combination of chemoimmunotherapies can efficiently break self-tolerance and induce antitumor immunity in a tolerogenic murine tumor model. Cancer Res 2007; 67: 7477-86.

262.   Sharma RK, Schabowsky RH, Srivastava AK, et al. 4-1BB ligand as an effective multifunctional immunomodulator and antigen delivery vehicle for the development of therapeutic cancer vaccines. Cancer Res 2010; 70: 3945-54.